

NASA/CR—1998-196710



**Flight Testing and Real-Time System Identification Analysis  
of a UH-60A Black Hawk Helicopter With an Instrumented  
External Sling Load**

*Allen H. McCoy*  
*Naval Postgraduate School, Monterey, California*

National Aeronautics and  
Space Administration

Ames Research Center  
Moffett Field, California 94035-1000

Prepared for Ames Research Center  
under Contract RTOP 581-30-22

---

**June 1998**

### **Acknowledgments**

Sincerest appreciation goes to Dr. Mark B. Tischler, Ames Research Center, and Dr. E. Roberts Wood, Naval Postgraduate School, for their boundless patience and support in what has been a challenging research endeavor. They were always available to help bring the pieces together and keep my perspective in check. A special thanks to Mr. Luigi Cicolani, Ames Research Center, for all those insightful conversations into the theoretical world of slung load dynamics and his meticulous attention to detail as second reader. Thanks to Mr. George Tucker for getting me up to speed on the project when I came aboard. Thanks also are due to Mr. Gary Villere and Mrs. Sharon Cioffi, Sterling Software, for their personal efforts to ensure I had access to and was able to use CIFER and all the other software packages which were the mainstay of the analysis. To Mr. Sunny Ng, Mrs. Mai Wei, Mr. Austin Somes, and all the exceptionally professional people at the flight test ground station, I pass along a hardy "well done" for your efforts in getting the ground station up to speed for the data acquisition and the real time data analysis. Lastly, a special thanks to Mr. Rick Simmons for his aggressive efforts in getting NASA 748 back in a flying status.

Available from:

NASA Center for AeroSpace Information  
7121 Standard Drive  
Hanover, MD 21076-1320

National Technical Information Service  
5285 Port Royal Road  
Springfield, VA 22161

## TABLE OF CONTENTS

I. INTRODUCTION .....	1
SUMMARY.....	1
A. BACKGROUND .....	1
B. UNITED STATES / ISRAELI MEMORANDUM OF AGREEMENT .....	2
II. TEST EQUIPMENT .....	5
A. HELICOPTER DESCRIPTION .....	5
1. General .....	5
2. Cargo Hook.....	6
B. LOADS.....	7
1. CONEX .....	8
2. Solid Block Loads.....	9
C. LIFTING SLING.....	9
D. LOAD INSTRUMENTATION PACKAGE.....	12
E. HELICOPTER INSTRUMENTATION .....	14
F. HELICOPTER VIDEO CAMERA.....	16
III. FLIGHT TEST PROGRAM.....	17
A. HISTORY .....	17
B. FLIGHT TEST PROFILE.....	17
C. DATA ACQUISITION.....	21
IV. DATA ANALYSIS.....	23
A. ANALYSIS TOOLS.....	23
1. CIFER®.....	23
2. Derived and Smoothed Variables Code.....	25
3. GetData .....	25
4. XPlot.....	26
5. Microsoft EXCEL® .....	26
B. HELICOPTER HANDLING QUALITIES.....	26
1. Bandwidth Frequency and Phase Delay .....	26
2. Determination of Bandwidth Frequency and Phase Delay.....	27

C. CONTROL SYSTEM STABILITY MARGINS .....	28
1. Gain Margin and Phase Margin.....	28
2. Determination of Gain and Phase Margins .....	29
D. LOAD MOTION ANALYSIS .....	31
1. Predicting Pendulum Mode Characteristics .....	31
2. Determination of Pendular Motion from Flight Measurements .....	32
a. Load Axis to Helicopter Axis Transformation Approximation.....	32
b. Determination of the Pendulum Mode Damping and Natural Frequency.....	32
E. NEAR-REAL TIME ANALYSIS VERSUS POST FLIGHT ANALYSIS.....	33
V. RESULTS.....	35
A. HELICOPTER HANDLING QUALITIES.....	35
B. CONTROL SYSTEM STABILITY MARGINS.....	41
C. LOAD MOTION CHARACTERIZATION.....	44
D. SIMULATION .....	46
1. Simulation Model.....	46
2. Comparison of Test Data to Simulation.....	46
VI. CONCLUSIONS AND RECOMMENDATIONS .....	49
A. CONCLUSIONS .....	49
B. RECOMMENDATIONS.....	50
APPENDIX A. SIGNAL LISTING FOR NASA 748, LOAD, AND STRIP CHARTS .....	53
APPENDIX B. DETAILED DRAWINGS OF THE 4K BLOCK AND CONEX.....	59
APPENDIX C. MOA TASK 8 FLIGHT TEST DATABASE SUMMARY.....	65
APPENDIX D. PILOT'S TEST FLIGHT DATA CARD .....	69
APPENDIX E. NEAR-REAL TIME DATA ANALYSIS PROCEDURES .....	73
A. OVERVIEW.....	74
B. TYPICAL SCENARIO .....	74
C. STEP-BY-STEP PROCEDURE FOR RUNNING CIFER® NEAR-REAL TIME.....	75
APPENDIX F. SISO ANALYSIS RESULTS SUMMARY.....	79
REFERENCES .....	81

## LIST OF FIGURES

Figure 1.1. U.S. Navy H-46D Performing Vertical Replenishment at Sea (VERTREP)	2
Figure 2.1. UH-60A Black Hawk helicopter general arrangement	5
Figure 2.2. UH-60A cargo hook with weigh system installed	7
Figure 2.3. Test loads and sling	8
Figure 2.4. Standard U.S. military 10,000-pound, 4-leg sling	9
Figure 2.5. Sling-load geometry	10
Figure 2.6. Stretch test of the 10,000-pound capacity, 4-leg sling	11
Figure 2.7. Installed sling swivel	12
Figure 2.8. Final installation of instrumentation package in CONEX	13
Figure 2.9. Sling-load instrumentation package	13
Figure 2.10. Simplified illustration of signal source locations on NASA 748	14
Figure 2.11. "Hell Hole" mounted video camera	16
Figure 3.1. Sample roll frequency sweep and helicopter roll rate response time histories	18
Figure 3.2. Sample roll step input and roll rate response time histories	19
Figure 3.3. Sample roll doublet input and roll rate response time histories	20
Figure 3.4. CONEX hook-up in progress	20
Figure 3.5. Schematic of MOA Task 8 data acquisition process	21
Figure 3.6. Ground station control room	22
Figure 4.1 Simplified model of the helicopter and slung load system	23
Figure 4.2. Major CIFER <sup>®</sup> utilities and data flow	24
Figure 4.3. Bandwidth frequency and phase delay definitions	27
Figure 4.4. Sample calculation of phase delay	28
Figure 4.5. Simplified model of the helicopter	29
Figure 4.6. Determination of phase and gain margins	30
Figure 4.7. NASA 748 with CONEX external load	31

Figure 4.8. Load axis to helicopter axis coordinate transformation	32
Figure 4.9. Example of second order fit to the load response	33
Figure 5.1. Handling qualities as a function of airspeed	36
Figure 5.2. ADS-33D handling qualities specification – 4K CONEX and no load	38
Figure 5.3. ADS-33D handling qualities specification – 2K CONEX and no load	38
Figure 5.4. ADS-33D handling qualities specification – 4K block and no load	39
Figure 5.5. ADS-33D handling qualities specification – 1K block and no load	39
Figure 5.6. Scaled drawing of the three external load configurations	40
Figure 5.7. Control system stability margins – pitch	42
Figure 5.8. Control system stability margins – roll	43
Figure 5.9. Load pendulum mode damping	45
Figure 5.10. Load pendulum natural frequency	45
Figure 5.11. Comparison of flight test and simulation time histories - longitudinal	47
Figure 5.12. Comparison of flight test and simulation time histories - lateral	48
Figure B.1. 4K block load	60
Figure B.2. CONEX dimensions (sheet 1 of 3)	61
Figure B.3. CONEX dimensions (sheet 2 of 3)	62
Figure B.4. CONEX dimensions (sheet 3 of 3)	63
Figure D.1. Pilot’s test flight data card (sheet 1 of 2)	70
Figure D.2. Pilot’s test flight data card (sheet 2 of 2)	71
Figure E.1. ‘fox-sparrow’ screen setup for real time analysis	78

## LIST OF TABLES

Table 2.1. NASA 748/UH-60A general specifications	6
Table 2.2. Test load and sling weights	7
Table 2.3. Results from NASA Ames calibration laboratory dynamic sling tests	11
Table 2.4. Gains and scaling factors for selected signals	15
Table 4.1. Comparison of near-real time results versus post flight results	34
Table 5.1. List of airspeed at which each load was flown	35
Table A.1. Telemetry signals for NASA 748 and load	54
Table A.2. Helicopter derived parameters and filtered signals	55
Table A.3. Load derived parameters and filtered signals	56
Table A.4. Strip chart signal listing	57
Table C.1. MOA Task 8, flight test database summary	66
Table C.2. MOA Task 8, flight test database summary (continued)	67
Table F.1. Summary of results from SISO analysis of flight data	80



# **FLIGHT TESTING AND REAL-TIME SYSTEM IDENTIFICATION ANALYSIS OF A UH-60A BLACK HAWK HELICOPTER WITH AN INSTRUMENTED EXTERNAL SLING LOAD**

Allen H. McCoy

## **I. INTRODUCTION**

### **SUMMARY**

Helicopter external slung load capabilities are crucial to many civilian and military operations. As such, it is of great interest to both the research and the operational worlds to increase the understanding of the dynamic interactions that exist when a helicopter is coupled with a slung load. The two main concerns being the safety of the crew and aircraft and the continual drive to decrease the costs associated with qualifying loads, slings, and helicopters for external cargo operations. In an effort to address some of the unique aspects of this area, the U.S. and Israel joined efforts through a Memorandum of Agreement. This thesis presents the results from the first series of flight tests conducted in support of this project. In particular, the effect of the suspended load on the helicopter's handling qualities and its control system's stability margins will be addressed. Load pendulum motion is analyzed. Also, presented is a discussion about the setup and use of CIFER<sup>®</sup> for near real-time data analysis.

### **A. BACKGROUND**

The helicopter external air transportation (HEAT) of cargo by both the military and the civilian market can be traced nearly to the beginning of the history of the helicopter itself. With the ability to handle heavy, oversized loads; to reach areas inaccessible by ground transportation; and to provide fast transit times; helicopter external load operations have found a home in such civilian industries as lumbering, construction, fire-fighting and oil exploration. In the military, HEAT is crucial to the success of the tactical transport and supply missions (fig. 1.1). Historically, the certification of a load, suspension system and helicopter for external air transport has been accomplished through flight testing (ref. 1). This is not only a time consuming task, especially considering the multitude of load, sling and helicopter combinations, but one which can be costly and dangerous. Even with prior flight clearance, problems with load and helicopter stability, sometimes with catastrophic results, arise when operational conditions do not match those of the original qualifying flight test.



Figure 1.1. U.S. Navy H-6D Performing Vertical Replenishment at Sea (VERTREP).

Certification of all Department of Defense (DOD) external loads is the responsibility of the U.S. Army Research, Development, and Engineering Center at Natick Maryland per the Joint Logistics Commanders Memorandum of Agreement on External Helicopter Transported Loads. This organization qualitatively assesses and certifies specific load and lifting configurations. No quantitative evaluation of stability margins or handling qualities is made (ref. 2).

As computers and modeling techniques advance it is a natural extension to apply these capabilities to helicopter external slung loads operations. To improve current simulations, it is necessary to improve the level of understanding of how the load, sling and helicopter interact. Some of the influences include; load weight and inertia, load aerodynamic characteristics, load mass as a fraction of the helicopter mass, sling configuration, length and elastic properties, helicopter dynamics and the power margin of the helicopter. Flight test data and system identification offer invaluable insight into these effects as well as provide the means to validate the model. This validated model can then be applied to estimate the expected helicopter and sling load flight envelope and in this way, pinpoint potential stability problems prior to flight testing. The obvious benefits are those of reduced cost and increased safety.

The U.S. Army and the National Aeronautics and Space Administration (NASA), in cooperation with the Israeli Air Force and Technion University, under a Memorandum of Agreement (MOA) have initiated a program to advance these concepts. This thesis presents initial results from the first phase of flight testing performed in support of this project.

## **B. UNITED STATES / ISRAELI MEMORANDUM OF AGREEMENT**

Initial cooperative efforts between the United States and Israel began in October 1986 with an investigation of the effects of biodynamic interference on panel-mounted and helmet-mounted displays. As follow-on to that project, a formal three-year agreement was drafted and signed in

November 1988. Due to the continued success of this initial endeavor, four years later in November 1992, a nine-year MOA for cooperative research on “Rotorcraft Aeromechanics and Man-Machine Integration Technology” was signed. This agreement was designed to bring together academia, industry and government research laboratories of both countries to work jointly on basic areas of research in the rotorcraft field. At present, nine specific research projects are identified. Three of these “Task 1: Biodynamic Interference in Helicopter Displays,” “Task 3: Human Factors Aspects of Thermal Imagery Interpretation,” and “Task 6: Active Armor Concepts” have been completed. The six remaining active programs are (ref. 3):

- Task 2: Rotorcraft Flight Mechanics Modeling
- Task 4: Unsteady Flow Control
- Task 5: Coupled Rotor/Airframe Analysis for Preliminary Design
- Task 7: Human Vision Modeling
- Task 8: Flight Mechanics of Helicopter/Sling-Load Systems
- Task 9: Human Performance Modeling in MIDAS

The study of helicopter external load operations falls under Task 8. This task was included in the MOA in 1995, in an effort to address some of the issues identified above in the Background. The main objectives of the task are (ref. 4):

- Study basic flight mechanics of rotorcraft/sling load systems.
- Develop numerical simulation modeling techniques, validated by flight test and system identification, which can accurately estimate the expected helicopter/sling load envelope in advance of flight testing.
- Develop near real-time data analysis capability for verifying aircraft and load stability margins during envelope confirmation flight testing.
- Analytical investigation of the potential of load stabilization, both passive and active, for improving mission performance.
- Use the numerical simulation to further investigate twin-lift operations to include performance, stability, pilot workload, and other related issues.

The main thrust of the U.S. efforts in support of Task 8 is to conduct the flight tests of a UH-60A Black Hawk helicopter with a range of external loads. These tests provide the opportunity to demonstrate the capability of near real-time analysis of the aircraft and load responses, using off-the-shelf technology. The specific goals of the analysis are to determine the effect of the load on both the handling qualities of the helicopter and on the control system’s stability margins, as well as to characterize the motion of the load. A long-term goal is to extract the aerodynamic

properties of the load from the flight test data. This data, along with analysis, will then be used in support of the simulation efforts.

## II. TEST EQUIPMENT

### A. HELICOPTER DESCRIPTION

#### 1. General

A Sikorsky UH-60A "Black Hawk" helicopter, Army serial number 83-23748 abbreviated to NASA 748, was utilized for this flight test program. This aircraft was employed for the previous ten years as the test bed for the joint U.S. Army and NASA "Airloads Project" which completed flight testing in 1994. The major system elements of the rotating data system (RDAS) were removed from the aircraft, while the aircraft data system (ADAS) remained intact. The ADAS is capable of providing over one hundred channels of pulse code modulation (PCM) encoded data from a full suite of existing sensors appropriate to a wide range of potential flight projects (ref. 5). A listing of the signals monitored during test flights is contained in Appendix A.

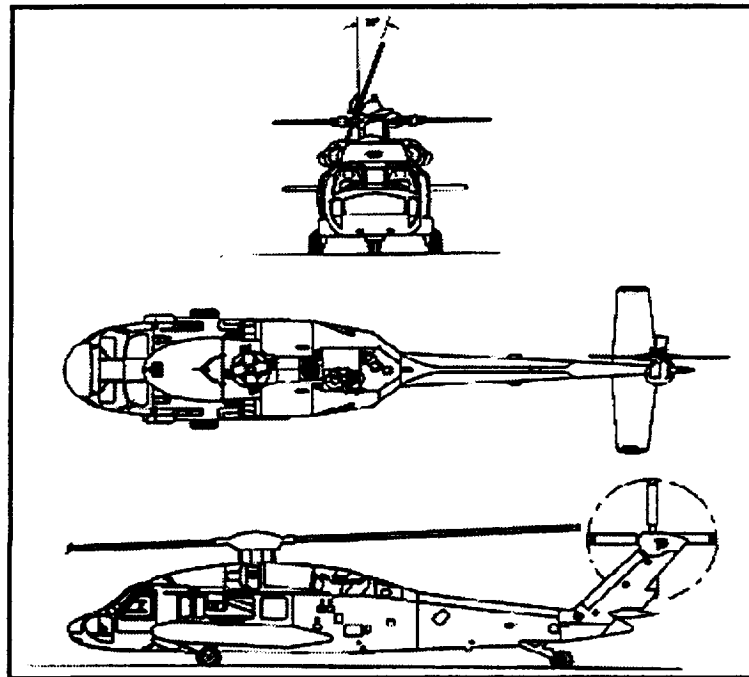


Figure 2.1. UH-60A Black Hawk helicopter general arrangement (after ref. 6).

The Black Hawk's primary mission for the U.S. Army is the tactical transport of troops, supplies and equipment. Its general configuration is shown in figure 2.1 and the major specifications and aircraft parameters are listed in table 2.1. The main and tail rotor systems each are comprised of four titanium/fiberglass blades. The drive train consists of a main transmission, intermediate gearbox, and tail rotor gearbox with interconnecting shafts. The aircraft is powered by two T700-GE-700 gas turbine engines with a maximum take-off power rating of 3,086 shaft horsepower (ref. 6) Other than the test instrumentation package installed on this aircraft, it is similar to Black Hawks currently operating in the field with the U.S. Army.

Table 2.1. NASA 748/UH-60A general specifications (from refs. 6, 7, & 8).

Empty Weight	11,563 lbs	
Fuel Weight, Typical	2,446 lbs	
Crew Weight: 2 Pilots, 1 Crew Chief	600 lbs	
Takeoff Weight, Typical	14,609 lbs	
Maximum Takeoff	20,250 lbs	
Engines (2)	T700-GE-700	
Maximum T.O. Rating	3,086 SHP	
Maximum Useable Power	2,828 SHP	
Maximum Hook Capacity	9,000 lbs	
<u>Rotor Parameters</u>	<u>Main Rotor</u>	<u>Tail Rotor</u>
Radius (ft)	26.83	5.5
Chord (ft)	1.73	0.81
Solidity	0.082	0.188
Number of Blades	4	4
Rotor Rotational Speed (rad/sec)	27.02	124.54
Tip Speed (ft/sec)	725	685
Hinge Offset Ratio	0.047	---

## 2. Cargo Hook

The standard UH-60A cargo hook was modified to include a load cell for determination of in-flight loads exerted on the hook. The system installed was an E-79 Electronic Load Weigh System from Onboard Systems of Portland, Oregon. It consists of a cockpit indicator; a load cell built into the cargo hook and an interconnecting wiring harness. The signal from the load cell was patched into the ADAS and included as an additional channel of recorded and telemetry data. Figure 2.2 shows the cargo hook and the basic weigh system components. The hook is installed along the helicopter's centerline at fuselage station 353.0 and is certified for a maximum load of 9,000 pounds. The hook can rotate about the longitudinal axis and cable angle should be limited to 30-degrees in pitch to avoid damage to the keeper (ref. 6).

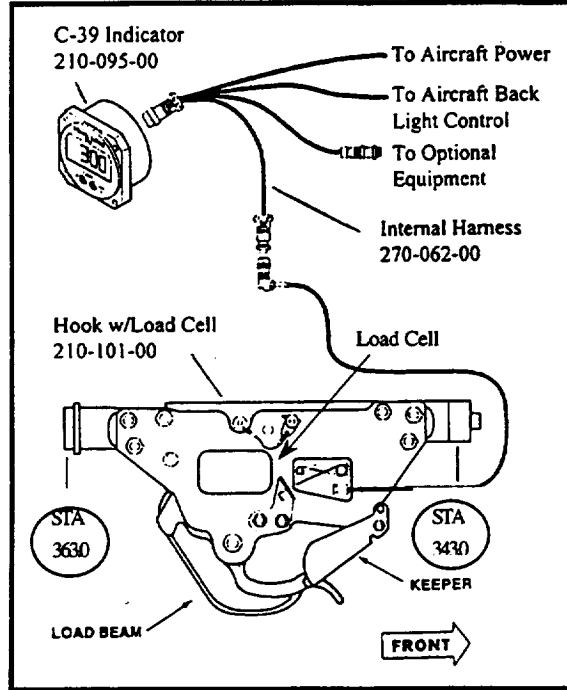


Figure 2.2. UH-60A cargo hook with weigh system installed (from ref. 9).

## B. LOADS

Four loads of varying sizes and weights flew as part of the test program. Load weights range from 1,070 pounds up to 6,164 pounds and they all are listed in table 2.2. Figure 2.3 gives a good perspective of the various sizes of the loads, from a flat plate to a container express box (CONEX).

Table 2.2. Test load and sling weights.

	Block Loads			CONEX		10K Capacity
	1K	4K	6K	2K	4K	4-Leg Sling
Weight (lbs)	1,070	4,154	6,164	1,794	4,105	52

Note: 1. Sling weight not included in load weights.  
 2. CONEX weight includes all instrumentation.

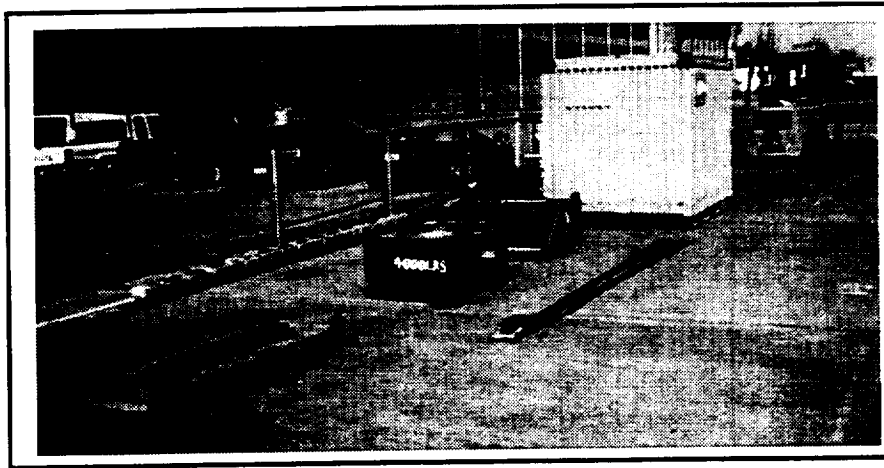


Figure 2.3. Test loads and sling (L to R, 1K, 4K, 6K, and CONEX).

## 1. CONEX

The primary load for this project is commonly referred to as a CONEX (container express box) (ref. 10). It is a basic steel container, 8.5 x 6.4 x 6.1 feet, with a flat floor and roof and corrugated sides as seen in figure 2.3. For determination of its center of gravity (CG), it is modeled as a box with its mass uniformly distributed throughout the sides, top and bottom. Detailed three-view drawings are included in Appendix B.

The CONEX was selected for several reasons. First, with an empty weight of 1800 pounds and the capability to be loaded to weights in excess of 6,000 pounds it provides a convenient platform to study the effect of changing load weights without altering the basic geometry. Second, a shelf could be easily built inside to support the instrumentation package. Third, it provided a simple geometric shape with significant aerodynamic properties, which could be easily modeled for wind tunnel testing to be conducted in Israel. Finally, it is representative of some operational loads currently being transported externally by helicopter.

A few minor modifications were made to the CONEX to facilitate instrumentation installation and improved safety. A shelf was installed inside the box. Constructed of aluminum, the shelf was designed to survive a 2.25g load. Incorporated into the design was the ability to raise and lower the shelf to accommodate a change in center of gravity. A magnetic compass, which provided the load heading, was mounted on an aluminum boom attached to the rear of the CONEX to reduce the magnetic interference effects of the steel box. The distance away from the box was determined through trial and error with the assistance of the compass' built in calibration process. The antenna for transmission of the telemetry data was placed on the front wall, opposite the compass, and was covered by a small kevlar bubble. For safety considerations and for the benefit of the ground/hook-up crew, a handle was installed over the doors. This provided a solid handhold when climbing up on to or down from the top of the CONEX.

## 2. Solid Block Loads

Three solid block loads were also flown at various stages of the flight test program. As stated in Table 2.2, their respective weights are 1,070 lbs, 4,154 lbs and 6,164 lbs. These loads provided the opportunity to isolate and study just the effect of varying weight with minimal influence from aerodynamic forces. The blocks were assumed to generate negligible aerodynamic specific forces and moments and were demonstrated to be stable over the range of airspeeds flown. The blocks are constructed of steel and concrete. The small 1k load was suspended from the helicopter with a standard 20-foot long single pendant sling with a four-leg bridle. As with the CONEX, the 4k and 6k loads each were suspended from the helicopter using the four-leg sling described below.

### C. LIFTING SLING

A standard U.S. Military 10,000-pound capacity sling was acquired for the test as the baseline configuration. It consists of an aluminum apex fitting (shackle) joining four legs together. Each leg is comprised of a twelve-foot long, 7/8-inch diameter nylon rope, with eye splices at each end, a grab-hook, and an eight-foot chain (fig. 2.4). The sling weighs 52 pounds. Each leg has a 2,500 pound capacity.

As shown in figure 2.4, the chain is doubled back through the lift point back to the grab-hook. For test standardization and safety, the sling was attached to the load in accordance with the "Multi-Service Helicopter External Air Transport: Basic Operations and Equipment Manual" (ref. 10). Attached in this fashion, the overall unloaded static length of the sling, from the lift point to the aircraft cargo hook was approximately 16.75 feet. Figure 2.5 illustrates the basic sling-load geometry for the 4k block and CONEX.

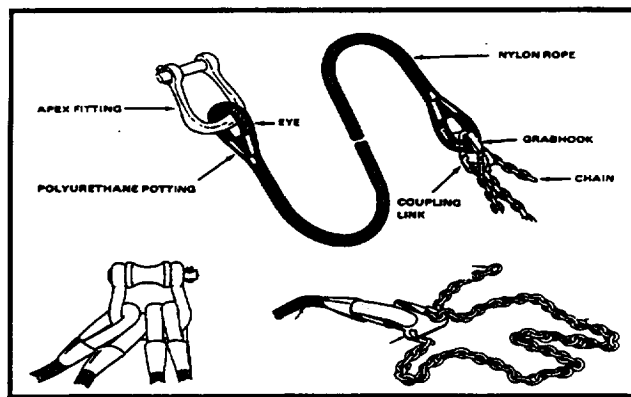


Figure 2.4. Standard U.S. military 10,000-pound, 4-leg sling (after ref. 10)].

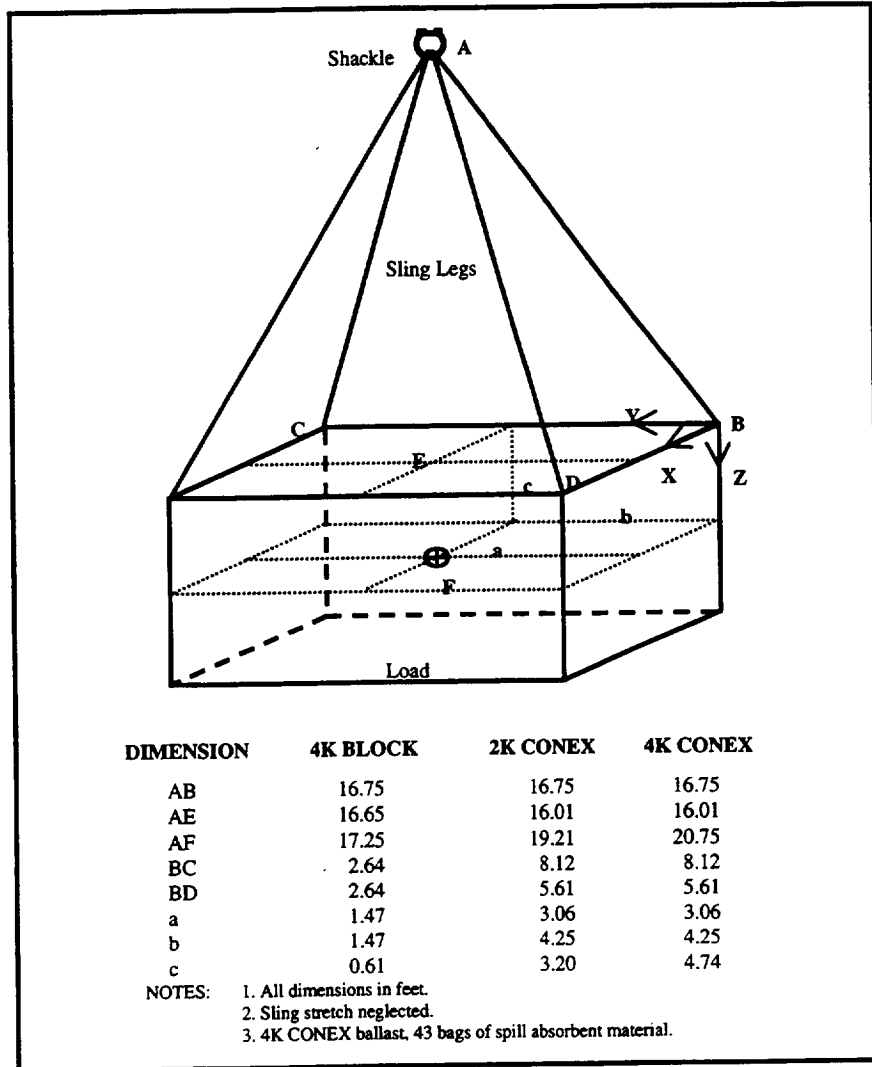


Figure 2.5. Sling-load geometry.

Limited data is available in regards to the spring constant and natural frequency of the sling. Dynamic testing of the sling performed at the NASA Ames calibration laboratory concluded that the spring constant of the four-leg sling varies with applied load (ref. 11). Tests conducted by the U.S. Army Aviation Troop Command, Directorate for Engineering, Ground Support Equipment Branch also concluded “the spring rate increases with load and with repeated application of load” (ref. 12). Results from the Ames test are listed in table 2.3. Investigations are ongoing into the effect age and use have on the characteristics of slings of this type.

Table 2.3. Results from NASA Ames calibration laboratory dynamic sling tests (ref. 11).

Load Weight (lbs)	Natural Frequency (Hz)	Damping	Spring Constant (lbs/in)
701.45	4.843	0.0157	1839
4197.0	2.54	0.0269	3215

In an effort to obtain more information about the sling’s elastic properties, a static suspension test was performed using each test load. Sling leg elongation up to 0.86-foot was recorded when the 6K block was suspended. The range of elongation for application of all four loads is between one to five percent. During the test, however, no time was allocated for the sling to “relax” between lifts. When the CONEX was lifted just after the 6K block, the amount of stretch was significantly less than the lighter 1K block, which was the first lift. This inconsistency is due to the build up of the hysteresis in the sling legs. This problem is seen as the dip in the data presented in figure 2.6, where the number above the data points indicates the lifting order.

Although these sling parameters are important to the overall task and future simulation modeling, the inconsistencies in the sling data did not play a critical role in this phase of the project. The concern at this point is the pendular characteristics of the slung load, which has a natural frequency around 0.24 hertz (1.5 rad/sec), well below the stretch frequencies.

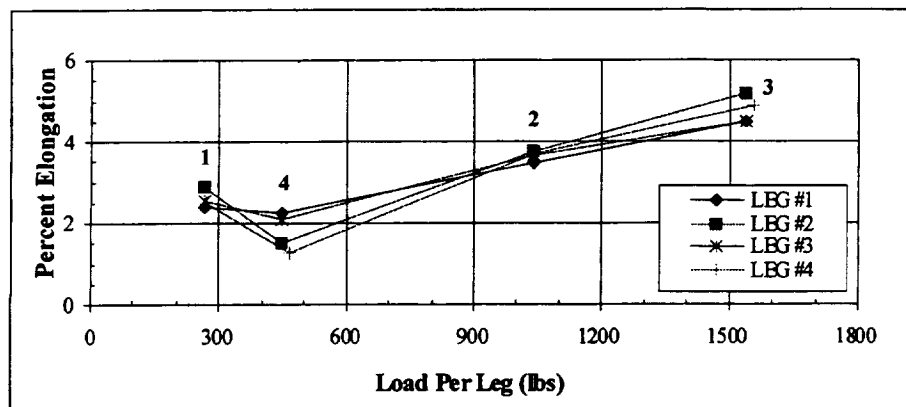


Figure 2.6. Stretch test of the 10,000-pound capacity, 4-leg sling.

In an attempt to eliminate the wind-up of the sling legs in flight due to the yaw rotation of the CONEX, a swivel (fig. 2.7) was installed at the shackle end of the sling. The swivel was load tested to 10,000 pounds and weighed 25 pounds. Unfortunately, due to the helicopter’s rotational downwash and load aerodynamics, the load developed yaw rates in excess of 50 degrees per second at hover and 30 knots. Concerns about possible instrumentation lags and the safety of prolonged flight with the swivel subjected to this condition led to its removal for the remaining test flights.



Figure 2.7. Installed sling swivel.

#### **D. LOAD INSTRUMENTATION PACKAGE**

The Israeli Air Force Flight Test Center, Instrumentation Department, designed and fabricated the load instrumentation package as one part of the joint aspect of the MOA. The package was designed to be compact, lending itself toward easy installation with minimum complexity. The package was installed on the shelf inside the CONEX without difficulty. Figure 2.8 is a photograph of the completed installation. Figure 2.9 shows the general layout of the package and identifies the major components. The main box and platform with instrumentation weighs 90 pounds. Power is supplied by a 24-volt lead-acid aircraft battery weighing 29 pounds. Total weight of the installed package is 119 pounds. A total of nine data signals are transmitted by the load, eight signals from the instruments in the package plus the magnetic compass signal. Signal sample rate is 260 hertz. A detailed list is included in Appendix A.

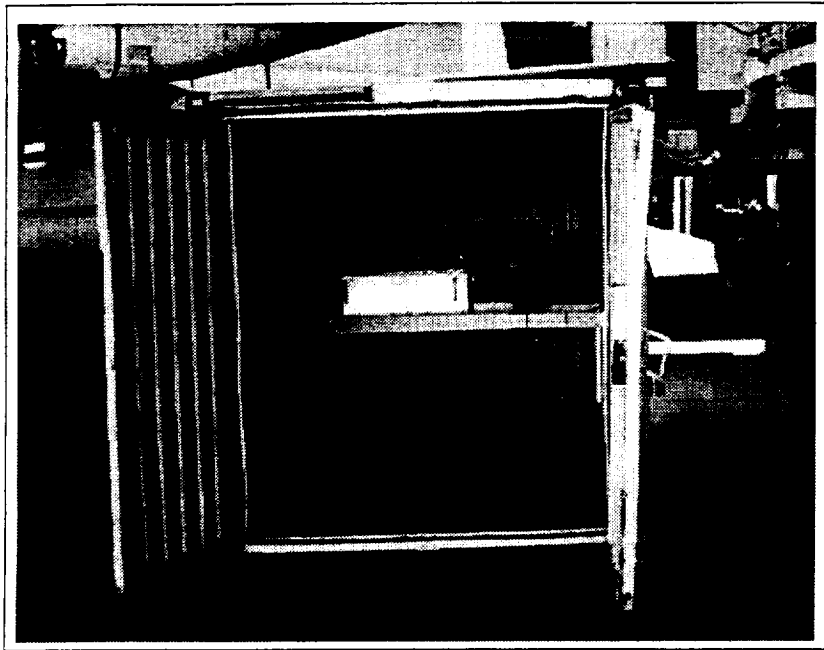


Figure 2.8. Final installation of instrumentation package in CONEX. Note compass arm on the right.

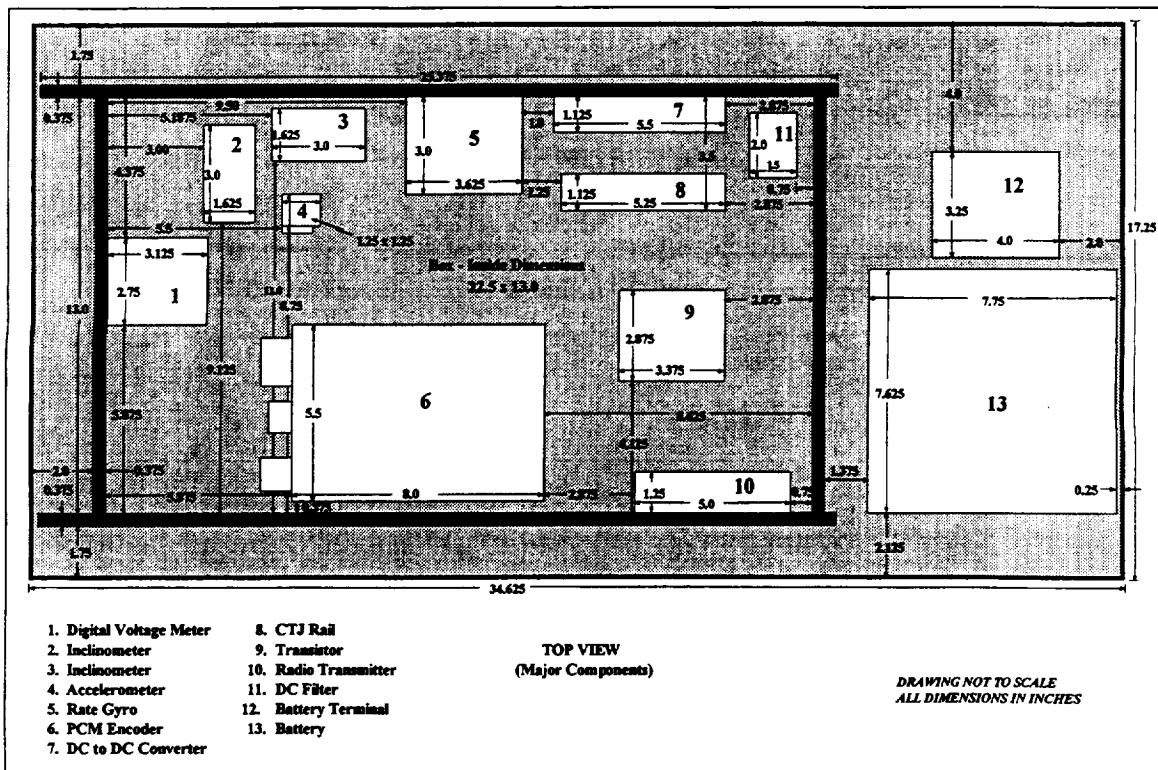


Figure 2.9. Sling-load instrumentation package.

## E. HELICOPTER INSTRUMENTATION

As mentioned in the description of the helicopter, a full compliment of instrumentation is installed in NASA 748. Appendix A gives a detailed list of those signals recorded during the MOA Task 8 test flights. Of particular interest are the control inputs, boost servo output, mixer inputs, and helicopter attitude and angular rate signals for all axes. Figure 2.10 is a simplified representation of the helicopter, which identifies the point where some of the signals are obtained. The sample rate is 209 hertz. The majority of scaling and gains values, some of which are listed in table 2.4, were obtained from the work done during the "Airloads Project," in which this helicopter was most recently involved.

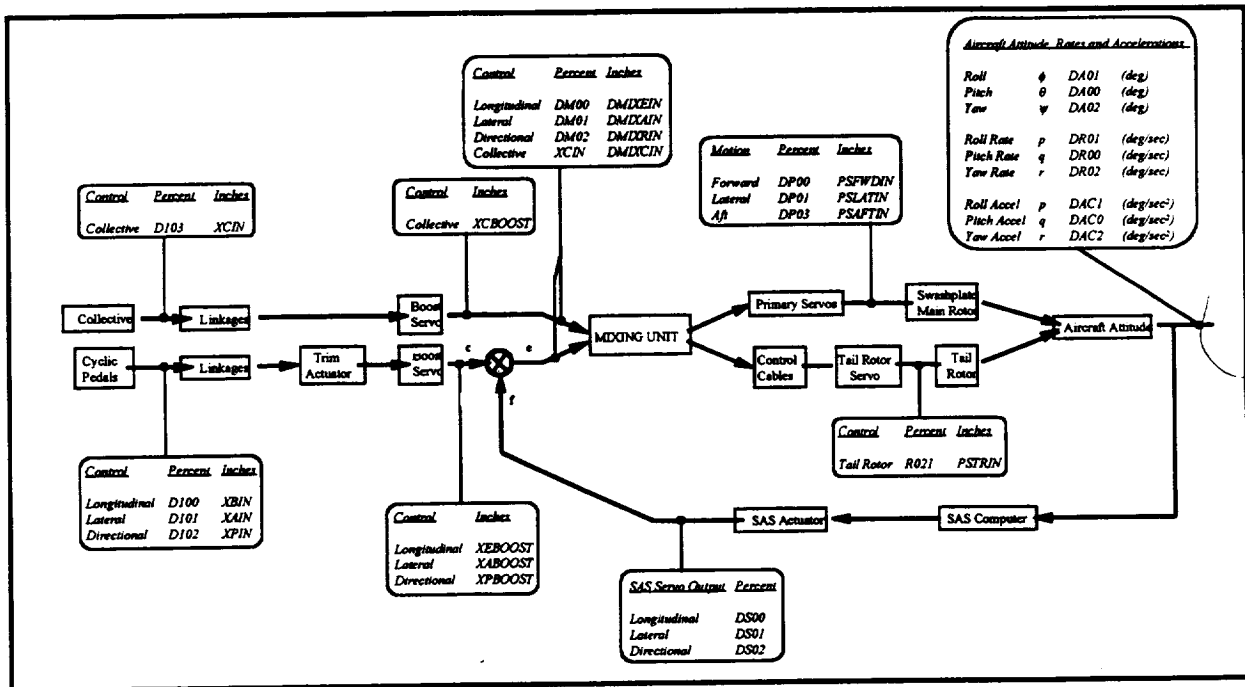


Figure 2.10. Simplified illustration of signal source locations on NASA 748.

Table 2.4. Gains and scaling factors for selected signals.

SIGNAL	ITEM CODE	UNITS	MULTIPLY BY	CONVERT TO	NEW SIGNAL
Longitudinal Stick	D100	Percent	0.1125	Inches	XBIN
Lateral Stick	D101	Percent	0.095625	Inches	XAIN
Pedals	D102	Percent	0.056875	Inches	XPIN
Collective	D103	Percent	0.10625	Inches	XCIN
Mixer Inputs:					
Longitudinal	DM00	Percent	0.02108	Inches	DMIXEIN
Lateral	DM01	Percent	0.02065	Inches	DMIXAIN
Directional	DM02	Percent	0.0189	Inches	DMIXRIN
Collective	XCIN	Inches	0.2025	Inches	DMIXCIN
Primary Servo Outputs:					
Forward	DP00	Percent	0.0406	Inches	PSFWDIN
Lateral	DP01	Percent	0.0327	Inches	PSLATIN
Aft	DP03	Percent	0.0429	Inches	PSAFTIN
Tail Rotor	R021	Percent	0.0308	Inches	PSTRIN
NOTE: These conversions are extracted from Mark Ballin and Mario-Alix Dalang-Secretan's derived variables routine for the UH-60A rotor system Phase IIA tests.					
DERIVATIONS:					
SIGNAL	CODE	EQUATION	UNITS		
Boost Servo Outputs:					
Longitudinal	XEBOOST	XBIN * 0.21	Inches		
Lateral	XABOOST	XAIN * 0.24	Inches		
Directional	XPBOOST	XPIN * 0.36	Inches		
Collective	XCBOOST	XCIN * 0.20	Inches		
NOTE: These equations were provided by Mark Tischler to account for the mechanical connections between the cockpit controls and the boost servo outputs.					

## F. HELICOPTER VIDEO CAMERA

A small video camera was installed against the starboard side of the cargo hook “hell hole,” looking down over the load as shown in figure 2.11. The video signal was recorded onboard in VHS format, as well as transmitted to the ground station. Unfortunately, due to tracking and reception problems the signal was only available to the flight test engineers when the aircraft was performing maneuvers at the field. The quality of the onboard video recording was excellent, however, providing a valuable source of information for post flight analysis.

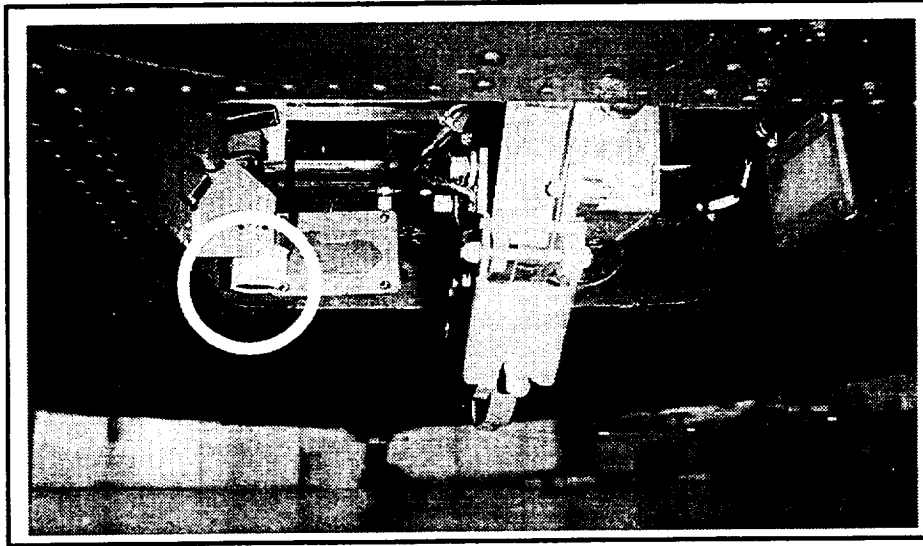


Figure 2.11. “Hell Hole” mounted video camera (left of the cargo hook).

### **III. FLIGHT TEST PROGRAM**

#### **A. HISTORY**

Shortly after Task 8 was included in the MOA, preparations were made to acquire the necessary equipment and begin the flight tests. Transfer of NASA 748, a UH-60A Black Hawk helicopter on extended loan from the U.S. Army, was completed at the end of January 1995. A search for practical and safe external loads resulted in the acquisition of the 1K block, 4K and 6K blocks, and the CONEX. A standard 10,000-pound capacity, four-leg sling and 20-foot long single pendant sling with a four-leg bridle were purchased. The four-leg 10K sling was used as the baseline sling configuration although initial flight with the 1K block used the single pendant and bridle sling.

All flight tests took place at or near Moffett Field, Ames Research Center, Mountain View, California. The first data flight, designated Flight 150, occurred in April 1995, and focused on initial procedure check out. Since that flight, 18 data flights and three calibration flights totaling 28 flight hours were flown in support of the project. A summary of the test flights is included in Appendix C. Prior to October 1996, test flights produced data mainly associated with the solid loads. Between October 1996 and July 1997, NASA 748 was grounded as a result of mechanical difficulties associated with the flight-control rigging. When cleared for flight in July 1997, data tests resumed in earnest. Between the end of July and the end of August 1997, eight data flights were flown, focusing on the CONEX load. Included in this series was a no-load flight (Flight 170) flown at hover, 30 knots and 50 knots, which established the baseline data set.

Flight 173, flown August 1997, concluded this first phase of flight testing in support of Task 8 of the MOA. Prior to beginning the next phase of flight tests, time has been allotted to further examine the data obtained. From this analysis and based on the original goals of the Task, additional flight phases will be developed and executed.

#### **B. FLIGHT TEST PROFILE**

The analysis of the test data was in the frequency domain. As such, the basic type of test inputs required for this analysis consisted of frequency sweeps. The frequency sweeps were used to generate a high quality, frequency response database. Steps and doublets were also conducted but were not used in the analysis discussed in this paper. They will be used in future analysis for time domain verification of the resulting models. Testing techniques and methodology are addressed in detail in reference 13.

The frequency sweeps were manually generated by the pilot applying a sinusoidal input to the controls, in the axis of interest. Each sweep begins and ends with a period of at least three seconds of trim data. The sweep is initiated with two complete input cycles at the minimum frequency. This is followed by a smooth and continuous increase in the frequency up to the maximum limit planned for the maneuver. By letting the pilots perform the sweeps, the excitation signals are typically spectrally richer than when the inputs are computer generated. Actual displacement of the controls remains within the range 0.5 to 1.5 inches, with the focus

being on a perceived continuous control movement by the pilot. To assist the pilot, the co-pilot calls out quarter cycles and the ground test engineers notify the pilot upon reaching 1.0 and 2.0 Hz. During the sweep, the pilot attempts to maintain the aircraft centered about the trim condition. Figure 3.1 depicts a typical frequency sweep input and the resulting aircraft response. A physical limitation to this sweep technique is the relatively large aircraft motions at the lower, long period frequencies (ref. 13).

The frequency limits of the sweep were established based on the following concerns. First, the natural frequency of the pendulum mode of the loads is estimated to be approximately 0.24 Hz (1.5 rad/sec) (see Section IV.D). Second, frequency ranges of 0.03 to 1.9 Hz (0.2 to 12 rad/sec) and 0.16 to 2.9 Hz (1.0 to 18.0 rad/sec) are recommended for handling qualities simulation and flight control system design models, respectively (ref. 14). Third, the lateral and vertical bending modes of the fuselage occur at 5.4 Hz (33.9 rad/sec) and 6.2 Hz (39.0 rad/sec), respectively. Fourth, the main rotor lag-regressive mode occurs at 2.4 Hz (15.1 rad/sec) (ref. 15). Therefore, to avoid possible excitation of the helicopter structural and rotor modes and still provide a wide, safe frequency spectrum, a range from 0.05 to 2.0 Hz (0.3 to 12.6 rad/sec) was selected. The resulting period of the low frequency limit was thus 20 seconds, with 5.0 second quarter-cycles. The total record length was typically greater than eighty seconds, which matches the length of 3-4 times the maximum period recommended by reference 13.

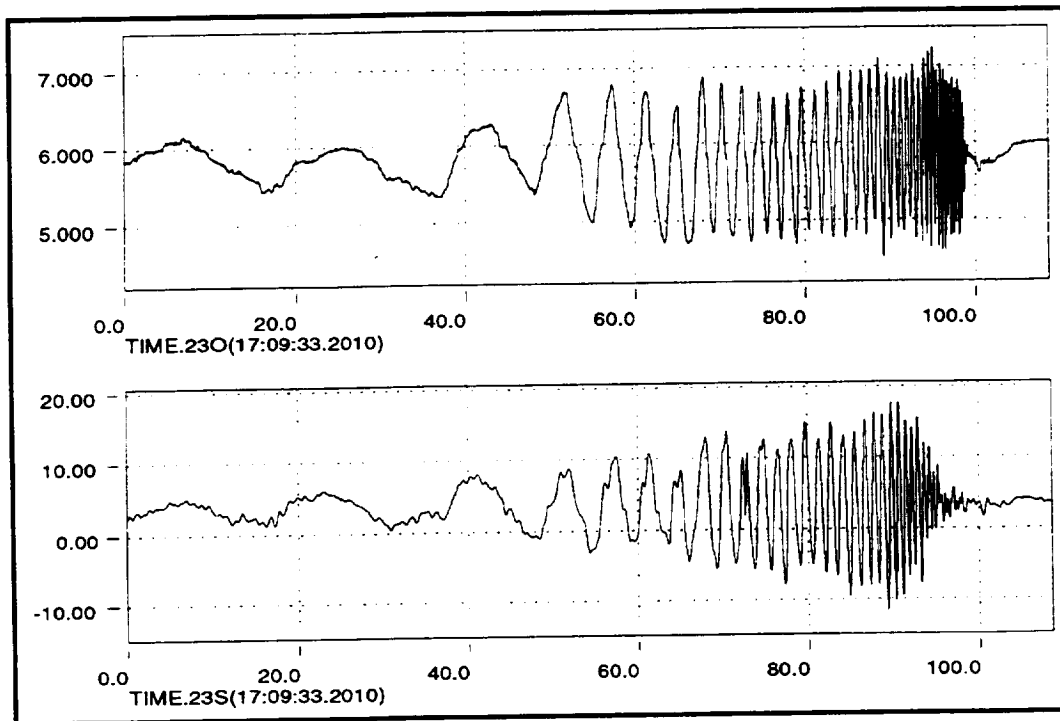


Figure 3.1. Sample roll frequency sweep and roll rate response time histories. Upper plot- lateral stick deflection ( $\delta_{Lat}$ ) in inches. Lower plot- roll rate ( $p$ ) in deg/sec.

Step and doublet inputs followed the sweeps. They were typically repeated twice, with the initial movement in the opposite direction on the second pass. The step input was held long enough to record about 10 to 15 seconds of data and then the pilot would return the controls to trim. Figures

3.2 and 3.3 illustrate typical step and doublet inputs and with corresponding on-axis aircraft response.

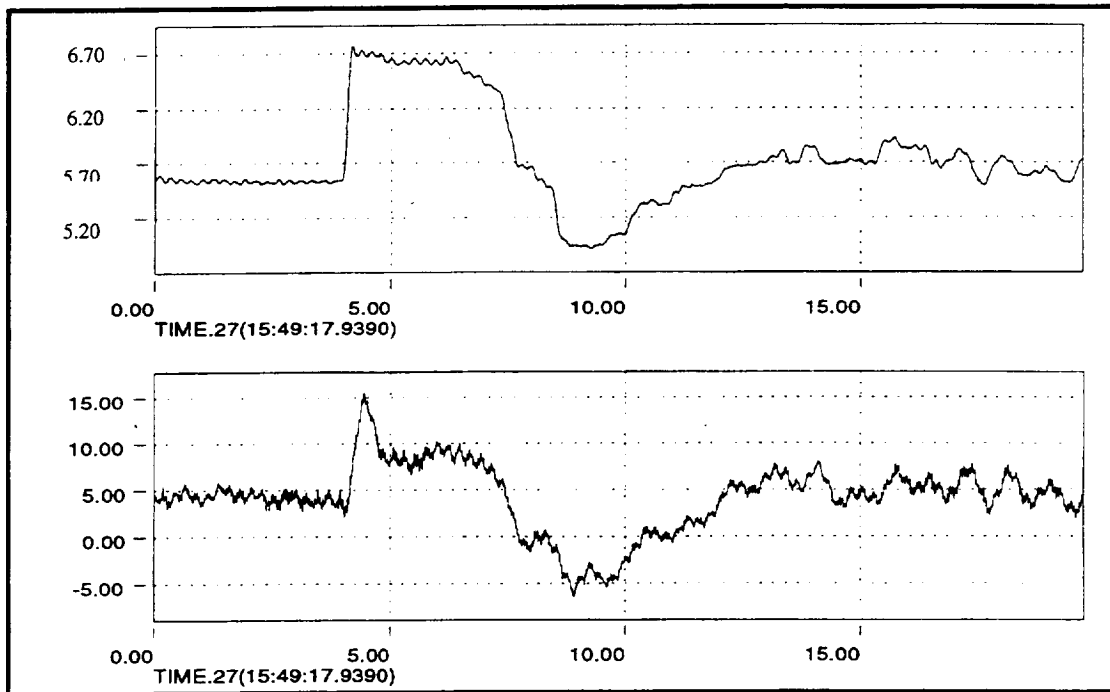


Figure 3.2. Sample roll step input and roll rate response time histories. Upper plot—lateral stick deflection ( $\delta_{Lat}$ ) in inches. Lower plot—roll rate ( $p$ ) in deg/sec.

The typical scenario for a data flight began with the crew brief. Required attendees were the aircrew, load handlers, and the flight test engineers. Main items covered in the brief were the test plan and any safety items. Following the brief, the pilots finished necessary preparations of the aircraft. The load handlers positioned the load at the pickup point and powered up the load instrumentation package. The engineers proceeded to the ground station and ensured all systems were ready there (see Section III.C). Once the helicopter was powered up, the pilots initiated the control throw checks and took the compass calibration data record. With all systems operating, the crew taxied the helicopter to pickup the load. The two load handlers waited by the load as the helicopter came to a lower hover over them and the load. If the test load was the CONEX, the handlers had to climb on top of the box for the hook-up as seen in figure 3.4. As soon as one handler grounded the cargo hook, the other placed the sling shackle on the hook. When the handlers were clear of the load, the helicopter lifted it and proceeded to setup at the first flight condition. A full test card (see Appendix D) consisted of a trim point, followed by three sweeps, two steps and two doublets. Each maneuver was recorded on the deck and in the aircraft as detailed in Section III.C. The maneuvers focused primarily in the lateral and longitudinal axes, although this varied some throughout the program. Once all maneuvers at each test condition were completed the load was set down and the aircraft taxied into the line. In the chocks, prior to shut down, a short end-of-flight compass calibration record was made, completing a typical full-card data flight.

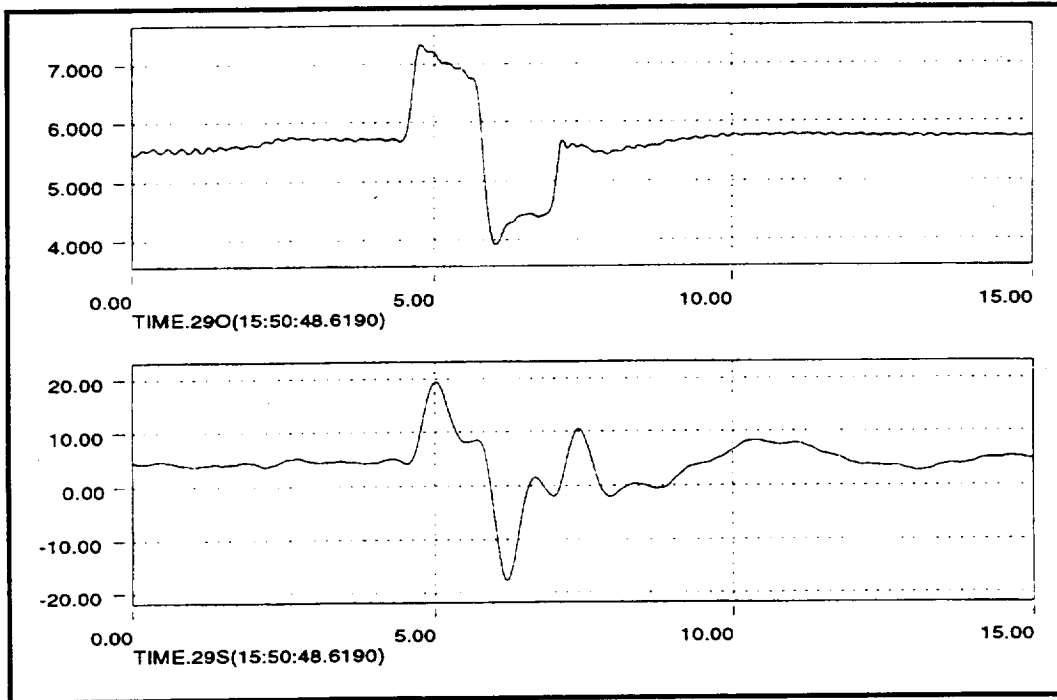


Figure 3.3. Sample roll doublet input and roll response time histories. Upper plot—lateral stick deflection ( $\delta_{Lat}$ ) in inches. Lower plot—roll rate ( $p$ ) in deg/sec.

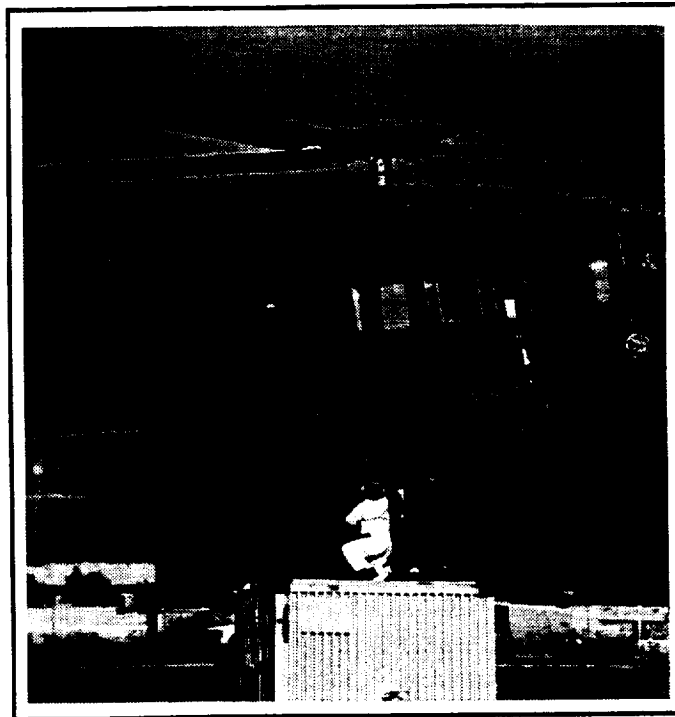


Figure 3.4. CONEX hook-up in progress.

It should be noted, that although pilot comments were welcomed and desired, no formal methodology was established to obtain qualitative analysis of the flights, such as in a Cooper-Harper rating. Pilot comments were simply used to adjust the test plan as appropriate to the flight conditions experienced.

### C. DATA ACQUISITION

Extensive effort was put forth to ensure high quality data was available for both the near real time and post flight analysis. Figure 3.5 illustrates all the major components involved in the process.

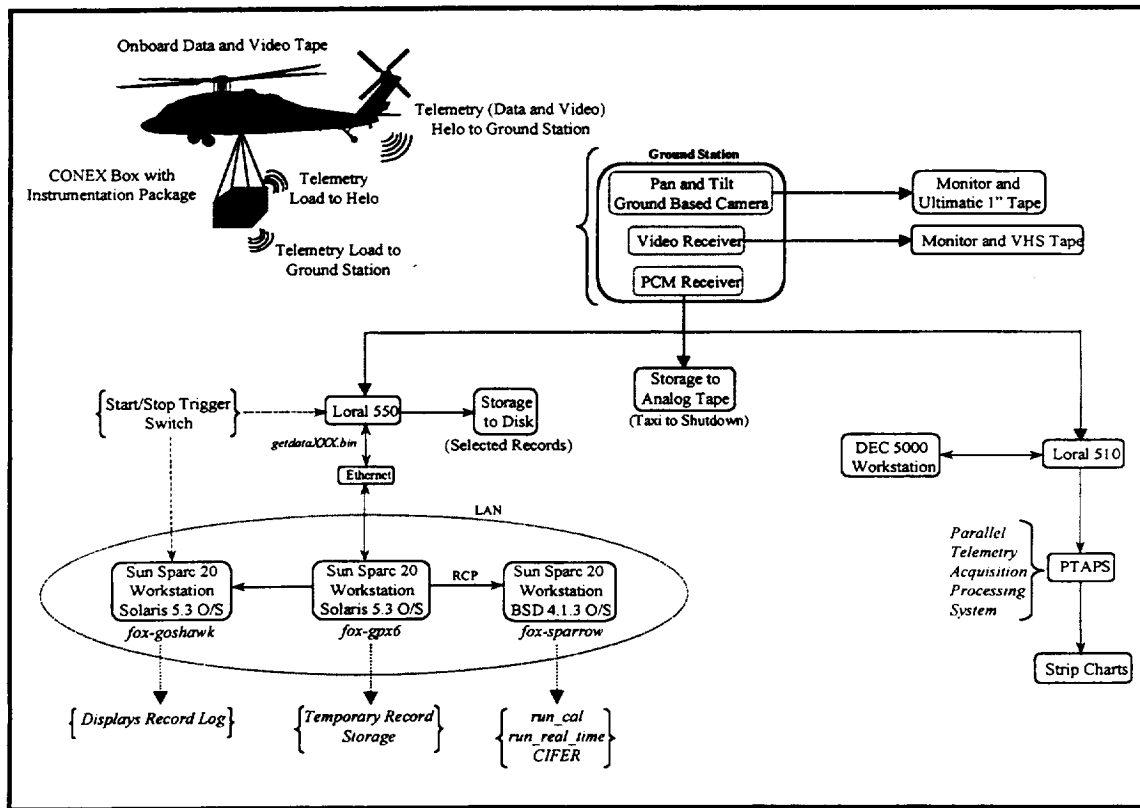


Figure 3.5. Schematic of MOA Task 8 data acquisition process.

Data signals were generated by the helicopter ADAS instrumentation and the load instrumentation package. ADAS signals were wired directly to an onboard data tape recorder and transmitted in a pulse code modulation (PCM) stream to the ground station. The load data telemetry signal was received and recorded both onboard the helicopter and at the ground station. The two data streams were recorded on separate tracks of the onboard tape. This tape was utilized as the primary data source for post flight analysis. The video signal from the “hell hole” camera was recorded directly onboard the helicopter in VHS format. Additionally, it was transmitted to the ground station.

At the ground station (fig. 3.6), the helicopter video signal was patched to monitors in the control room and to a VHS recorder. Additional video coverage came from the “pan and tilt” camera located on the antenna tower at the test facility. This camera provided an excellent method of observing the test while the helicopter was at the field.

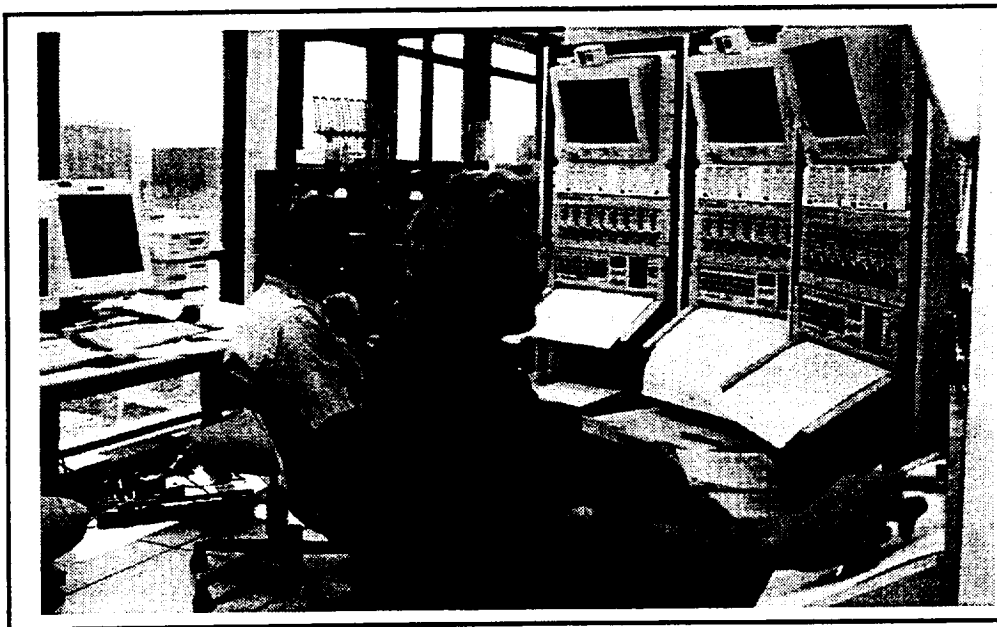


Figure 3.6. Ground station control room. Shown (L to R) are Mark Tischler and Luigi Cicolani, U.S. Army/NASA Rotorcraft Division, Ames Research Center, monitoring real time strip charts during a test flight for MOA Task 8. CIFER<sup>®</sup> was run on “fox-sparrow” located behind Mark Tischler.

Once received at the ground station, the data signals travel three distinct routes (see fig. 3.5). First, the raw PCM stream was recorded on an analog tape. This recording was continuous from initial taxi to final shutdown. Second, the data was processed through the Loral 510 System and the parallel telemetry acquisition processing system (PTAPS) finally coming out at the strip charts. These were observed in real time. The final data path lead to the near real time analysis.

By using a trigger switch, one of the flight test engineers started and stopped the recording of data for each maneuver. Each cycle of the switch created a permanent backup record, which was stored to disk, and a temporary record, which was stored on “fox-gpx6”, a Sun Workstation. When the engineer running the near real time analysis in the control room was ready, the file was then transferred via remote copy protocol (RCP) to “fox-sparrow,” the workstation on which CIFER<sup>®</sup> was installed. It was during this process that the signals were converted from counts to engineering units, decimated to a sample rate of 50 Hz, and scaled (see table 2.4). The load angular rate coordinate transformation was also applied (see Section IV.D) at this time. Once this manipulation was complete, the record was ready to be processed through CIFER<sup>®</sup>. Further details of this process are discussed in Section IV and Appendix E.

## IV. DATA ANALYSIS

The goals of the analysis of the flight test data were threefold. First, the handling qualities, bandwidth frequency and phase delay, were determined from the on-axis closed loop responses of the helicopter,  $p/\delta_{LAT}$  and  $q/\delta_{LON}$  as represented in figure 4.1. These rate responses were then integrated to produce the roll and pitch attitude responses. The second analysis objective was to obtain values for the phase and gain margins of the control system for stability analysis. These were calculated from the control system feedback loop. Third, characterization of the load motion was accomplished by analysis of the damping and natural frequency of the load pendulum modes. These parameters were obtained from the response of the transformed load angular rates to control input,  $p_2'/\delta_{LAT}$  and  $q_2'/\delta_{LON}$  (fig. 4.1). The analysis tools employed and the details of the analysis methodology are described in this section.

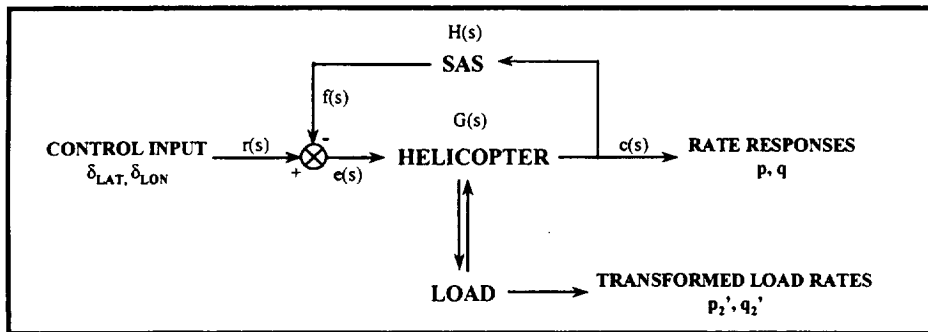


Figure 4.1. Simplified model of the helicopter and slung load system.

### A. ANALYSIS TOOLS

#### 1. CIFER<sup>®</sup>

The analysis of the flight test data was accomplished employing the Comprehensive Identification from Frequency Responses (CIFER<sup>®</sup>) integrated software package developed by Dr. Mark Tischler, U.S. Army / NASA Rotorcraft Division, Ames Research Center. CIFER<sup>®</sup> has been developed and exercised over the past ten years on numerous flight test and simulation projects including the BO-105, AH-64, and UH-60 helicopters and the XV-15, V-22, and AV-8B fixed wing aircraft. Over 20 U.S. research/industry organizations currently utilize the CIFER<sup>®</sup> software. CIFER<sup>®</sup> allows frequency domain analysis of time history test data through an interactive framework. It extracts a set of non-parametric input-to-output frequency responses without a-priori assumptions. The analysis applications of CIFER<sup>®</sup> include rapid identification of transfer function models, spectral signal analysis, handling qualities analysis, determination of crossover characteristics, and time and frequency domain comparisons of identification versus simulation model predictions. Also incorporated into the software are routines for response arithmetic and several methods of data presentation, including plotting. Figure 4.2 illustrates the basic components of the CIFER<sup>®</sup> software package. For the analysis performed here, only a few of the utilities were utilized (ref. 16).

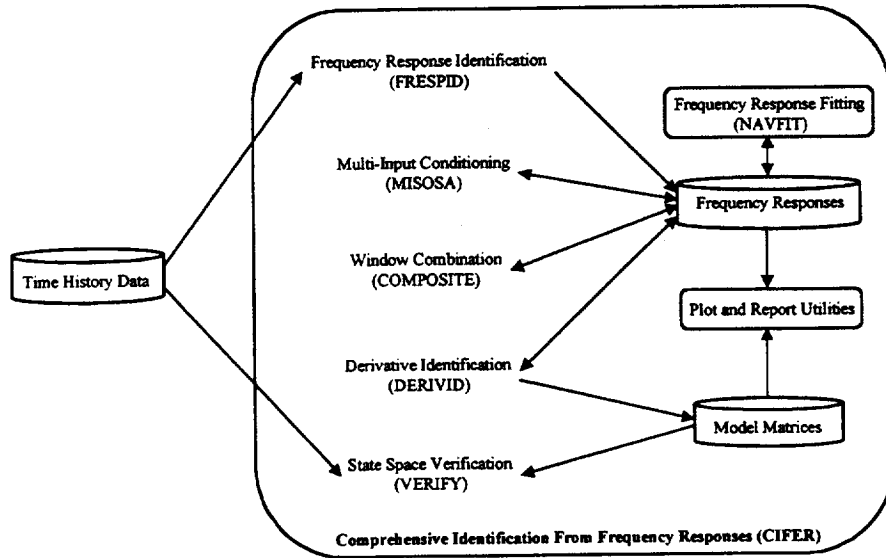


Figure 4.2. Major CIFER<sup>®</sup> utilities and data flow (from ref. 14).

To start, the frequency response for each axis and each set of input and output variables was calculated in FRESPID. FRESPID calculates the responses through a Chirp-Z Transform (CZT). The CZT is a flexible form of the Fast Fourier Transform (FFT), which does not require that the number of time history points and number of frequency points be equal. The CZT also allows the user to calculate the FFT over any frequency range. As with any FFT the input and output functions must be bounded, and by ensuring the frequency sweep starts and ends in trim, this condition was met. When possible multiple sweep records, performed at the same flight conditions, were concatenated in order to increase the number of averages, reducing the random error and thus increasing the coherence. This translates into a higher signal to noise ratio and improved calculated frequency response (ref. 14).

The coherence function is a numerical measure of the accuracy of the frequency response and was critical to the success of the identification. It is the “fraction of the output that is linearly related to the input power.” The value of the coherence is always less than one. This is due to three effects; 1) the non-linearity of the actual physical system, 2) the noise associated with the output, and 3) secondary inputs, including off-axis control inputs and external inputs such as gusts. A coherence of 0.6 or greater is considered acceptable (refs. 13 & 14).

Current analysis focused on the single input, single output (SISO) approach; meeting the primary objectives of the analysis by investigating only the on-axis responses of the aircraft and load to control deflection inputs. For each flight condition, three frequency responses were calculated; 1) the helicopter’s closed loop attitude response, 2) the broken loop response of the control system, and 3) for those flights with a load, the response of the load. For each of the three, up to five individual frequency responses were calculated in FRESPID based on selected windowing, one response for each size window. A window is simply a method of analyzing the signal time histories in blocks of time. The window is sequenced and overlapped across the entire sweep

record or concatenated records. A larger window improves the low-frequency identification but reduces the number of averages. This results in a poorer frequency response at high frequencies where averaging is needed to counter lower signal to noise ratios. Smaller windows, on the other hand, increase the number of averages, improving the high frequency response, but in turn, degrade the low-frequency identification. The COMPOSITE algorithm eliminates the need for the user to manually optimize window size selection. It produces a quality compromise between the responses calculated based on the chosen windows. For the near real-time analysis, only one window, sized to 20 seconds, was selected and therefore, COMPOSITE was not required to optimize the response. For the post flight analysis however, five windows, sized to 10, 20, 25, 30, and 40 seconds, were chosen and COMPOSITE was required in order to produce a single response. This response was then used for the stability and handling qualities analysis (ref. 14).

The load motion characteristics, damping and natural frequency, discussed in detail in Section IV.D, were determined by fitting a second order system to the load's frequency response. This was accomplished through the CIPHER<sup>®</sup> routine called NAVFIT. "NAVFIT determines the transfer-function coefficients based on a non-linear (Rosenbrock) least-squares minimization of the cost function" (ref. 14). The cost function is simply a mathematical measure of how well the model fits the data. A fit is considered good any time the 'cost' is less than 100. In most cases for this analysis, the cost was less than 40. The flexibility of the routine allows the user to 'fix' or 'free' specified coefficients, apply a time delay, select the transfer function order, and define the frequency range of interest. For this analysis, the coefficients and time delay were not fixed, a zero-over-second order transfer function was selected, and the frequency range was typically between 0.5 and 3 rad/sec.

Handling qualities and stability margins, discussed in further detail in Sections IV.B and C, were calculated from generated frequency responses by Utility #8. Plots were generated within each routine, as well as by using general plotting functions of Utility #19. All generated frequency responses were automatically organized and stored in a database, which CIPHER<sup>®</sup> created and managed.

## **2. Derived and Smoothed Variables Code**

For the post flight analysis, a set of programs were created by Mr. Luigi Cicolani, U.S. Army/ NASA Rotorcraft Division, Ames Research Center. Among the many functions these routines performed were the application of the necessary scaling of control signals (see table 2.4) and the coordinate transformations of the load angular rates (see Section IV.D). Although not required for this analysis some of the additional calculations included; application of instrumentation correction for airspeed and altitude, calculation of the calibrated, equivalent and true airspeeds, correction of the inertial accelerations due to sensor location and changes in center of gravity, smoothing of angular rate and linear acceleration signals by applying a 2.5 Hz cutoff frequency, and the derivation of the angular acceleration from the angular rate signals. A complete list of the derived and smoothed signals for the helicopter and the load is contained in table A.2 and table A.3, respectively.

### 3. GetData

GetData, Version 3.2.5, developed at NASA Dryden Flight Test Facility, is a Fortran utility program for manipulating time history data (ref. 17). This utility was used to extract specific sensor signals from the flight test data files. These signals were then modified or used to calculate other parameters necessary for analysis. GetData's ability to manipulate and merge signal time histories and work with the compressed UNC3 data format was extensively used in this project, in particular in the derived and smoothed signal programs.

### 4. XPlot

XPlot, Version 3.06, developed at NASA Dryden Flight Test Facility is an XY plotting package designed to plot out time history and frequency response data (ref. 18). It was extensively utilized post-flight, to plot and scrutinize the flight data. The utility allows the user to "zoom" in and out as necessary to get a detailed look at the form and consistency of the data. XPlot also provides a means of performing simple math functions on individual or multiple time histories.

### 5. Microsoft EXCEL®

EXCEL® was utilized as common software for the development of databases to track each test flight, the real time and post-flight analysis results, and the CIFER® case-name catalog. Due to its commonality across both Macintosh and Windows operating systems, it provided a convenient tool for this purpose.

## B. HELICOPTER HANDLING QUALITIES

The bandwidth frequency ( $\omega_{BW}$ ) and phase delay ( $\tau_p$ ) parameters were computed from the closed-loop frequency responses of the helicopter,  $p/\delta_{LAT}$  and  $q/\delta_{LON}$  (fig. 4.1). These two parameters together provide a quantitative measure of the handling qualities of an aircraft. The Aeronautical Design Standard (ADS)-33D-PRF (ref. 19) is the current standard with regards to handling qualities. However, it does not adequately address cargo/utility helicopters, and more specifically, handling qualities for slung load operations. A separate program is currently in progress to expand the coverage of this specification to include cargo/utility helicopters with and without slung loads (ref. 20).

### 1. Bandwidth Frequency and Phase Delay

Bandwidth frequency is an indicator of how well an aircraft will track control inputs (ref. 21). The larger the bandwidth the more agile the aircraft, where as, a lower bandwidth results in a slower, smoother response. For rate responses, the bandwidth is the lesser of the gain and phase bandwidth frequencies, which are defined in figure 4.3. The bandwidth frequency assures at least 6 dB of gain margin and 45 degrees of phase margin from the neutral stability frequency.

Phase delay is a measure of the slope of the phase plot between the 180-degree frequency ( $\omega_{180}$ ) and twice the 180-degree frequency ( $2\omega_{180}$ ), usually determined by a linear least squares fit (ref. 19). A small phase delay, shallow slope, means that minor control deflections near the

180-degree frequency will not produce a significant phase change. This can be translated into good response predictability. As the phase delay becomes larger, small control disturbances result in major changes in the phase, and therefore, a less predictable response. Aircraft with large phase delays are more prone to pilot induced oscillations (PIO) (ref. 13). Although the expression for the phase delay seems to establish a well-defined criterion, in actuality the linear assumption made is not always valid in this area of the phase plot. In addition, the slope of the phase curve often changes dramatically within the range of  $\omega_{180}$  and  $2\omega_{180}$ . Compounding these concerns is the fact that the data at  $2\omega_{180}$  is often unreliable based on the poor coherence of the response. One possible reason for the poor coherence is the fact that since the objective of the test is to identify the frequency response, accurate knowledge of  $2\omega_{180}$  is not available prior to the flight. Therefore, the sweep range may not adequately cover this frequency. The definition of the phase delay is shown on figure 4.3.

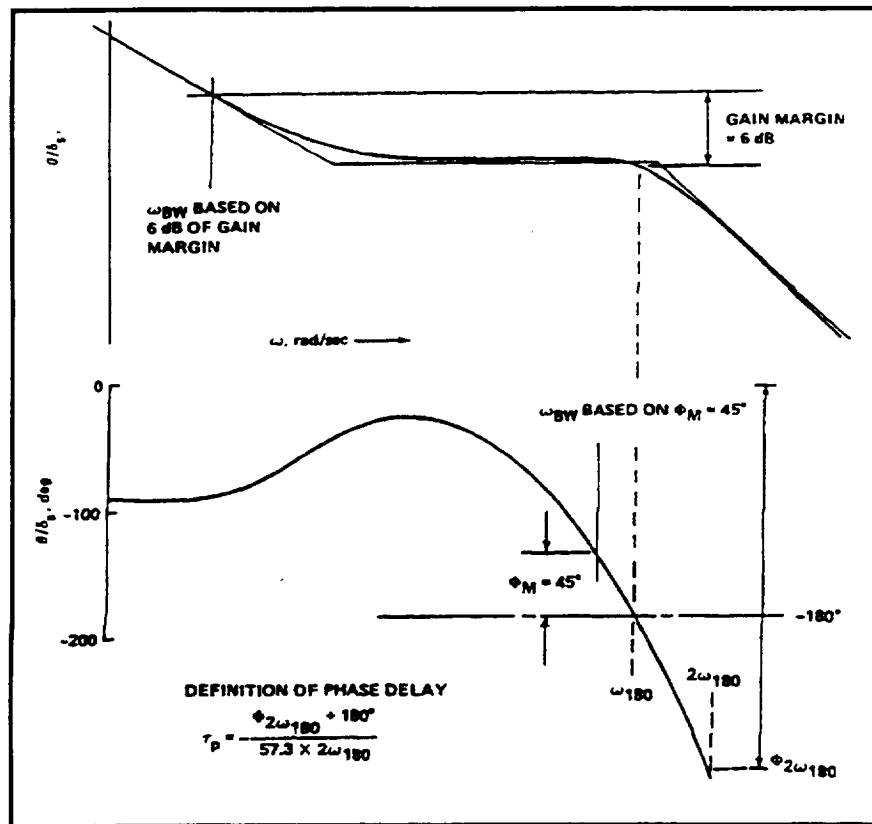


Figure 4.3. Bandwidth frequency and phase delay definitions (from ref. 13).

## 2. Determination of Bandwidth Frequency and Phase Delay.

As mentioned earlier, the  $\omega_{BW}$  and  $\tau_p$  were determined from the closed loop response of the helicopter; roll to lateral stick deflection ( $\phi/\delta_{Lat}$ ) and pitch to longitudinal stick deflection ( $\theta/\delta_{Lon}$ ). Initially, the closed loop frequency responses were calculated in FRESPID using the aircraft's angular rates ( $p$  and  $q$ ) rather than the attitudes ( $\phi$  and  $\theta$ ) because the rate variables possess greater mid and high frequency content. The responses were then integrated by applying a  $1/s$

conversion through CIPHER<sup>®</sup>'s Utility #8. This choice is better suited for the determination of the bandwidth and delay (ref. 22). The bandwidth and phase delay values were calculated by applying the definitions described above to the attitude response. In particular, for this analysis, phase delay was calculated by a linear, least squares fit to the phase curve around  $\omega_{180}$ , as shown in figure 4.4. This particular case is a lateral sweep in a hover with the 4K CONEX. Note the poor coherence near  $2\omega_{180}$  and the significant change in slope between  $\omega_{180}$  and  $2\omega_{180}$ .

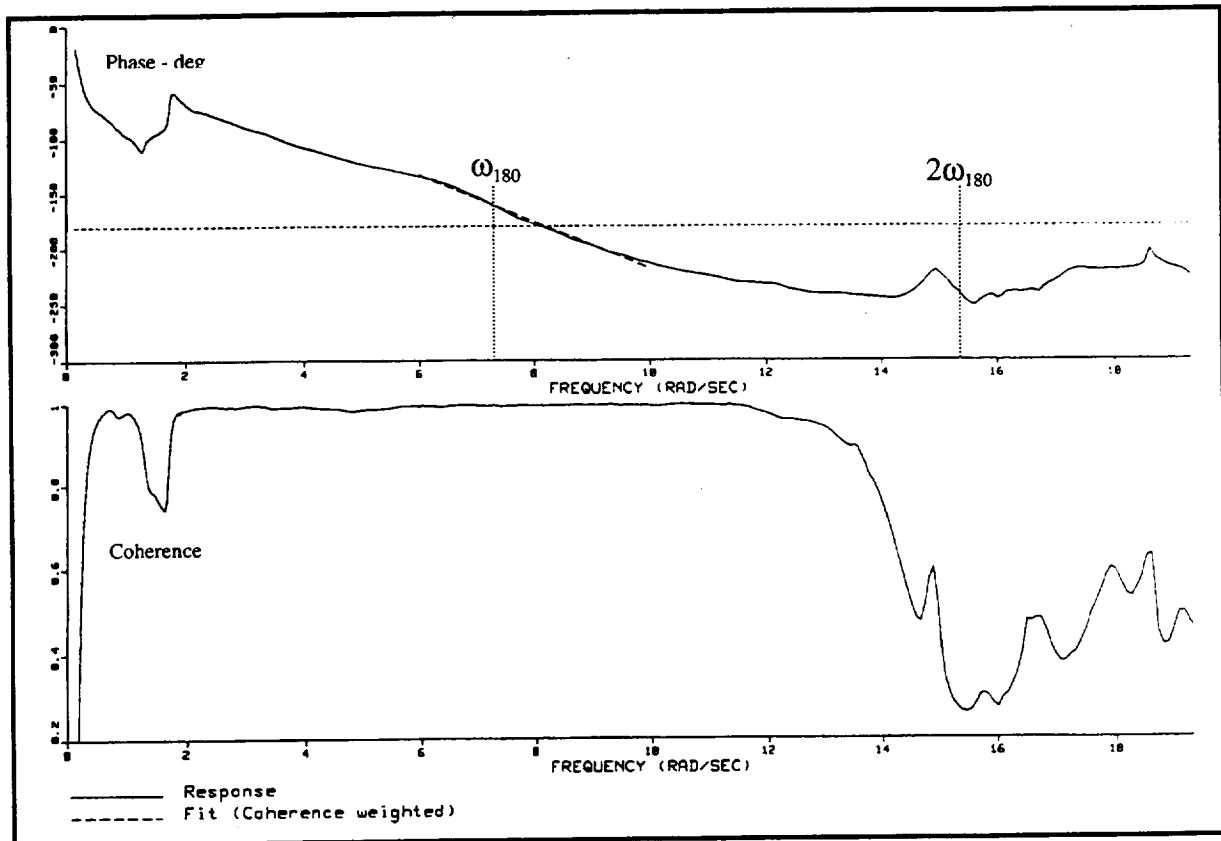


Figure 4.4. Sample calculation of phase delay.

## C. CONTROL SYSTEM STABILITY MARGINS

### 1. Gain Margin and Phase Margin

Gain margin is the reciprocal of the magnitude,  $|G(j\omega)|$ , of the open loop response at the frequency where the phase angle is equal to  $-180^\circ$  ( $\omega_{180}$ ) (ref. 21). In the physical sense it is “the amount by which the pilot can change his gain without threatening the stability” of the aircraft (ref. 13). For a system to be stable, the gain margin must be positive.

Phase margin is the “amount of additional phase lag at the gain crossover frequency required to bring the system to the verge of instability. The gain crossover frequency ( $\omega_c$ ) is the frequency at which the magnitude of the open loop transfer function,  $|G(j\omega)|$ , is unity.” In decibels, this corresponds to when the magnitude curve crosses 0 dB. The phase margin is  $180^\circ$  plus the phase

angle of the open loop response at the gain crossover frequency. A positive phase margin indicates a stable system (ref. 21).

For satisfactory performance, it is desired that the gain margin be greater than 6 dB and the phase margin be greater than  $45^\circ$ . A 6 dB gain margin is a factor of two and the  $45^\circ$  phase margin corresponds to a phase shift of  $-135^\circ$ .

## 2. Determination of Gain and Phase Margins

The identification of the control system broken loop response and subsequent determination of the stability margins are obtained by analyzing the output of the stability augmentation system (SAS) with respect to the mixer input. Referring to figure 4.5, the broken loop response is defined as  $f(s)/e(s)$ . An alternative, indirect method to determine  $f(s)/e(s)$  is by calculating the error response, mixer input to the control boost output,  $e(s)/r(s)$ , and applying basic control system block diagram algebra to determine the broken loop response. Comparative analysis from the first test flights showed a good agreement between these two methods. In general, however, the error response method had better coherence and therefore, it was adopted for the remainder of the analysis.

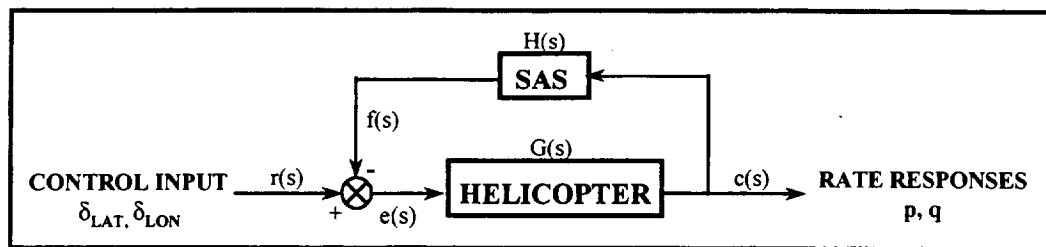


Figure 4.5. Simplified model of the helicopter.

The desired open-loop transfer function is

$$\frac{f(s)}{e(s)} = G(s)H(s) \quad (\text{Equation 4.1})$$

and

$$e(s) = r(s) - f(s) \quad (\text{Equation 4.2})$$

Substituting equation 4.1 into equation 4.2, eliminating  $f(s)$  gives

$$e(s) = r(s) - e(s)G(s)H(s) \quad (\text{Equation 4.3})$$

Rearranging terms

$$\frac{e(s)}{r(s)} = \frac{1}{1 + G(s)H(s)} \quad \text{(Equation 4.4)}$$

Recalling equation 4.1 and substituting into equation 4.4, the result is

$$\frac{f(s)}{e(s)} = \left( \frac{e(s)}{r(s)} \right)^{-1} - 1 \quad \text{(Equation 4.5)}$$

Applying equation 4.5 to the error response was done through the frequency response arithmetic routine, Utility #9 of CIPHER<sup>®</sup>. The phase and gain margins were calculated using the CIPHER<sup>®</sup> Utility #8. Due to the complexity of the system, multiple crossover frequencies often occurred. In these cases, the critical crossover frequency was determined by selecting the crossover frequency associated with the minimum margin, which occurred within the frequency range of interest, 0.05 to 2.0 Hz (0.3 to 12.6 rad/sec). Figure 4.6 is an example of the typical broken loop response magnitude and phase plots used for the determination of the margins. This particular case was for a lateral sweep in a hover with the 4K CONEX.

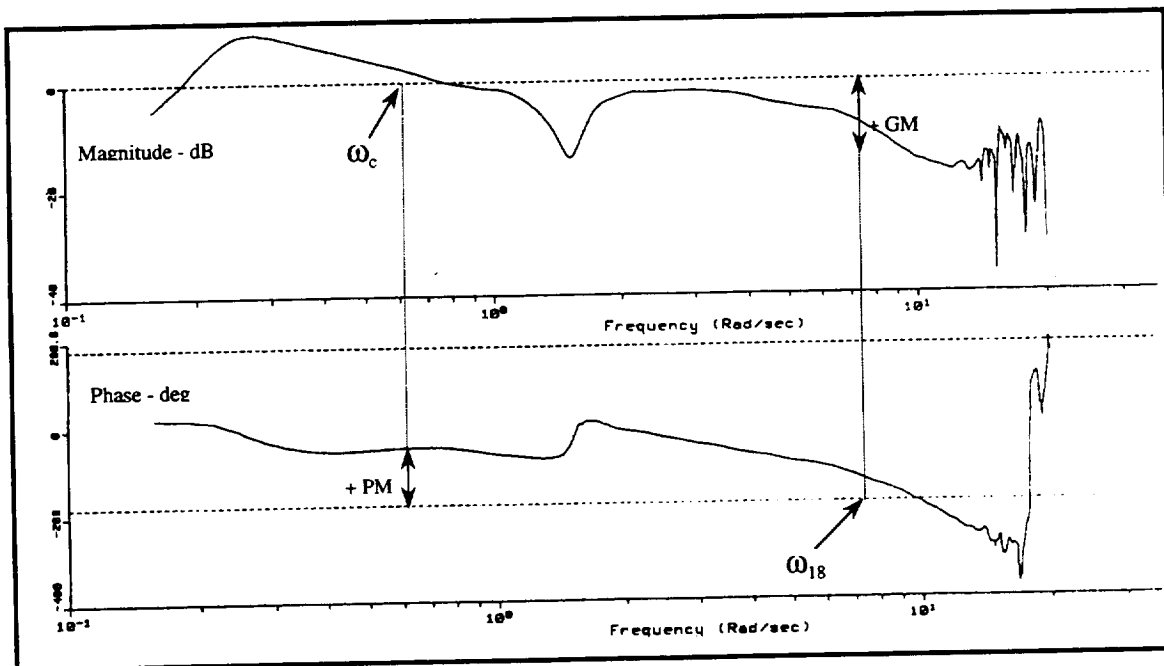


Figure 4.6. Determination of phase and gain margins.

## D. LOAD MOTION ANALYSIS

The helicopter-load configuration with an elastic sling (fig. 4.7) is a two-body system with twelve rigid body degrees of freedom and corresponding natural modes. The new modes due to the load and sling consist of two oscillatory pendulum modes (lateral and longitudinal), two load yaw modes, and three oscillatory stretching modes (one vertical and two load attitude modes) (ref. 23). The modes of particular interest here are the two pendulum modes. One of the complications encountered in the analysis of the pendulum modes is the need to transform or refer the load angular velocity to the helicopter heading.

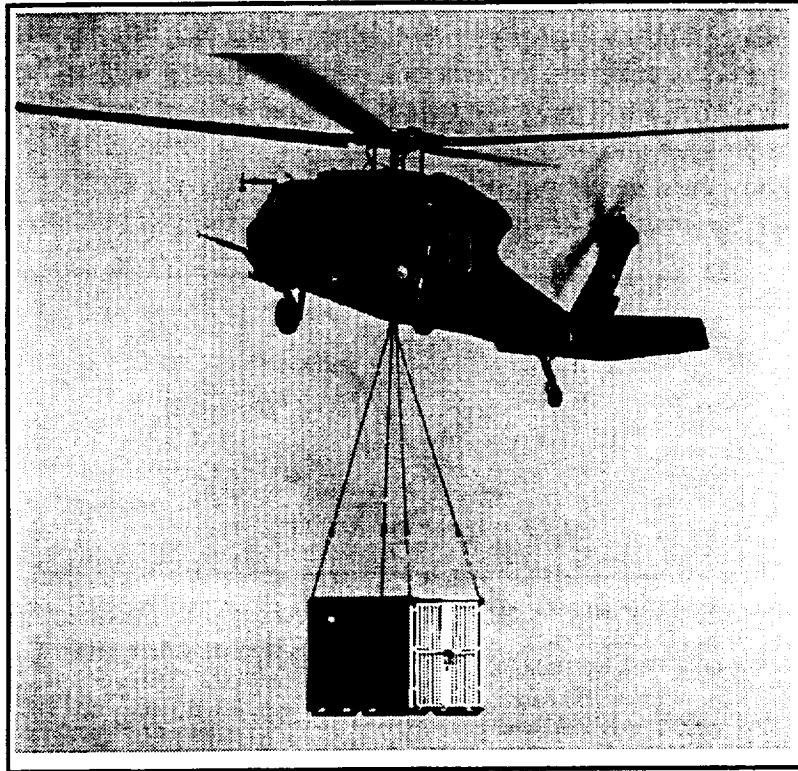


Figure 4.7. NASA 748 with CONEX external load.

### 1. Predicting Pendulum Mode Characteristics

Pendulum frequencies are dependent on sling length and load-helicopter weight ratio. Equation 4.6 gives an analytical estimate of the frequencies for both pendulum modes based on a point-mass dumbbell model. The variables of the equation are:  $g$  – gravitational acceleration,  $l$  – distance

$$\omega_p = \sqrt{\frac{g}{l} \left( 1 + \frac{m_2}{m_1} \right)} \quad (\text{Equation 4.6})$$

between load and helicopter,  $m_1$  – helicopter mass, and  $m_2$  – load mass (ref. 23). The estimated natural frequencies are 1.05, 1.58, 1.50, and 1.61 rad/sec for the 1K block, 4K block, 2K CONEX and 4K CONEX, respectively.

Pendulum damping depends on the coupling with the helicopter attitude. This, in turn, requires hook offset from the helicopter center-of-gravity (CG) and varies inversely with helicopter inertia. Linear analysis by Cicolani (ref. 23) estimates the damping of the longitudinal mode to be 5% while the lateral mode estimate was significantly higher at 38%.

## 2. Determination of Pendular Motion from Flight Measurements

*a. Load Axis to Helicopter Axis Transformation Approximation.* The analysis of the load response was facilitated by referring the measured load pitch and roll rates to the helicopter heading as shown in figure 4.8. The key to this transformation was the knowledge of the relative yaw angle between the load and the aircraft. The new axes,  $x_2'$  and  $y_2'$ , are in the horizontal plane of the load body axes. Assuming small roll ( $\phi_2$ ) and pitch ( $\theta_2$ ) angles then  $x_2'$  is nearly that direction in the load horizontal plan which has the current helicopter heading.

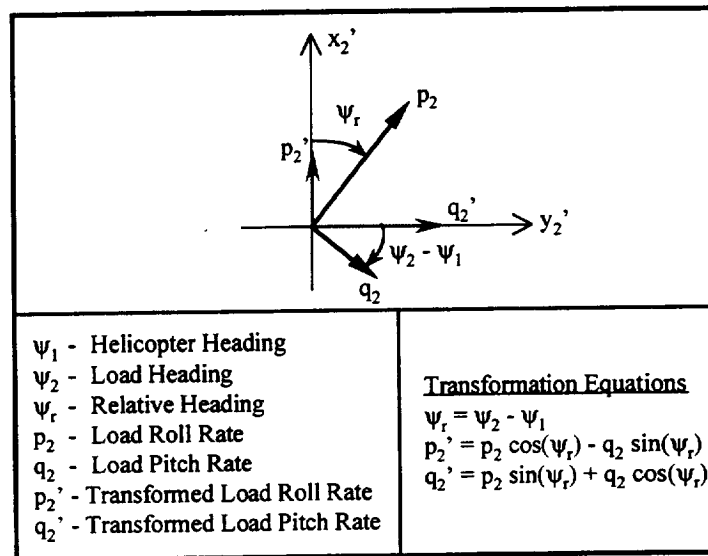


Figure 4.8. Load axis to helicopter axis coordinate transformation.

*b. Determination of the Pendulum Mode Damping and Natural Frequency.* The pendulum mode characteristics were obtained from the test data by assuming that within a small frequency range near the load's natural frequency the load's response can be represented by a second order system (equation 4.7). Even though the overall response is obviously one of a higher order

$$G(s) = \frac{k}{s^2 + 2\zeta\omega_n^2 + \omega_n} \quad (\text{Equation 4.7})$$

system, the load's pendulum motion is dominant in this frequency range. By making this simplifying assumption, the analysis focuses on two well-understood parameters, the damping ( $\zeta$ ) and the undamped natural frequency ( $\omega_n$ ).

Utilizing the NAVFIT function in CIPHER®, a second order fit was applied to the load's response,  $p_2'/\delta_{Lat}$  and  $q_2'/\delta_{Lon}$ . This process required a bit of trial and error in selecting a minimum and maximum frequency for the fit in order to get the cost function below 100. The damping and natural frequency were given as part of the output from NAVFIT. Figure 4.9 shows an example of NAVFIT output. This particular case was for a lateral sweep in hover with the 4K CONEX.

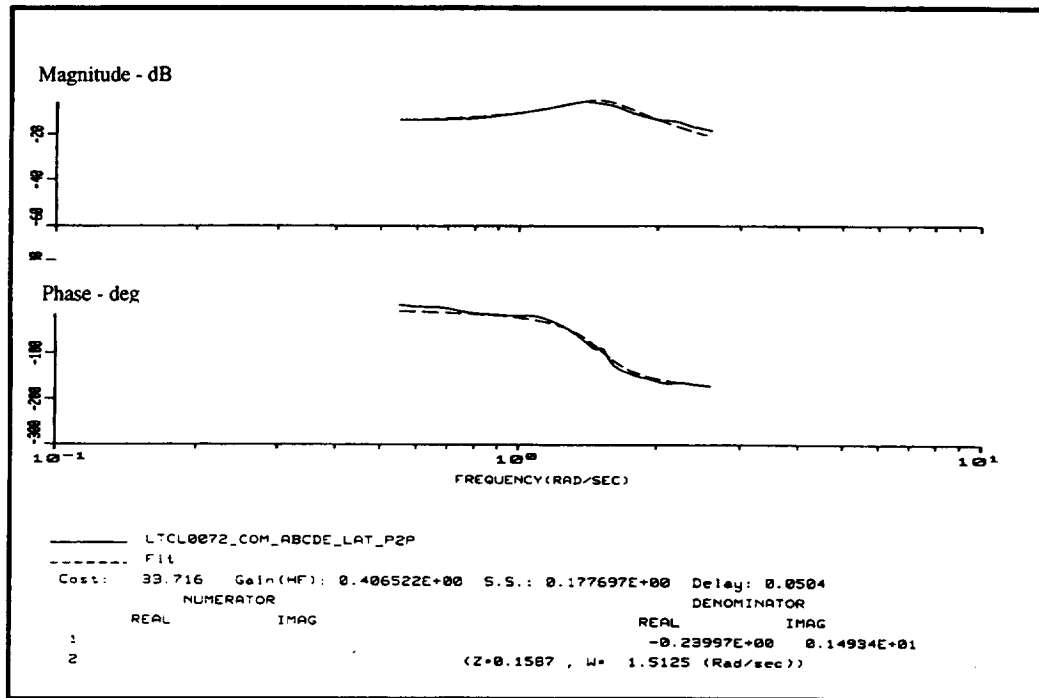


Figure 4.9. Example of second order fit to the load response.

## E. NEAR REAL TIME ANALYSIS VERSUS POST FLIGHT ANALYSIS

The basic principles and procedures described above and in earlier sections generally apply to both the real time analysis and the post flight analysis except as noted here. In order for the real time analysis to be useful, it must be completed in a short time and provide reasonably accurate results.

As with any time the source of data is from telemetry, data dropouts occasionally occur. The CIPHER® analysis generally proved insensitive to minor dropouts and data spikes since these appear as high frequency noise, outside the frequency range of interest. However, continuous periods of excessive data dropouts are incompatible, requiring that that particular record be removed from the analysis. Recall that "garbage in is garbage out." Eliminating sweep records, meant fewer possible concatenations and therefore less averages, hampering the ability to reduce

the random errors. Data dropouts were rarely a problem with the onboard data tape; therefore, it was used as the source for the time histories during post flight analysis. A significant timesaving was achieved by reducing the sample rate from the post flight processing rate of 100 Hz to 50 Hz for the real time processing.

As noted earlier in this section, only a single window, sized at 20-seconds, was used during the real time response identification. This had a two-fold effect in reducing the total processing time. First, with only one window, FRESPID had to calculate only one response for each case; helicopter closed loop response, broken loop response, and load response. Second, without multiple windows there was no need to run the COMPOSITE routine. In contrast, the post flight analysis, utilized five windows and COMPOSITE to generate an optimized response.

A comparative study was conducted between the analysis performed real time and the post flight analysis. It was determined that the effect of data dropouts, lower data sample rate, and single window on the near real time analysis results was minimal. Listed in table 4.1 is a sample set of results comparing the real time analysis to the post flight analysis. Differences do exist, as one would expect, however, they are relatively small. Overall, the comparison is good and it validates the real time processing procedure.

Table 4.1. Comparison of near real time results versus post flight results.

Flt	Maneuver	Analysis	$\omega_{BW}$	$\tau_p$	PM	$\omega_c$	GM	$\omega_{180}$	$\zeta$	$\omega_n$
170	Hover, Lon Sweep, No Load	Real Time	2.67	0.19	82.15	2.23	36.88	8.09		
		Post Flight	2.24	0.19	87.41	2.00	22.45	6.5		
170	30 kts, Lon Sweep, No Load	Real Time	2.50	0.18	110.76	1.88	17.27	6.73		
		Post Flight	2.38	0.15	110.50	1.71	20.29	6.38		
170	30 kts, Lon Sweep, 4K CONEX	Real Time	3.17	0.20	91.08	2.76	19.93	7.18	0.19	1.47
		Post Flight	3.06	0.20	106.60	2.20	20.38	7.02	0.11	1.42
172	Hover, Lat Sweep, 4K CONEX	Real Time	2.68	0.18	126.30	0.82	15.39	9.95	0.19	1.60
		Post Flight	2.86	0.19	125.69	0.79	13.82	9.81	0.16	1.58
172	30 kts, Lat Sweep, 4K CONEX	Real Time	4.16	0.16	121.89	0.79	13.84	9.75	0.21	1.48
		Post Flight	3.90	0.19	118.69	0.82	14.32	9.97	0.20	1.35

## V. RESULTS

The following paragraphs summarize the data obtained during the flight test program that pertains to the aircraft handling qualities, control system stability margins, and the suspended load motion. A significant amount of data beyond that required to investigate these areas exists and is available for future work. A summary of the airspeed at which each load was flown is given in table 5.1. Except in the load pendulum motion plots, data for the no load baseline, 1K block, 4K block, 2K CONEX, and 4K CONEX is presented. Since only the CONEX was flown with the load instrumentation package, only those cases are presented in the plots of load damping and natural frequency. A complete listing of all resultant quantities is available in Appendix F. All data presented was determined based on a SISO response, using five windows (10, 20, 25, 30, and 40 secs) and concatenating all available sweep records of the same maneuver, which were of sufficient quality.

Table 5.1. List of airspeeds at which each load was flown.

Load	Airspeed
No Load	Hover, 30, 50 and 80 kts
1K Block	Hover and 80 kts
4K Block	Hover and 80 kts
2K CONEX	Hover
4K CONEX	Hover, 30, 50, 60 and 70 kts

### A. HELICOPTER HANDLING QUALITIES

Figure 5.1 shows the effect changing airspeed has on the bandwidth frequency and phase delay for the various loads. The pitch bandwidth was generally less than the roll bandwidth. Comparing the no load case with the 4K CONEX in pitch, there is an appreciable increase in bandwidth for the loaded aircraft. Whereas, comparing the same cases in roll shows some loss due to changes in the load configuration. The phase delay, for the 4K CONEX case in both axes, remained fairly constant between 0.15 and 0.20 seconds, but was higher than the no load case, indicating a slight degradation of the response to control inputs. Continuation of this trend could lead to possible PIO as pilot workload increases.

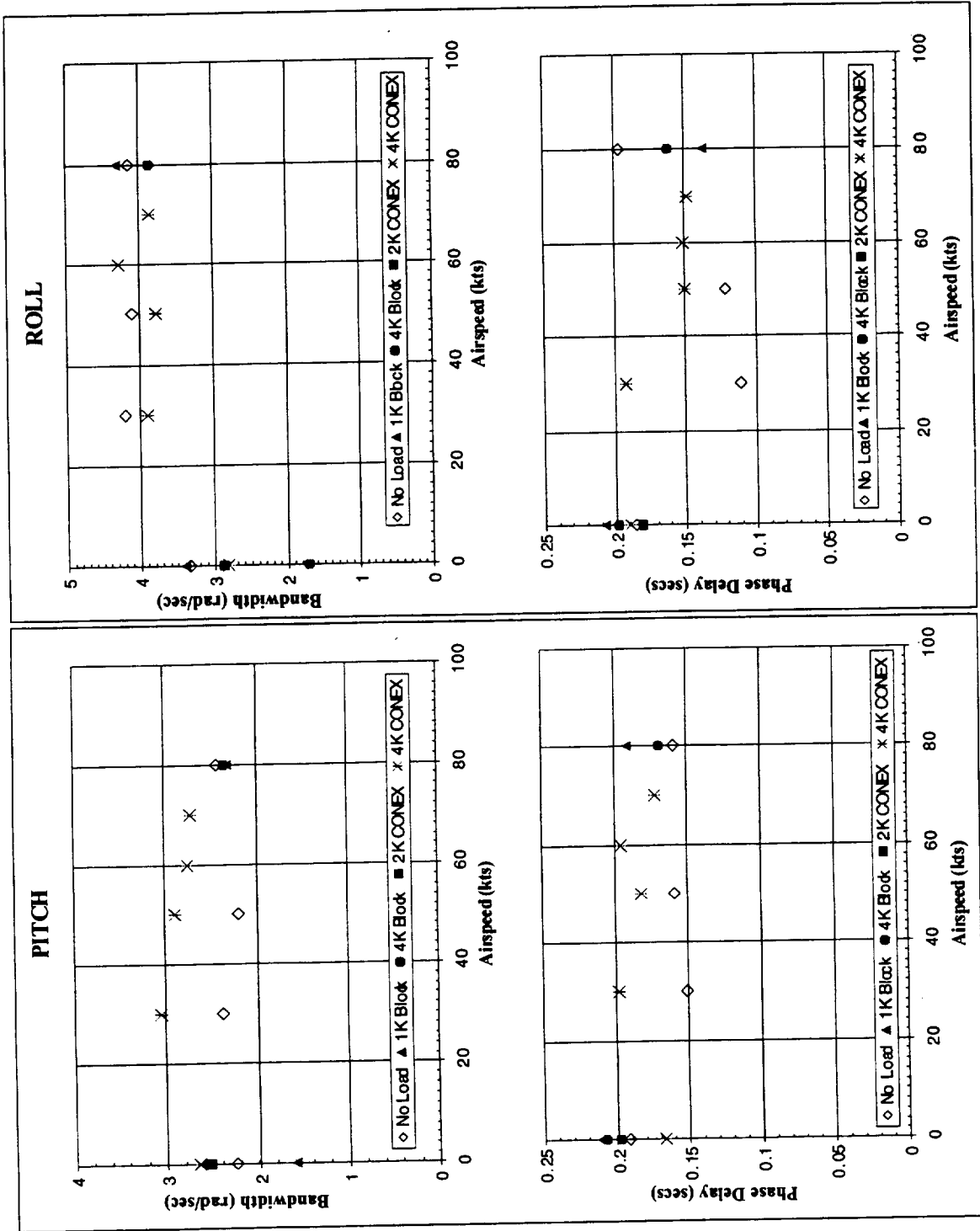


Figure 5.1. Handling qualities as a function of airspeed.

As mentioned in Section IV.B, ADS-33D does not fully address utility/cargo helicopters and external load operations. However, since work is currently being performed in an attempt to extend the specification to this class of helicopters and operations, the handling qualities determined from these flight tests were plotted in the specification format. Figures 5.2 through 5.5 show the results plotted against the requirement for “all other MTEs (mission task elements) and a UCE (usable cue environment) greater than one and/or divided attention operations.” This requirement is the same for hover, low speed and forward flight and is the most restrictive of all the specifications associated with the “all other MTE” category (ref. 19). The actual flight conditions of the test flights would likely have been rated as a UCE of one and the operations classified as fully attended. The frequency sweep maneuver, however, is not an ADS-33D testing requirement. Therefore, this MTE and UCE requirement was chosen as a representative, conservative case. For comparison, the no load baseline case is shown in each plot.

For the 4K CONEX, 2K CONEX and the 4K Block, figures 5.2, 5.3 and 5.4, it is noted that in pitch the addition of the load actually improves the response of the helicopter. There is an increase in both the bandwidth and the phase delay that drives the response further into the Level 1 region for all airspeeds. In roll, however, it is noted that the response is actually degraded somewhat. In particular, there is a significant decrease in the hover bandwidth, driving that case toward the Level 1/Level 2 boundary. The loss of bandwidth is so significant for the 4K Block case, figure 5.4, that the response does enter the Level 2 region. This demonstrates that for these configurations the roll response is more critical than pitch in regards to handling qualities.

This trend does not hold for the 1K Block case, figure 5.5. Here, in pitch, the bandwidth is decreased and the phase delay is increased by the addition of the load. This combined effect is to drive the response from Level 1 to Level 2. At hover, the response is degraded to a point well within Level 2. In roll, there is no significant change in response; only a slight increase in phase delay with little change in the bandwidth.

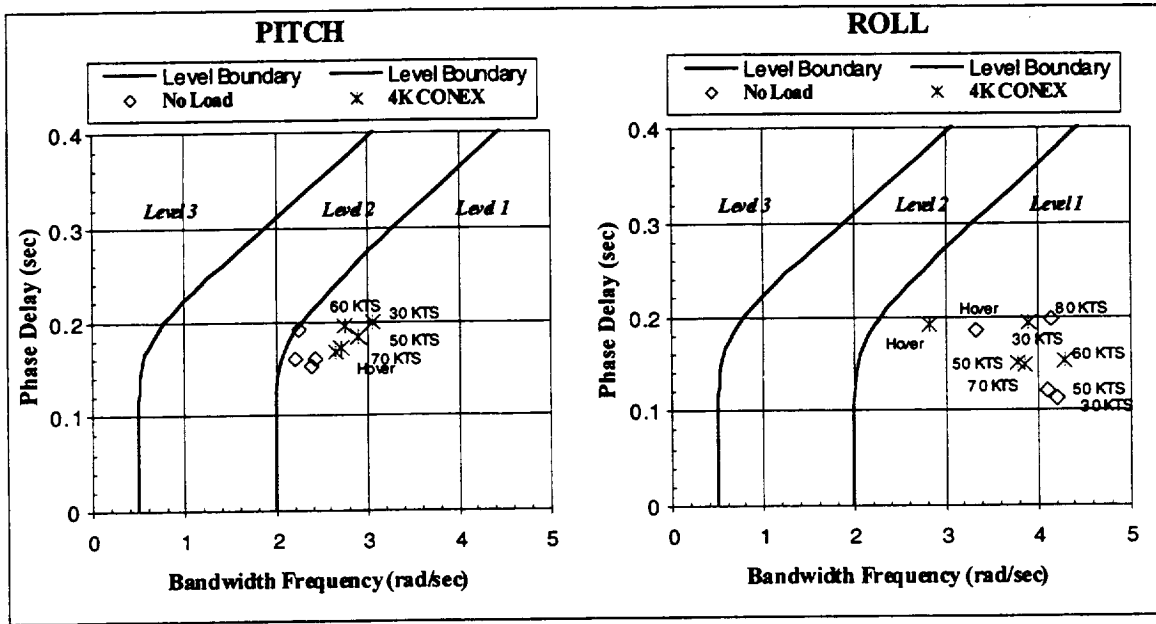


Figure 5.2. ADS-33D handling qualities specification - 4K CONEX and no load.

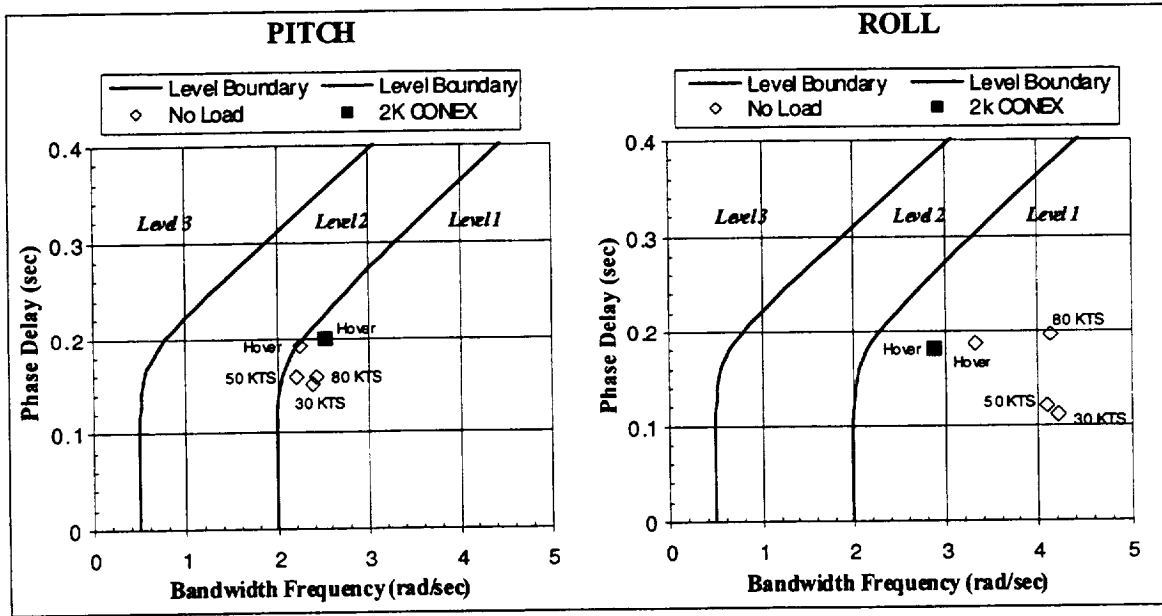


Figure 5.3. ADS-33D handling qualities specification - 2K CONEX and no load.

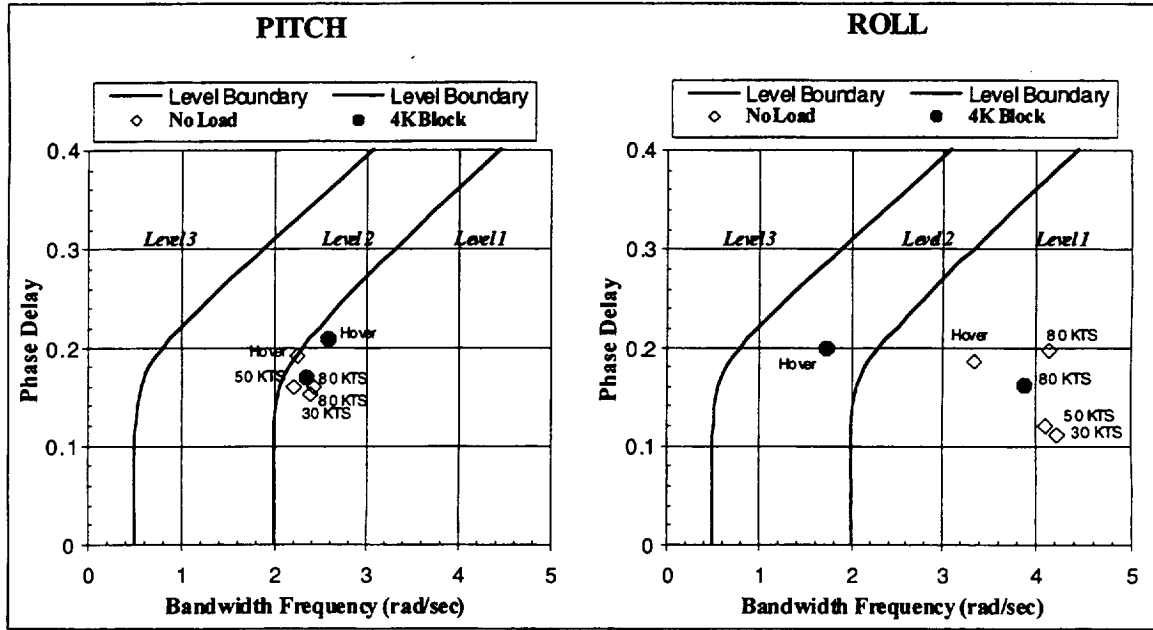


Figure 5.4. ADS-33D handling qualities specification - 4K Block and no load.

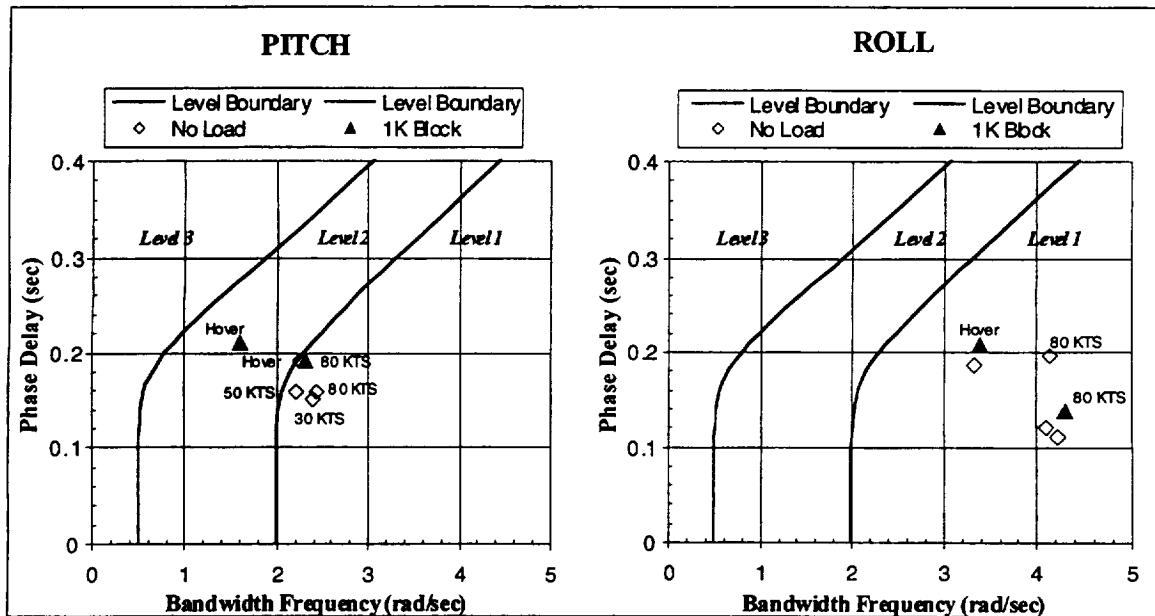


Figure 5.5. ADS-33D handling qualities specification - 1K Block and no load.

The difference in the trends may be due to the differences in the load and sling geometry. Figure 5.6 depicts, to scale, the three configurations. Recall, internal ballast was used with the CONEX to increase its weight from 2K to 4K, and the 1K Block was slung using a different bridle

assembly. From this drawing, many differences can be seen, in particular the wetted area of the loads and the distance between the load and the helicopter. The area differences will effect the aerodynamic drag and downwash effects experienced by the load. The sling length, discussed previously, greatly influences the pendulum response of the load and thus the response of the helicopter to the load.

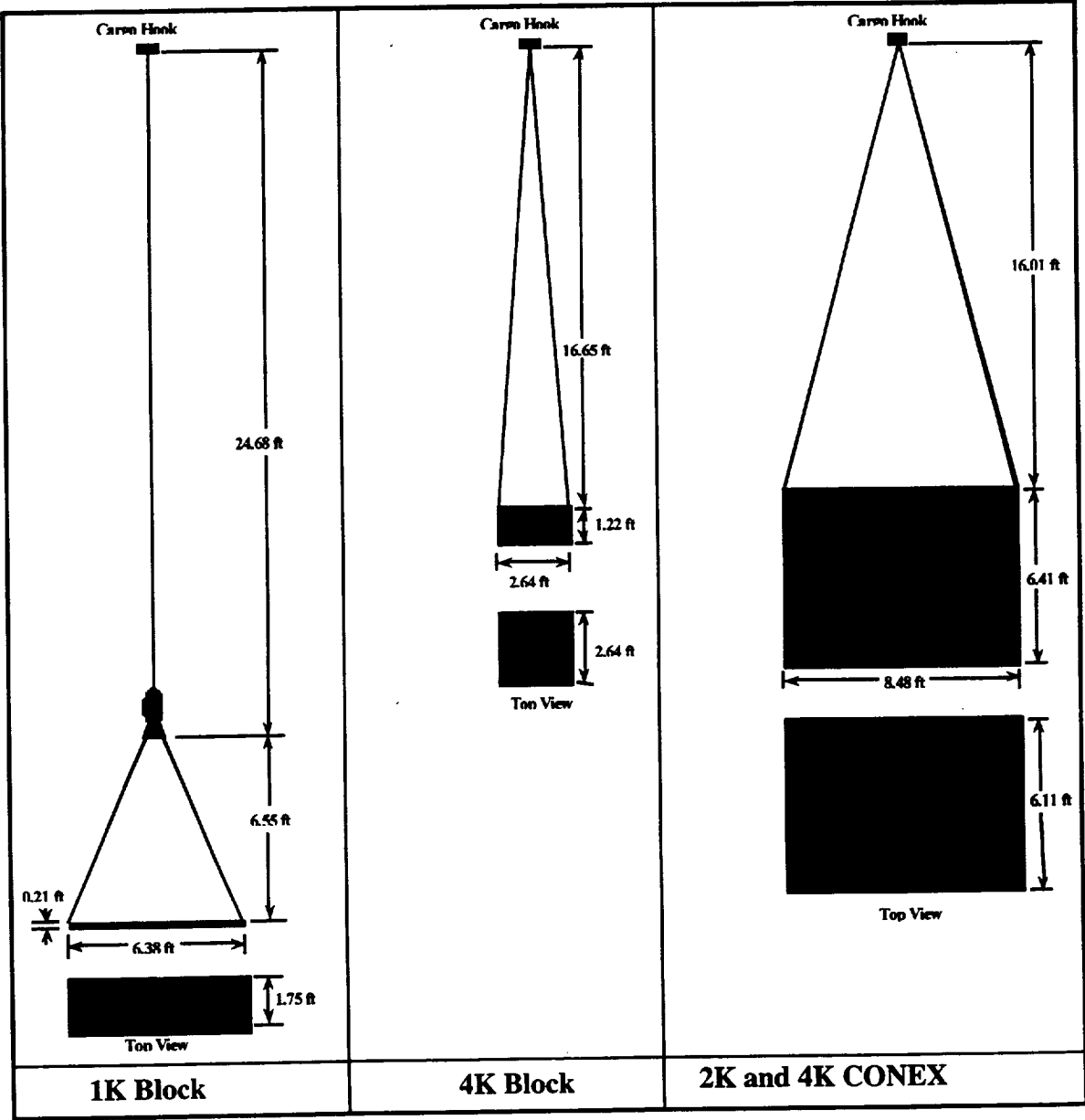


Figure 5.6. Scaled drawing of the three external load configurations.

## B. CONTROL SYSTEM STABILITY MARGINS

Figure 5.7 compares the results of the phase and gain margins and their associated crossover frequencies for the pitch response. In general, there was only a small decrease in the margins for the 4K CONEX case in comparison to the no load baseline. The addition of the 1K Block to the system at hover, however, resulted in a phase margin increase of 39 degrees with an associated decrease in the cross-over frequency of 1.3 rad/sec. As with the handling qualities, this may be due to differences in the configurations of the loads, in particular the sling length. At 80 knots, the results for the 1K Block were in line with the other loads. Further flights at this condition will determine if this is a repeatable tendency.

The roll response margins and crossover frequencies are presented in figure 5.8. Unlike the longitudinal case, a significant reduction in both margins in roll is apparent between the no load and 4K CONEX cases. Phase margin was reduced by as much as 37 degrees (30 knots), while gain margin decreased by as much as 4 dB (hover). At hover the 1K Block caused a decrease in the phase margin of 35 degrees, opposite its effect in pitch. Due to the Black Hawk's large stability margins, these reductions did not place the overall stability of the helicopter in jeopardy. However, for helicopters designed with much smaller stability margins, reductions of this magnitude represent a serious degradation in the system and could possibly lead to an unstable condition.

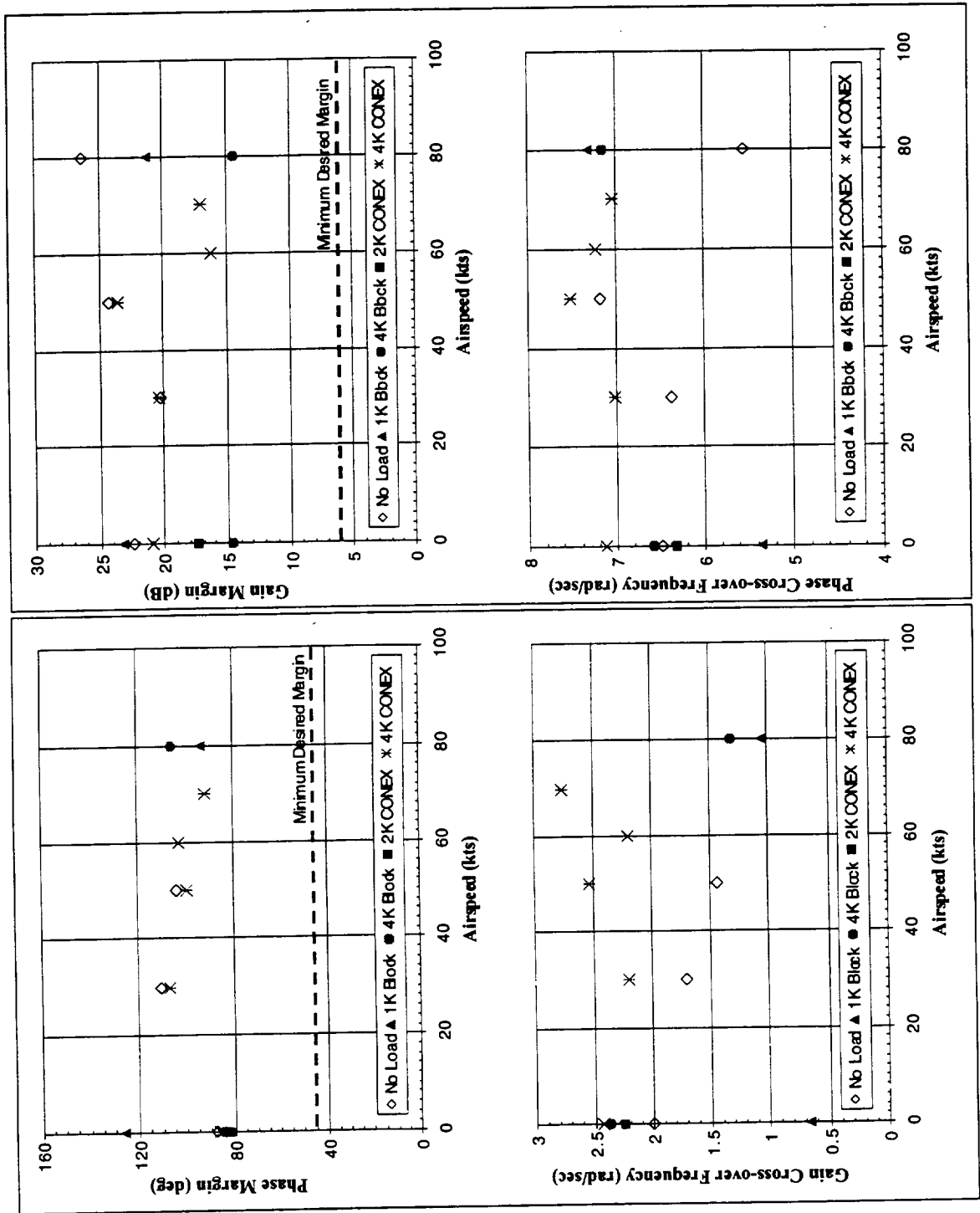


Figure 5.7 Control system stability margins — pitch.

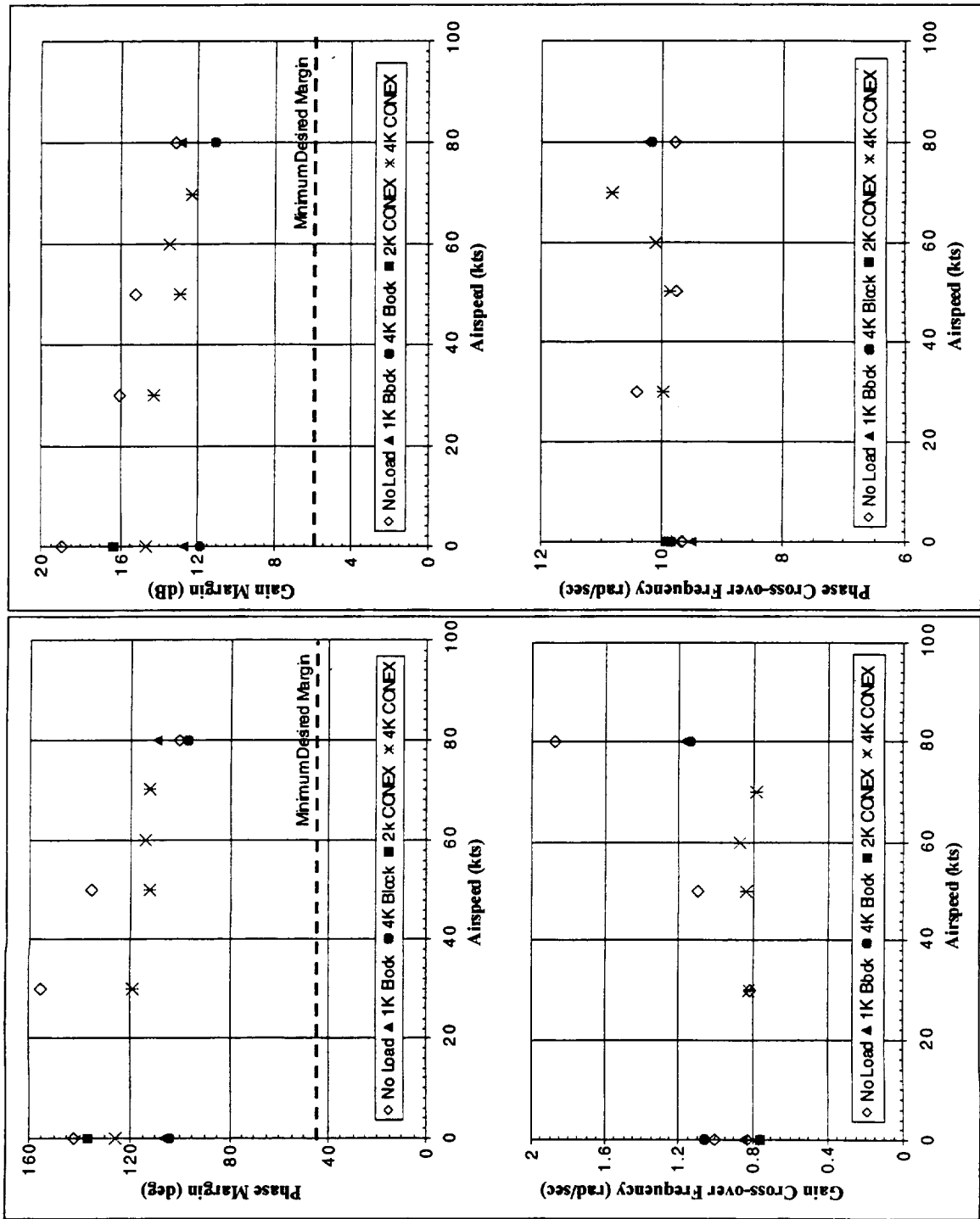


Figure 5.8. Control system stability margins – roll.

## C. LOAD MOTION CHARACTERIZATION

Before looking at the results, it is necessary to point out a few of the limitations encountered during the analysis of the load pendulum motion. First, as noted in Section IV.D.2a, knowledge of the relative yaw angle between the load and the helicopter is critical to the determination of the damping and natural frequency of the load pendular modes. Early in 1997, while researching the instrumentation installed on the helicopter, it was learned that a bias problem existed with the heading gyro used in the helicopter instrumentation rack. Evidently, each time the helicopter test instrumentation is powered up, the gyro stabilizes on a different heading (ref. 24). It was thought that by simply referencing the initial gyro reading with that of the pilots heading gyro, a correction could be made. Unfortunately, later test flights proved that not only is there a bias upon initialization, but that during the flight, the gyro drifts. In an attempt to compensate for this, a post flight compass calibration record was taken and the pilot's heading noted just prior to shut down. Assuming the drift rate was constant throughout the flight, a linear correction was applied to the heading signal. This correction was applied to the data from Flights 172 and 173. Although only limited data is available, it appears that on top of the bias and drift, the drift rate is not consistent from one flight to the next. In short, the heading signal is unreliable at the best and a replacement for the gyro should be sought before further flight testing is performed.

A second problem was associated with the fact that at the higher airspeeds the load motion itself was small except in yaw. Above 50 knots, the load tended to trail slightly aft and remain in a stable position under the aircraft. In fact, according to the pilots comments, supported by the recorded data, the CONEX was minimally excited in pitch and roll above 50 knots. The main motion was the sling wind-up experienced. At some points, up to nine full revolutions were noted. This brings another dimension of complexity to the puzzle; in essence, the sling geometry was constantly changing. As the number of twists varied, so too did the total distance between load and helicopter, and the geometry of the sling. It may prove beneficial to fly the load with the swivel again on future flights.

With the above comments in mind, the calculated load pendulum damping is shown in figure 5.9. One apparent observation is the difference between the lateral and the longitudinal mode. In all cases, pitch damping was less than roll damping, as predicted by analysis. However, the simulation and linear analysis predicted a much lower longitudinal damping. Although further testing is required, the apparent trend is one of a minimum damping in both pitch and roll at low airspeeds, then increasing with increasing airspeed, with the pitch case as the most critical. It is important to remember that these results are strongly dependent upon load and sling configuration.

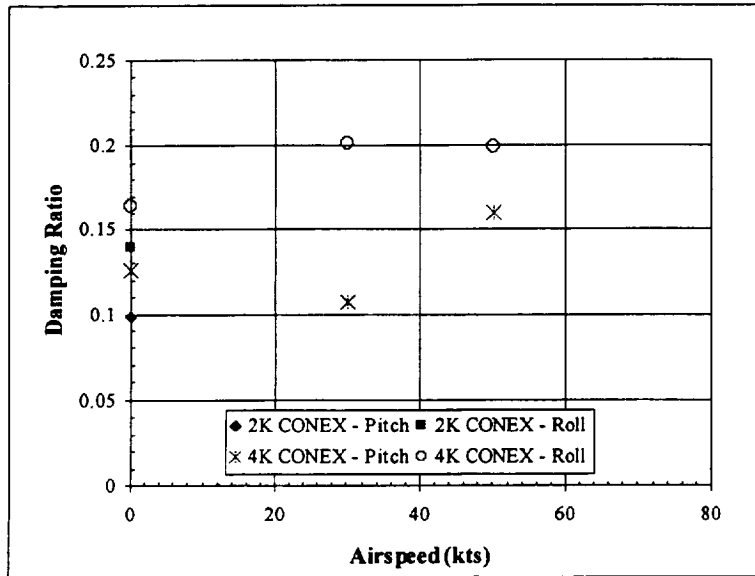


Figure 5.9. Load pendulum mode damping.

Figure 5.10 shows the undamped natural frequency associated with the load's pendulum mode. The frequency compares well with the predicted values of 1.5 and 1.6 rad/sec for the 2K and 4K CONEX, respectively. The frequency is nearly the same for both the pitch and roll modes, decreasing slightly with increasing airspeed.

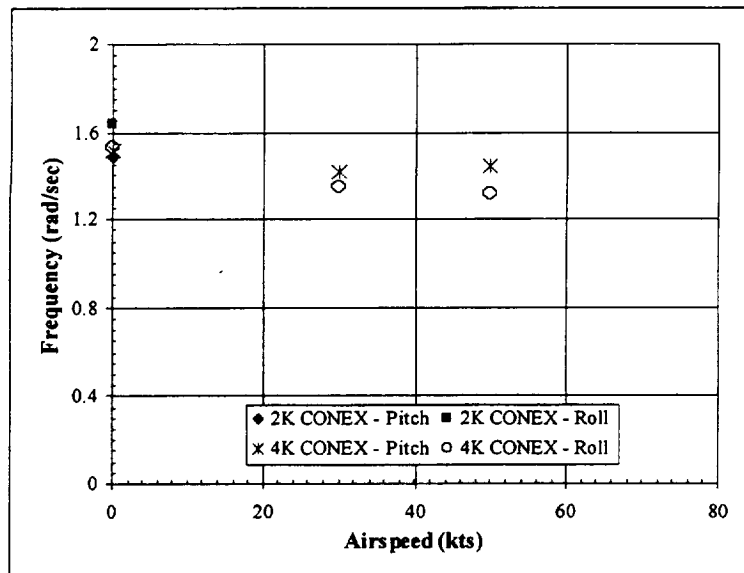


Figure 5.10. Load pendulum natural frequency.

## **D. SIMULATION**

### **1. Simulation Model**

Mr. Cicolani is currently developing the simulation model used for comparison. It is a generic helicopter called 'ESD.' This is a linearized, uncoupled, six-degree of freedom model, which is stable in response to any control input. Rotor actuator dynamics and rotor downwash are not incorporated. The load was modeled as a 4,000-pound box with inertia matching that of the 4K CONEX. It was subjected to a drag force only, with minimal yaw. A four-leg inelastic sling matching the actual test flight sling geometry was incorporated into the system as well. The actual flight test control input time histories were used to drive the simulation and the results of this initial effort are discussed below.

### **2. Comparison of Test Data to Simulation**

Comparison of the time histories of the longitudinal and lateral control sweep inputs and the resulting on-axis helicopter and load time domain rate responses are shown in figures 5.11 and 5.12, respectively. Good agreement is shown in both the helicopter's pitch rate and roll rate responses. In the lateral case, the load response also demonstrates good agreement in amplitude and damping. The load pitch rate response comparison indicates a significant difference between the test flight data and the simulation, particularly with respect to damping and magnitude of the response. Improved aerodynamic models of the load may help to reconcile the differences.

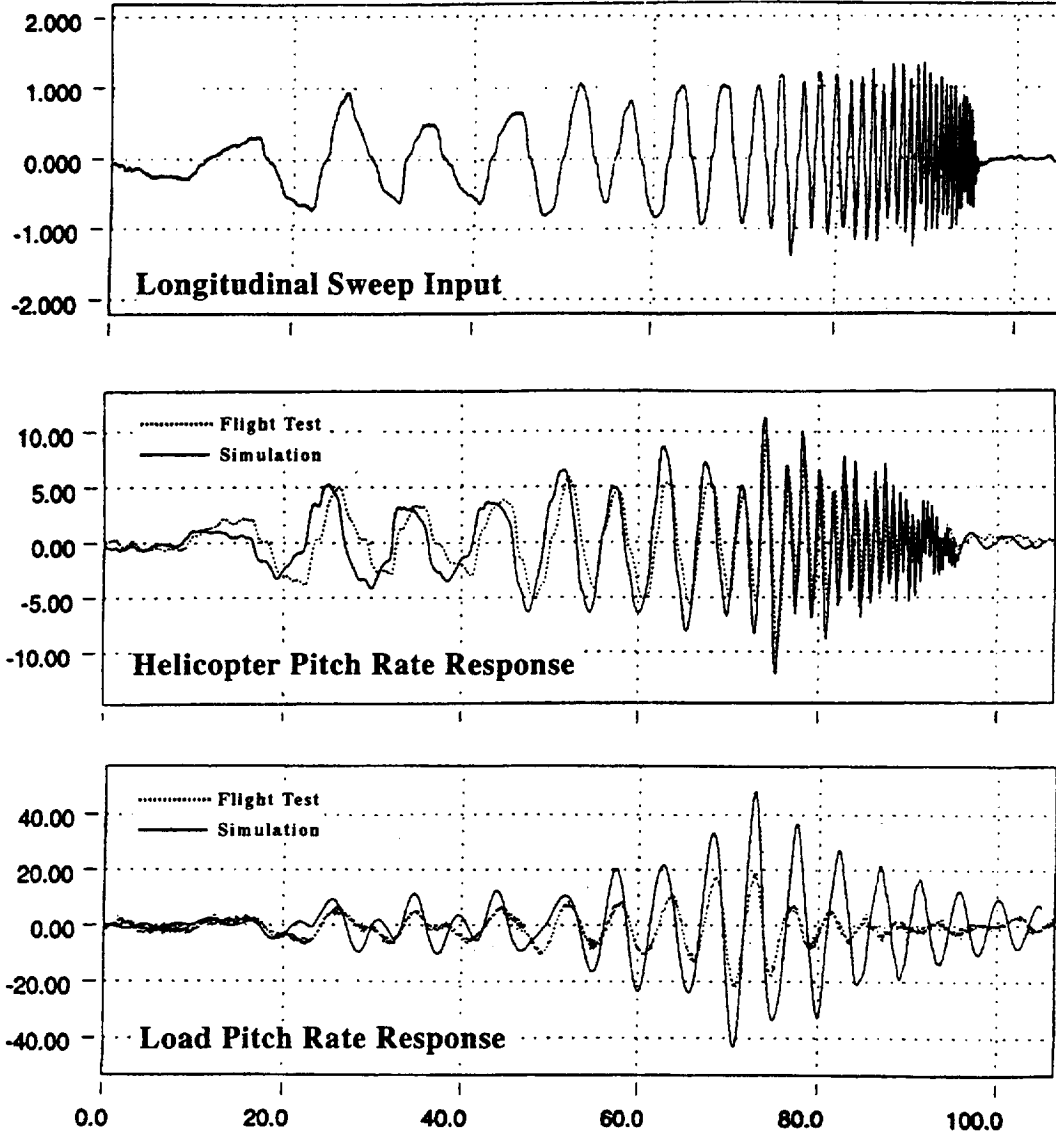


Figure 5.11. Comparison of flight test and simulation time histories – longitudinal control sweep, hover with the 4K CONEX.

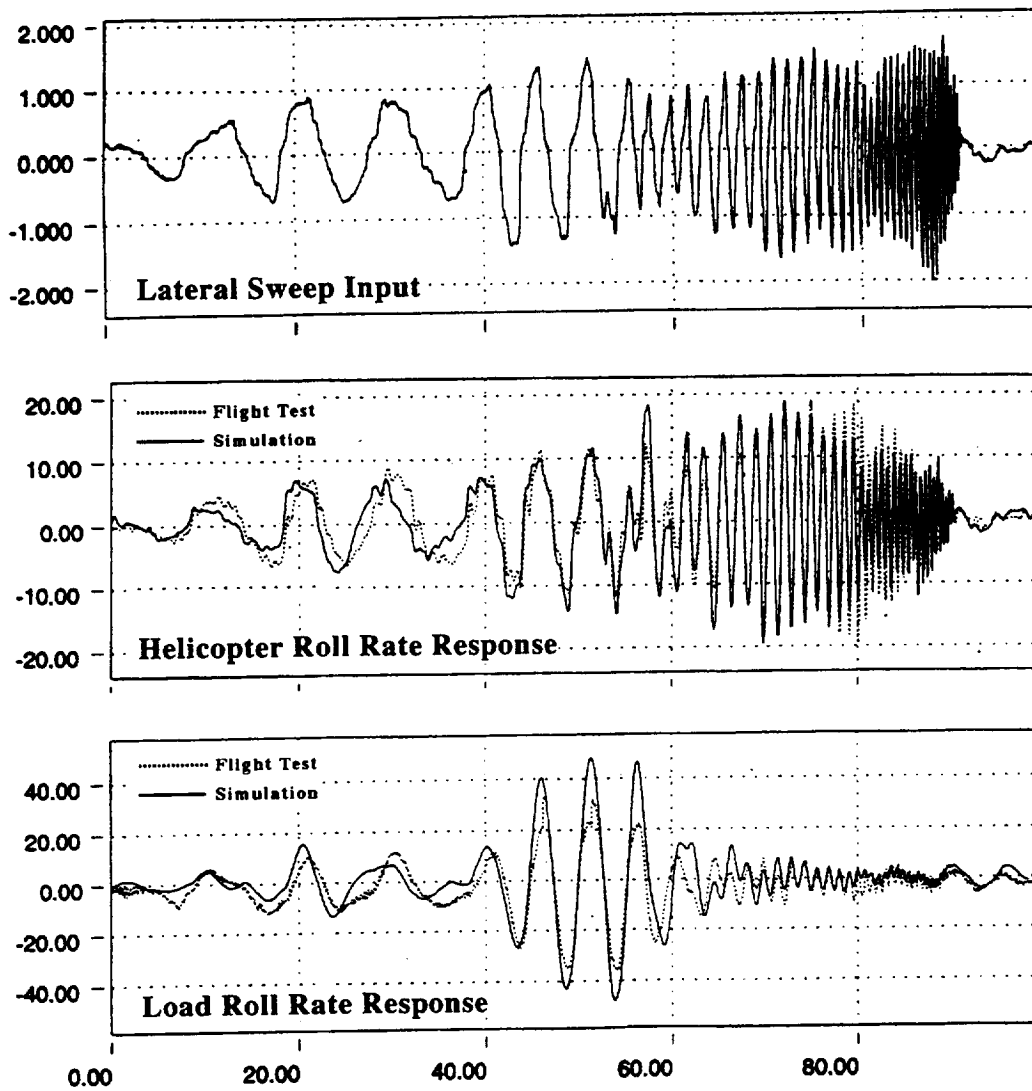


Figure 5.12. Comparison of flight test and simulation time histories – lateral control sweep, hover with the 4K CONEX.

## VI. CONCLUSIONS AND RECOMMENDATIONS

### A. CONCLUSIONS

This report presents a detailed description of the first phase of flight testing associated with the U.S./Israeli MOA, Task 8: Flight Mechanics of Helicopter/Sling-Load Dynamics. The focus of this early testing consisted of five main points. The first was to determine the effect the load has on the helicopter's handling quantities, quantified by the bandwidth frequency and phase delay parameters. The second point was to observe the effect the load has on the helicopter's control system stability margins, quantified through the phase and gain margins. Third, characterization of the load's lateral and longitudinal pendular motion was sought by evaluating the motions damping and natural frequency. Demonstration of a near-real time flight test data analysis and system identification technique was the fourth goal of the project. The last point was to compare flight test with simulation results and begin investigation of improvements to the current simulation model.

Included in this report is a detailed description of the equipment used, covering the UH-60A Black Hawk helicopter, test loads, slings and the helicopter and load instrumentation. A brief history of the flight test program from Flight 150 in April 1995 to Flight 173 in August 1997 was outlined followed by a discussion of frequency domain flight testing. The basic flight profile was laid out, highlighting the frequency sweep technique. Data acquisition specifics were also covered, emphasizing the multiple data paths and the redundancy in the recording of the data stream. The discussion of the analysis described all the software tools utilized, focusing on CIPHER<sup>®</sup>. CIPHER<sup>®</sup> produced the frequency responses from the time history data and facilitated the calculation of the desired parameters. Differences between the near-real time and post flight analysis were noted.

The work done for this first phase of the MOA Task 8 has shown:

- Although variations exist in the results between the near-real time and the post flight analysis methods, the overall conclusion is the real time analysis technique demonstrated in this program did provide expeditious and satisfactory answers.
- Handling qualities results show that the roll axis tends to be the more critical than the pitch axis, especially at hover, with the exception of the 1K Block case that showed the opposite tendency. In pitch, the addition of the CONEX improved the helicopter's response, where in roll the response was degraded.
- The stability margins of the control system are degraded by picking up an external load. In particular, at low airspeeds, the roll axis is more sensitive than pitch, with a decrease of up to 37 degrees of phase margin and four dB of gain margin. These results parallel those of the handling qualities.
- The pendulum damping of the load is lowest at low airspeeds and in the pitch axis.
- The natural frequency of the load's pendulum motion is almost identical for both pitch and roll axis, with a slight decrease noted as airspeed increases.

- Current simulation models the lateral response of the helicopter and load and longitudinal response of the helicopter very well. However, the model significantly under-predicts the damping of the load in the longitudinal case.

## **B. RECOMMENDATIONS**

Although a significant amount of data was obtained in this stage of the Task, it is not possible to draw any all-encompassing conclusions about external load operations at this point. Several reasons exist for this. First and foremost, the results are very dependent upon the load and configuration. In addition, the load instrumentation package was only flown with the CONEX, and only the CONEX with ballast was flown at more than two airspeeds. Thus, now that the majority of the groundwork has been laid, future flight testing should concentrate on increasing the database size. Emphasis should be placed on acquiring further data on the 1K Block and empty CONEX at various airspeeds, matching the ballasted CONEX database, as well as utilizing the load instrumentation package on the block loads.

Effort needs to be put into improving available instrumentation. In particular, instrumentation better suited to provide load attitude and improvement in the directional heading of the helicopter. The latter may simply be a matter of determining a more accurate prediction of the compass drift or complete replacement of the instrument.

For the near-real time analysis, the main recommendation is to stream line the user interaction and data entry process. One possible solution may be to develop a 'front end' for CIPHER<sup>®</sup>. The idea being that since most of the data entry is repetitive in nature, it should be possible to condense the entries. This could possibly be a single page with a few lines indicating which time histories to use, window size, signals, and plotting options. This would then be used in one simple stroke to run the FRESPID routine of CIPHER<sup>®</sup> and produce the desired frequency responses. Use of modern GUI techniques may add to the versatility of this real time analysis, add-on software package. Additional improvements in running the analysis real time would be realized as the software becomes available on more operating systems. Taking CIPHER<sup>®</sup> into the field, say via a PC or laptop, would certainly open the door to many more possibilities.

Extracting the load motion damping and natural frequency at airspeeds below 50 knots proved possible and produce fairly good results. Above 50 knots however, the inability to generate a pendular response with sufficient magnitude combined with the wind up of the sling significantly limited the extraction of these parameters for the 4K CONEX case. Work is on going to improve these results. Use of the swivel may be reintroduced into the flight procedure to eliminate the excessive amount of wind-up experienced during the higher forward airspeeds. The lighter 2K CONEX may produce responses that are more dramatic at the higher airspeed.

The work comparing the actual flight test data with the simulation data is truly in its infancy. Although comparisons showed significant agreement between test data and simulation, many improvements can be accomplished in the future. These improvements include using a stabilized UH-60A Black Hawk model vice the ESD model, incorporating load aerodynamic data acquired through wind tunnel tests, use of an elastic sling configuration, and incorporation of a rotor downwash model.

As a final note, it is intended that all significant data from these tests will be incorporated into the Tilt Rotor Engineering Database System (TRENDS). TRENDS is an interactive, flight test, relational database developed by NASA to support rotorcraft research studies. It is designed to provide all of the project information a user needs without having to contact the flight test engineer. By including the slung load data in TRENDS it will become available to a much larger audience in a standardized, readily accessible format (ref. 25).



**APPENDIX A. SIGNAL LISTING FOR NASA 748, LOAD, AND STRIP CHARTS**

### HELICOPTER PCM MEASUREMENTS (37)

ITEM CODE	MNEMONIC	DESCRIPTION	POSITIVE DIRECTION	UNITS	RANGE		SAMPLE RATE
					MIN	MAX	
D100	LONGSTK	Longitudinal Control Position	AFT	%	0	100	209
D101	LATSTK	Lateral Control Position	RIGHT	%	0	100	209
D102	PEDAL	Directional Control Position	RT PEDAL	%	0	100	209
D103	COLLSTK	Collective Control Position	UP	%	0	100	209
D003	STABLR	Stabilator Angle	TE DOWN	deg	-10	40	209
DM00	DMXE	Longitudinal Mixer Input Posit	AFT	%	0	100	209
DM01	DMXA	Lateral Mixer Input Position	RIGHT	%	0	100	209
DM02	DMXR	Directional Mixer Input Posit	RT PEDAL	%	0	100	209
DP00	PSFWD	Primary Servo, Forward	UP	%	0	100	209
DP01	PSLAT	Primary Servo, Lateral	UP	%	0	100	209
DP03	PSAFT	Primary Servo, Aft	UP	%	0	100	209
R021	TRIP	Tail Rotor Impress Pitch	LT PEDAL	deg	0	100	209
DS00	SASE	Longitudinal SAS Output	AFT	%	0	100	209
DS01	SASA	Lateral SAS Output	RIGHT	%	0	100	209
DS02	SASR	Directional SAS Output	RIGHT	%	0	100	209
DA00	PITCHATT	Pitch Attitude	NOSE UP	deg	-50	50	209
DA01	ROLLATT	Roll Attitude	RIGHT	deg	-100	100	209
DA02	HEADING	Aircraft Heading	NOSE RT	deg	0	360	209
DAA0	ALPHA	Aircraft Angle of Attack	NOSE UP	deg	-100	100	209
DSS0	BETA	Aircraft Sideslip Angle	NOSE LT	deg	-100	100	209
DR00	PTCHRATE	Aircraft Pitch Rate	NOSE UP	deg/s	-50	50	209
DR01	ROLLRATE	Aircraft Roll Rate	RIGHT	deg/s	-50	50	209
DR02	YAWRATE	Aircraft Yaw Rate	NOSE RT	deg/s	-50	50	209
DAC0	PTCHACC	Pitch Angular Acceleration	NOSE UP	deg/s <sup>2</sup>	-600	600	209
DAC1	ROLLACC	Roll Angular Acceleration	RIGHT	deg/s <sup>2</sup>	-200	200	209
DAC2	YAWACC	Yaw Angular Acceleration	NOSE RT	deg/s <sup>2</sup>	-100	100	209
DL00	AXCG	X-axis Linear CG Acceleration	FORWARD	g's	-2	2	209
DL01	AYCG	Y-axis Linear CG Acceleration	RIGHT	g's	-2	2	209
DL02	AZCG	Y-axis Linear CG Acceleration	UP	g's	-2	4	209
V001	V001	Aircraft Airspeed, Boom		in Hg	0	2	209
H001	H001	Static Pressure, Boom (Altitude)		in Hg	20	32	209
VX03	LSSX	LASSIE Forward Airspeed	FORWARD	kts	-35	165	209
VY03	LSSY	LASSIE Lateral Airspeed	RIGHT	kts	-50	50	209
VZ03	LSSZ	LASSIE Vertical Airspeed	UP	ft/min	-300	2000	209
T100	T100	Stagnation Temperature		°C	-20	50	209
H003	RALT	Radar Altimeter		ft	0	1500	209
HKLD	HKLD	Hook Load		lbs			

### LOAD PCM MEASUREMENTS (9)

ITEM CODE	MNEMONIC	DESCRIPTION	POSITIVE DIRECTION	UNITS	RANGE		SAMPLE RATE
					MIN	MAX	
DAL1	PANGL	Load Pitch Angle	NOSE UP	deg			260
DAL2	RANGL	Load Roll Angle	RIGHT	deg			260
DAL3	YAWANG	Load Yaw Angle	NOSE RIGHT	deg			260
DRL1	PITCHRATE	Load Pitch Rate	NOSE UP	deg/s			260
DRL2	ROLLRATE	Load Roll Rate	RIGHT	deg/s			260
DRL3	YAWRATE	Load Yaw Rate	NOSE UP	deg/s			260
AL01	LNGACC	Load Longitudinal Acceleration	FORWARD	g's			260
AL02	LATACC	Load Lateral Acceleration	RIGHT	g's			260
AL03	NORMACC	Load Normal Acceleration	UP	g's			260

Table A1. Telemetry signals for NASA 748 and load.

## HELICOPTER DERIVED AND SMOOTHED MEASUREMENTS (51)

MNEMONIC	DESCRIPTION	POSITIVE DIRECTION	UNITS
XAIN	Lateral Stick Position	RIGHT	in
XBIN	Longitudinal Stick Position	AFT	in
XPIN	Pedal Position	RIGHT	in
XCIN	Collective Position	UP	in
XABOOST	Lateral Output from Boost Actuator	RIGHT	in
XEBOOST	Longitudinal Output from Boost Actuator	AFT	in
XPBOOST	Pedal Output from Boost Actuator	RIGHT	in
XCBOOST	Collective Output from Boost Actuator	UP	in
DMIXAIN	Lateral Mixer Input	RIGHT	in
DMIXEIN	Longitudinal Mixer Input	AFT	in
DMIXPIN	Pedal Mixer Input	RIGHT	in
DMIXCIN	Collective Mixer Input	UP	in
PSFWDIN	Servo Output, Forward	FORWARD	in
PSFAFTIN	Servo Output, Aft	AFT	in
PSLATIN	Servo Output, Lateral	RIGHT	in
PSTRIN	Servo Output, Tail Rotor		in
DR00S	Smoothed Pitch Rate, Cutoff Freq. = 2.5 Hz	NOSE UP	deg/sec
DR01S	Smoothed Roll Rate, Cutoff Freq. = 2.5 Hz	RIGHT	deg/sec
DR02S	Smoothed Yaw Rate, Cutoff Freq. = 2.5 Hz	NOSE RIGHT	deg/sec
DR00D	Derivative of DR00S	NOSE UP	deg/sec <sup>2</sup>
DR01D	Derivative of DR01S	RIGHT	deg/sec <sup>2</sup>
DR02D	Derivative of DR02S	NOSE RIGHT	deg/sec <sup>2</sup>
DL00S	Smoothed X-axis Linear Accel., Cutoff Freq. = 2.5 Hz	FORWARD	g's
DL01S	Smoothed Y-axis Linear Accel., Cutoff Freq. = 2.5 Hz	RIGHT	g's
DL02S	Smoothed Z-axis Linear Accel., Cutoff Freq. = 2.5 Hz	UP	g's
DVISNX	X-axis Inertial CG Acceleration	FORWARD	ft/sec <sup>2</sup>
DVISNY	Y-axis Inertial CG Acceleration	RIGHT	ft/sec <sup>2</sup>
DVISNZ	Z-axis Inertial CG Acceleration	UP	ft/sec <sup>2</sup>
VICB	Boom Indicated Airspeed (IAS)	FORWARD	kts
VCALB	Boom Calibrated Airspeed (CAS)	FORWARD	kts
VEB	Boom Equivalent Airspeed (EAS)	FORWARD	kts
VTB	Boom True Airspeed (TAS)	FORWARD	kts
VBODYBC	CG Velocity, u Component from Boom Data	FORWARD	ft/sec
VBODYBC	CG Velocity, v Component from Boom Data	RIGHT	ft/sec
WBODYBC	CG Velocity, w Component from Boom Data	UP	ft/sec
VT	Estimated TAS for Boom and/or Lassie	FORWARD	
LSSXC	u Comp Calibrated Airspeed from Lassie Data	FORWARD	
LSSYC	v Comp Calibrated Airspeed from Lassie Data	RIGHT	
V001S	Smoothed Boom Airspeed, Cutoff Freq. = 2.5 Hz		
VTBS	True Airspeed from Smoothed Data		kts
VICBS	Indicated Airspeed from Smoothed Data		kts
H001S	Smoothed Boom Static Pressure, Cutoff Freq. = 0.05 Hz		
HDB	Density Altitude from Boom Data		ft
HDBS	Density Altitude from Smoothed Data		ft
HMHRWS	Pressure Altitude from Smoothed Data		ft
HMHRWD	Rate of Change of Altitude (Derivative of HMHRWS)		ft/sec
H003D	Rate of Change of Altitude (Derivative of H003)		ft/sec
T100S	Smoothed Stagnation Temperature, Cutoff Freq. = 2.5 Hz		
TA	Ambient Temperature from Boom Data		°C
TASMTH	Ambient Temperature from Smoothed Data		°C
SIGMAB	Density Ratio from Boom Data		

Table A.2. Helicopter derived parameters and filtered signals.

### LOAD DERIVED AND SMOOTHED PARAMETERS (16)

MNEMONIC	DESCRIPTION	POSITIVE DIRECTION	UNITS
DAL3C	Load Heading Corrected for 360 Jump Transients	RIGHT	deg
DRL1S	Smoothed Load Pitch Rate, Cutoff Freq. = 2.5 Hz	UP	des/sec
DRL2S	Smoothed Load Roll Rate, Cutoff Freq. = 2.5 Hz	RIGHT	des/sec
DRL3S	Smoothed Load Yaw Rate, Cutoff Freq. = 2.5 Hz	RIGHT	des/sec
DRL1D	Derivative of DRL1S		deg/sec <sup>2</sup>
DRL2D	Derivative of DRL2S		deg/sec <sup>2</sup>
DRL3D	Derivative of DRL3S		deg/sec <sup>2</sup>
AL01S	Smoothed Load X-axis Accel., Cutoff Freq. = 2.5 Hz		g's
AL02S	Smoothed Load Y-axis Accel., Cutoff Freq. = 2.5 Hz		g's
AL03S	Smoothed Load Z-axis Accel., Cutoff Freq. = 2.5 Hz		g's
PS2H1DEG	Continuous Load Heading, No Jumps at 0/360 deg		
P2P	Load Roll Rate Transformed to Helo Heading Axis	RIGHT	deg/sec
Q2P	Load Pitch Rate Transformed to Helo Heading Axis	NOSE UP	deg/sec
PS2P	Load Heading Minus Helicopter Heading	RIGHT	deg
ABSPQ2	Magnitude of Load Roll and Pitch Rates		
ANGKASK2	Angle btwn Load Apparent Gravity and Load Vertical		

Table A.3 Load derived parameters and filtered signals.

Gp	Li	Param	Tag	C	Chn	Min Value	Max Value	Scale 0	Scale 1	Scale 2	Scale 3	Description	Units	Proc
0	A	DAL1	3111	0	1	-45	45	0.000000E+00	1.000000E+00	0.000000E+00	0.000000E+00	PANGL - Pitch Angle	deg	120
0	A	DAL2	3110	0	2	-45	45	0.000000E+00	1.000000E+00	0.000000E+00	0.000000E+00	RANGL - Roll Angle	deg	120
0	A	DAL3	3114	0	3	0	360	-1.990000E+01	1.220000E+01	0.000000E+00	0.000000E+00	YAWANG - Yaw Angle	deg	-1
0	A	DRL1	3107	0	4	-20	20	-6.000000E+01	2.899999E+02	0.000000E+00	0.000000E+00	PITCHRATE - Pitch Rate	d/s	-1
0	A	DRL2	3106	0	5	-20	20	-9.000000E+01	4.400000E+02	0.000000E+00	0.000000E+00	ROLLRATE - Roll rate	d/s	-1
0	A	DRL3	3108	0	6	-40	40	-1.200000E+02	5.900000E+02	0.000000E+00	0.000000E+00	YAWRATE - Yaw rate	d/s	-1
0	A	AL01	3102	0	7	-0.5	0.5	-2.500000E+00	1.250000E+03	0.000000E+00	0.000000E+00	LNGACC - Longitudinal Accel	g's	-1
0	A	AL02	3103	0	8	-0.5	0.5	-2.520000E+00	1.230000E+03	0.000000E+00	0.000000E+00	LATACC - Lateral Accel	g's	-1
0	A	D100	57	1	1	25	75	-9.819500E+00	2.342299E+02	4.608600E-07	2.331900E-10	Control Pos Long	%	-1
0	A	DR00	63	1	2	-10	10	1.539400E+02	-1.017800E+01	0.000000E+00	0.000000E+00	Angular Rate Pitch	d/s	-1
0	A	DA00	51	1	3	-30	30	-1.801800E+02	8.805400E+02	0.000000E+00	0.000000E+00	Pitch Attitude	deg	-1
0	A	DS00	105	1	4	0	100	-6.632400E+01	5.086300E+02	0.000000E+00	0.000000E+00	SAS Out Pos Long	%	-1
0	A	D101	61	1	5	25	75	-3.525800E+01	3.288989E+02	-8.511100E+00	7.4576900E-10	Control Pos Lat	%	-1
0	A	DR01	67	1	6	-20	20	2.408999E+02	-1.008800E+01	0.000000E+00	0.000000E+00	Angular Rate Roll	d/s	-1
0	A	DA01	55	1	7	-45	45	1.780390E+02	-8.717200E+00	2.0.000000	0.000000E+00	Roll Attitude	deg	-1
0	A	DS01	109	1	8	0	100	1.483200E+02	-4.940700E+00	2.0.000000	0.000000E+00	SAS Out Pos Lat	%	-1
0	A	D102	65	2	1	0	100	-5.244700E+01	5.099600E+02	-7.543700E+00	6.1.025400E-09	Control Pos Dir	%	-1
0	A	DR02	71	2	2	-40	40	-2.163300E+02	1.002000E+01	0.000000E+00	0.000000E+00	Angular Rate Yaw	d/s	-1
0	A	DA02	59	2	3	0	360	0.000000E+00	8.789099E+02	0.000000E+00	0.000000E+00	Heading	deg	-1
0	A	DS02	113	2	4	0	100	-1.274300E+02	7.485000E+02	0.000000E+00	0.000000E+00	SAS Out Pos Dir	%	-1
0	A	D103	69	2	5	0	100	-6.109800E+01	3.455999E+02	1.380999E+06	-1.202500E-11	Control Pos Coll	%	-1
0	A	DL02	95	2	6	-1	3	-5.108500E+00	2.510489E+03	0.000000E+00	0.000000E+00	Lim Accel Cg-Normal	g's	-1
0	A	AL03	3104	2	7	0	2	-1.250000E+01	6.130000E+03	0.000000E+00	0.000000E+00	NORMACC - Normal Accel	g's	-1
0	A	HKLD	70	2	8	0	10000	0.000000E+00	1.221000E+00	0.000000E+00	0.000000E+00	CRCOHLKD - Cargo Hook Load	lbs	-1
0	A	LSSXC	94	3	1	-20	30	-3.968839E+01	4.943753E+02	0.000000E+00	0.000000E+00	LowairX(LASSIE)	kts	-1
0	A	V001	86	3	2	0	0.4	-4.584600E-	02.5154099E-04	0.000000E+00	0.000000E+00	Airspeed (boom)	inHg	-1
0	A	\$VRMR	0	3	3	242	296	0.000000E+00	1.000000E+00	0.000000E+00	0.000000E+00	Refered Main Rotor Speed	RPM	121
0	A	H003	82	3	4	0	2500	-1.844900E+01	3.617500E+01	0.000000E+00	0.000000E+00	Altitude (Radar)	ft	-1
0	A	\$VICB	0	3	5	10	60	0.000000E+00	1.000000E+00	0.000000E+00	0.000000E+00	Calibrated Airspeed (boom)	Knots	122

Table A.4. Strip chart signal listing.



**APPENDIX B. DETAILED DRAWINGS OF THE 4K BLOCK AND CONEX.**

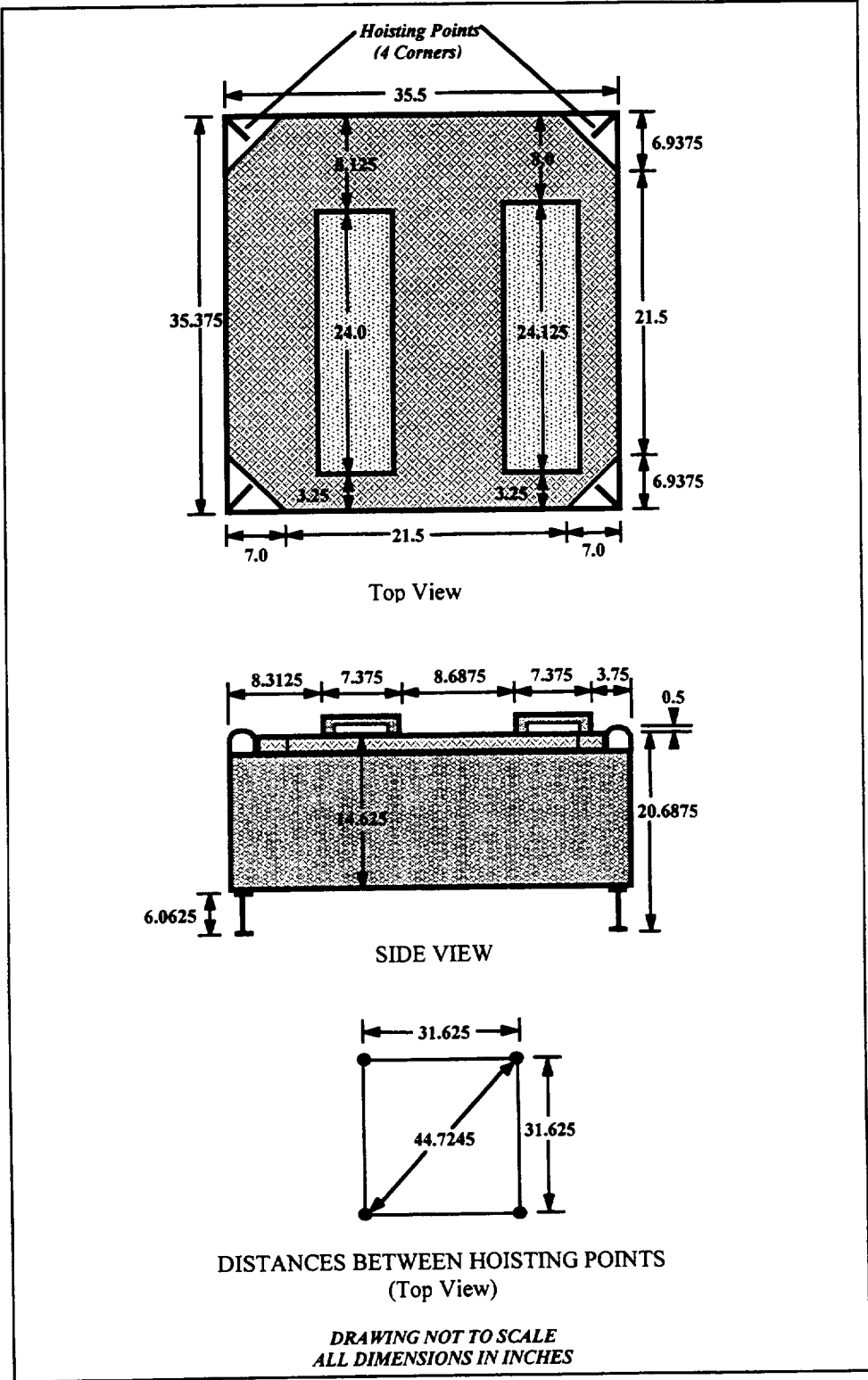


Figure B.1. 4K block load

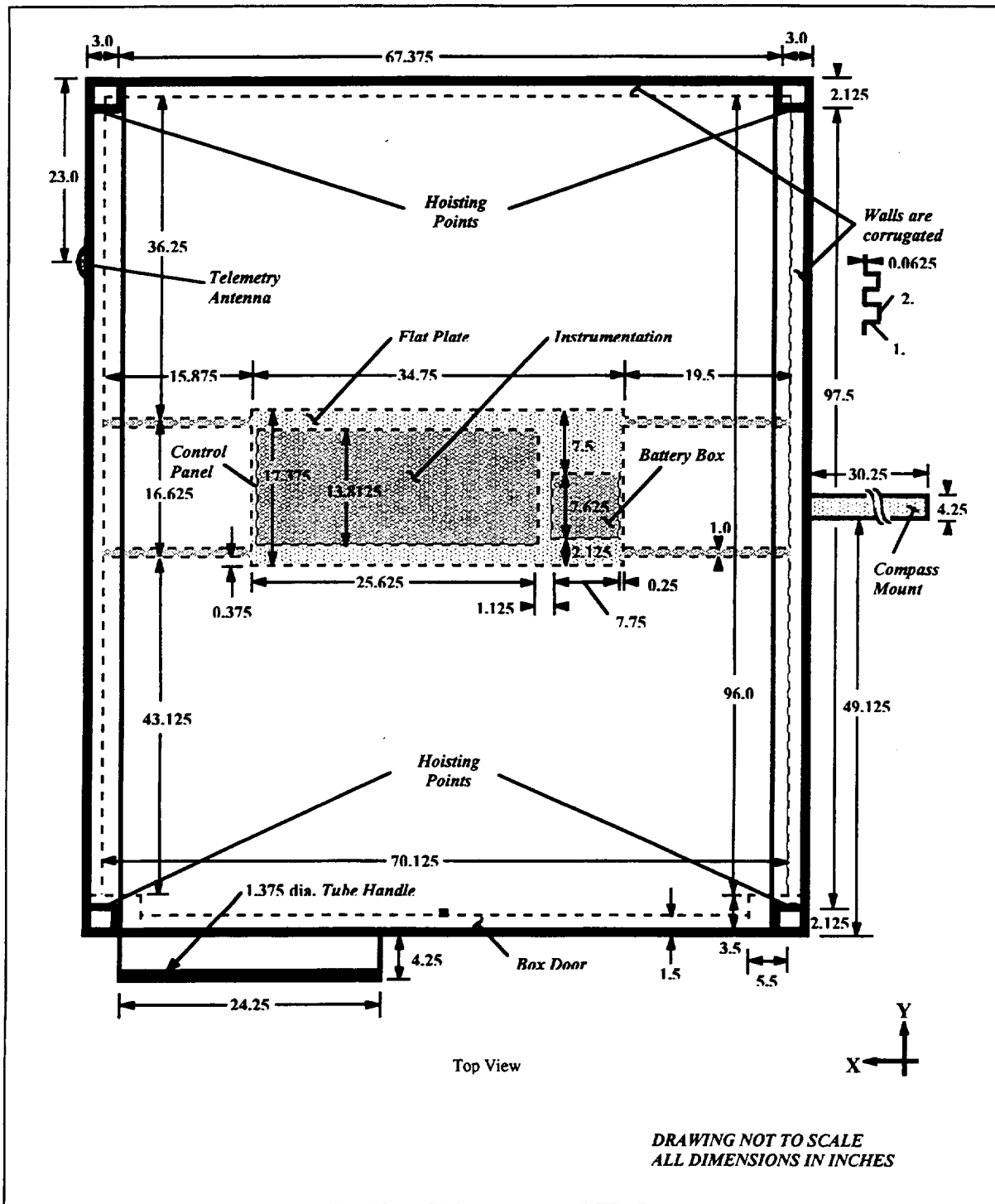


Figure B.2. CONEX dimensions (sheet 1 of 3).

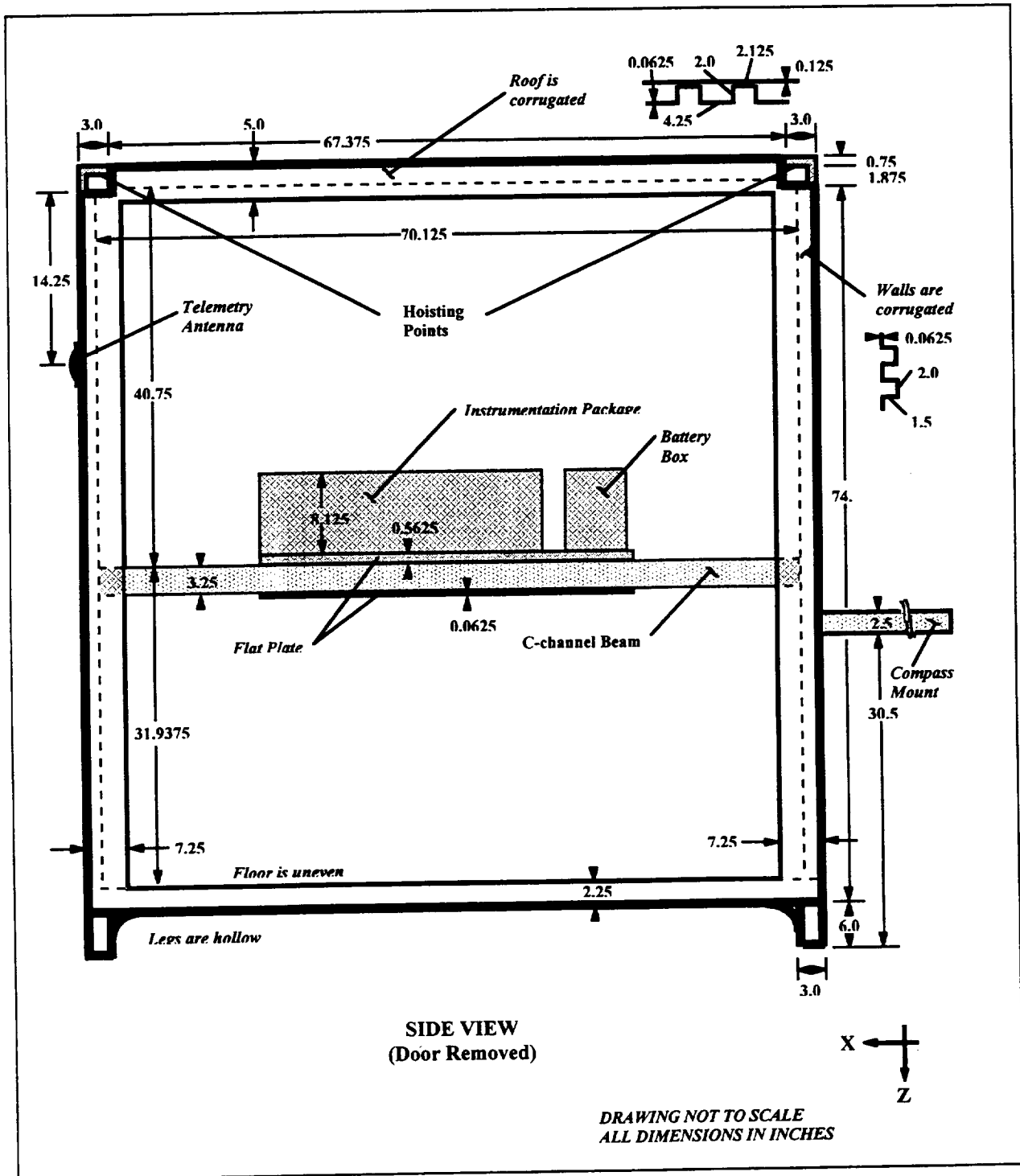


Figure B.3. CONEX dimensions (sheet 2 of 3).

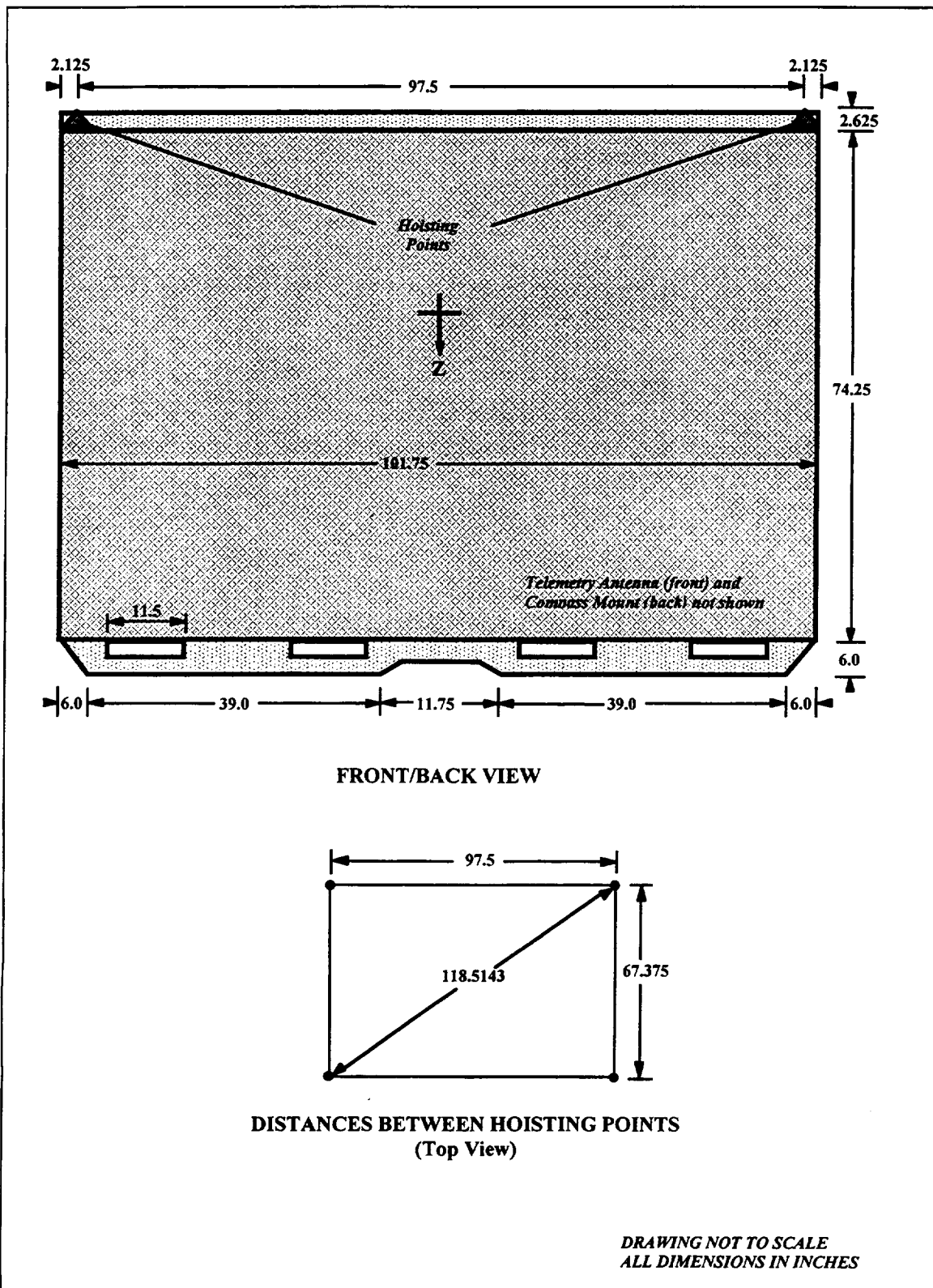


Figure B.4. CONEX dimensions (sheet 3 of 3).



## **APPENDIX C. MOA TASK 8 FLIGHT TEST DATABASE SUMMARY**

Table C.1. MOA Task 8, flight test database summary.

SUMMARY BY FLIGHT NUMBER

FLIGHT #	DATE	LOAD	AIRSPEED	CONTROL AXIS	CONTROL INPUT
150	4/14/95	None	0	DATA LOST	
151	5/3/95	1k External	0	Pitch	Sweeps, Doublets
			0	Roll	Sweeps, Doublets
			0	Yaw	Sweeps, Doublets
			0	Collective	Sweeps, Doublets
152	5/11/95	1k Internal	0	Pitch	Sweeps, Doublets
			0	Roll	Sweeps, Doublets
			0	Yaw	Sweeps, Doublets
			0	Collective	Sweeps, Doublets
153	6/23/95	1k Internal	80	Pitch	Sweeps, Doublets
			80	Roll	Sweeps, Doublets
			80	Yaw	Sweeps, Doublets
			80	Collective	Sweeps, Doublets
154	8/10/95	1k Internal	80	Pitch	Sweeps, Doublets
			80	Roll	Sweeps
155	1/10/96	None	0, 10, 20, 30, 40	Trim	Lassie Check
156	1/23/96	4k External	0, 20, 40, 60, 80, 100, 120	Trim	
			0, 20, 40, 60, 80, 100, 120	Pitch	Steps, Doublets
			0, 20, 40, 60, 80, 100, 120	Roll	Steps, Doublets
			0, 20, 40, 60, 80, 100, 120	Yaw	Steps, Doublets
157	3/20/96	None	0 thru 130 steps of 10	Trim	Airspeed & Altitude Calibration
158	4/25/96	4k External	0, 60, 80, 100	Trim	
			0, 60, 80, 100	Pitch	Steps, Doublets
			0, 60, 80, 100	Roll	Steps, Doublets
			0, 60, 80, 100	Yaw	Steps, Doublets
			0, 60, 80, 100	Collective	Steps, Doublets
159	6/6/96	4k External	0	Trim	
			0	Pitch	Sweeps, Steps, Doublets
			0	Roll	Sweeps, Steps, Doublets
			0	Yaw	Sweeps, Steps, Doublets
			0	Collective	Sweeps, Steps, Doublets
160	7/19/96	1k External	80	Trim	
			80	Pitch	Sweeps, Steps, Doublets (SAS on & off)
			80	Roll	Sweeps, Steps, Doublets (SAS on & off)
161	9/30/96	4k External	80	Trim	
			80	Pitch	Sweeps, Steps, Doublets
			80	Roll	Sweeps, Steps, Doublets
			80	Yaw	Sweeps, Steps, Doublets
			80	Collective	Sweeps, Steps, Doublets
162	10/16/96	2k Conex	0, 30, 40, 50, 60	Trim	
163				Post Maintenance Functional Check Flight	
164		2k Conex	40	Roll	Sweep
165	1/16/97			Post Maintenance Functional Check Flight	
166	7/25/97	4k & 6k External	0	Trim	Hook Calibration
				Conex on Forklift	
167	7/28/97	2k Conex	0	Trim	
			0	Pitch	Sweeps, Steps, Doublets
			0	Roll	Sweeps, Steps, Doublets
			0	Collective	Doublets
168	7/28/97	4k Conex	0	Trim	
			0	Pitch	Sweeps, Steps, Doublets
			0	Roll	Sweeps, Steps, Doublets
			0	Collective	Doublets
169	8/6/97	4k Conex	0, 30	Trim	
			0	Roll	Sweeps
			30	Pitch	Sweeps
170	8/7/97	None	0, 30, 50	Trim	
			0, 30, 50	Pitch	Sweeps, Steps, Doublets
			0, 30, 50	Roll	Sweeps, Steps, Doublets
			0, 30, 50	Collective	Doublets
171	8/18/97	None	0, 30	Trim	
			0, 30	Pitch	Sweeps

Table C.2. MOA Task 8, flight test database summary (continued).

**SUMMARY BY FLIGHT NUMBER (con't)**

FLIGHT #	DATE	LOAD	AIRSPEED	CONTROL AXIS	CONTROL INPUT
172	8/20/97	4k Conex	0, 30, 50 30, 50 0, 30, 50	Trim Pitch Roll	Sweeps, Steps, Doublets Sweeps, Steps, Doublets
173	8/21/97	4k Conex	0, 60, 70 0, 60, 70 60, 70	Trim Pitch Roll	Sweeps, Steps, Doublets Sweeps, Steps, Doublets

**SUMMARY BY LOAD**

LOAD	FLIGHT #	DESCRIPTION
None	155	LASSIE (low air speed) instrumentation check.
	157	Airspeed and altitude calibration flight.
	163	Post maintenance functional check flight.
	165	Post maintenance functional check flight.
	170	Hover, 30 kts, and 50 kts, pitch, roll and collective sweeps, steps and doublets.
	171	Trim and pitch sweeps at hover and 30 kts -- Pilot proficiency training.
1k Block	151	Hover, 4 axis sweeps and doublets, 1k load external.
	152	Hover, 4 axis sweeps and doublets, 1k load internal.
	153	80 kts, 4 axis sweeps and doublets, 1k load internal.
	154	80 kts, pitch and roll sweeps and doublets, 1k internal.
	160	80 kts, pitch and roll sweeps, steps, and doublets, 1k load external.
4k Block	156	Hover, 20 kts, 40 kts, 60 kts, 80 kts, 100 kts and 120 kts, 4 axis steps and doublets, 4k load external
	158	Hover, 60 kts, 80 kts, and 100 kts, 4 axis steps and doublets, 4k load external
	159	Hover, 4 axis sweeps, steps and doublets, 4k load external
	161	80 kts, 4 axis sweeps, steps and doublets, 4k load external.
	166	Hover, hook calibration flight with 6k and 4k load external.
2k Conex	162	Hover, 30 kts, 40 kts, 50 kts and 60 kts, trim conditions, first Conex box flight
	164	40 kts, roll sweep.
	167	Hover, pitch and roll sweeps, steps and doublets.
4k Conex	168	Hover, pitch and roll sweeps, steps and doublets, and collective doublets.
	169	Roll sweeps in hover, pitch sweeps at 30 kts. Swivel installed.
	172	30 kts and 50 kts, pitch and roll sweeps, steps and doublets. Roll sweep in hover.
	173	60 kts and 70 kts, pitch and roll sweeps, steps and doublets. Pitch sweeps in hover.



**APPENDIX D. PILOT'S TEST FLIGHT DATA CARD**

**UH-60 Slung Load Project (Aircraft 748)**

Date: \_\_\_\_\_ Flight #: \_\_\_\_\_  
 Pilots: \_\_\_\_\_ / \_\_\_\_\_  
 Take-off Conditions  
 Winds: \_\_\_\_\_ GW: \_\_\_\_\_  
 OAT: \_\_\_\_\_ Fuel: \_\_\_\_\_  
 Alt Set ting: \_\_\_\_\_ Moment Arm: \_\_\_\_\_  
 OG: \_\_\_\_\_

**UH-60 Slung Load Project (Aircraft 748)**

Date: \_\_\_\_\_ Flight #: \_\_\_\_\_  
 Event Rec # Start Time Stop Time Fuel / Hook Load

Maneuver Condition: Airspeed: \_\_\_\_\_ Altitude: \_\_\_\_\_  
 Axis: Pitch / Roll / Yaw / Collective  
 Load: None / CONEX / 1.2k / 4k / 6k  
 SAS 1 on / off SAS 2: on / off FPS: on / off

Trim \_\_\_\_\_  
 Sweep 1 ( ) \_\_\_\_\_  
 Sweep 2 ( ) \_\_\_\_\_  
 Sweep 3 ( ) \_\_\_\_\_  
 Step 1 ( ) \_\_\_\_\_  
 Step 2 ( ) \_\_\_\_\_  
 Doublet 1 ( ) \_\_\_\_\_  
 Doublet 2 ( ) \_\_\_\_\_

**UH-60 Slung Load Project (Aircraft 748)**

Compass Cal \_\_\_\_\_ Ind Hdq: \_\_\_\_\_  
 Pre-Flight Control Throws:  
 X - Cal \_\_\_\_\_  
 R-Cal \_\_\_\_\_  
 1 \_\_\_\_\_  
 2 \_\_\_\_\_  
 3 \_\_\_\_\_  
 4 \_\_\_\_\_  
 5 \_\_\_\_\_  
 6 \_\_\_\_\_  
 7 \_\_\_\_\_  
 8 \_\_\_\_\_  
 9 \_\_\_\_\_

Maneuver Condition: Airspeed: \_\_\_\_\_ Altitude: \_\_\_\_\_  
 Axis: Pitch / Roll / Yaw / Collective  
 Load: None / CONEX / 1.2k / 4k / 6k  
 SAS 1 on / off SAS 2: on / off FPS: on / off

Trim \_\_\_\_\_  
 Sweep 1 ( ) \_\_\_\_\_  
 Sweep 2 ( ) \_\_\_\_\_  
 Sweep 3 ( ) \_\_\_\_\_  
 Step 1 ( ) \_\_\_\_\_  
 Step 2 ( ) \_\_\_\_\_  
 Doublet 1 ( ) \_\_\_\_\_  
 Doublet 2 ( ) \_\_\_\_\_

Post Flight Control Throws:  
 X - Cal \_\_\_\_\_  
 R-Cal \_\_\_\_\_  
 1 \_\_\_\_\_  
 2 \_\_\_\_\_  
 3 \_\_\_\_\_  
 4 \_\_\_\_\_  
 5 \_\_\_\_\_  
 6 \_\_\_\_\_  
 7 \_\_\_\_\_  
 8 \_\_\_\_\_  
 9 \_\_\_\_\_

Figure D.1. Pilot's test flight data card (sheet 1 of 2).

**UH-60 Slung Load Project (Aircraft 748)**

Date: \_\_\_\_\_ Flight #: \_\_\_\_\_

Event   Rec #   Start Time   Stop Time   Fuel / Hook Load

Maneuver Condition:   Airspeed: \_\_\_\_\_   Altitude: \_\_\_\_\_  
 Axis:Pitch / Roll / Yaw / Collective  
 Load:None / CONEX / 1.2k / 4k / 6k  
 SAS:1 on / off   SAS 2: on / off   FPS: on / off

Trim \_\_\_\_\_  
 Sweep 1 ( ) \_\_\_\_\_  
 Sweep 2 ( ) \_\_\_\_\_  
 Sweep 3 ( ) \_\_\_\_\_  
 Step 1 ( ) \_\_\_\_\_  
 Step 2 ( ) \_\_\_\_\_  
 Doublet 1 ( ) \_\_\_\_\_  
 Doublet 2 ( ) \_\_\_\_\_  
 \_\_\_\_\_  
 \_\_\_\_\_  
 \_\_\_\_\_

Maneuver Condition:   Airspeed: \_\_\_\_\_   Altitude: \_\_\_\_\_  
 Axis:Pitch / Roll / Yaw / Collective  
 Load:None / CONEX / 1.2k / 4k / 6k  
 SAS:1 on / off   SAS 2: on / off   FPS: on / off

Trim \_\_\_\_\_  
 Sweep 1 ( ) \_\_\_\_\_  
 Sweep 2 ( ) \_\_\_\_\_  
 Sweep 3 ( ) \_\_\_\_\_  
 Step 1 ( ) \_\_\_\_\_  
 Step 2 ( ) \_\_\_\_\_  
 Doublet 1 ( ) \_\_\_\_\_  
 Doublet 2 ( ) \_\_\_\_\_  
 \_\_\_\_\_  
 \_\_\_\_\_  
 \_\_\_\_\_

**UH-60 Slung Load Project (Aircraft 748)**

Date: \_\_\_\_\_ Flight #: \_\_\_\_\_

Event   Rec #   Start Time   Stop Time   Fuel / Hook Load

Maneuver Condition:   Airspeed: \_\_\_\_\_   Altitude: \_\_\_\_\_  
 Axis:Pitch / Roll / Yaw / Collective  
 Load:None / CONEX / 1.2k / 4k / 6k  
 SAS:1 on / off   SAS 2: on / off   FPS: on / off

Trim \_\_\_\_\_  
 Sweep 1 ( ) \_\_\_\_\_  
 Sweep 2 ( ) \_\_\_\_\_  
 Sweep 3 ( ) \_\_\_\_\_  
 Step 1 ( ) \_\_\_\_\_  
 Step 2 ( ) \_\_\_\_\_  
 Doublet 1 ( ) \_\_\_\_\_  
 Doublet 2 ( ) \_\_\_\_\_  
 \_\_\_\_\_  
 \_\_\_\_\_  
 \_\_\_\_\_

Maneuver Condition:   Airspeed: \_\_\_\_\_   Altitude: \_\_\_\_\_  
 Axis:Pitch / Roll / Yaw / Collective  
 Load:None / CONEX / 1.2k / 4k / 6k  
 SAS:1 on / off   SAS 2: on / off   FPS: on / off

Trim \_\_\_\_\_  
 Sweep 1 ( ) \_\_\_\_\_  
 Sweep 2 ( ) \_\_\_\_\_  
 Sweep 3 ( ) \_\_\_\_\_  
 Step 1 ( ) \_\_\_\_\_  
 Step 2 ( ) \_\_\_\_\_  
 Doublet 1 ( ) \_\_\_\_\_  
 Doublet 2 ( ) \_\_\_\_\_  
 \_\_\_\_\_  
 \_\_\_\_\_  
 \_\_\_\_\_

Figure D.2. Pilot's test flight data card (sheet 2 of 2).



## APPENDIX E. NEAR-REAL TIME DATA ANALYSIS PROCEDURES

## **A. OVERVIEW**

One of the main goals of Task 8 of the U.S./Israel MOA was to modify existing hardware and software to allow for the capture and immediate analysis of flight test data in near-real time. The necessary modifications are complete and a protocol has been established for executing the analysis. The entire procedure was demonstrated during actual flight tests with good results. As experience in the routine increases, improvements allowing the process to be streamlined and easily modified to support any flight test operation will be incorporated. This appendix specifically details the procedures followed to carry out the near-real time analysis at Ames Research Center during this project. Detailed information on the data acquisition set up and hardware and software used is contained in Section III and IV of the main text.

There are three results of interest for the near-real time data analysis with respect to Task 8. The first is to determine the effect of the load on the handling qualities, the bandwidth, and the phase delay of the helicopter itself. Second is to determine the effect of the load on the stability margin of the automatic flight control system (AFCS), in particular the stability augmentation system (SAS). Third, it is desired to characterize the motion of the load through its damping ratio and natural frequency. These results are obtained from the frequency sweeps performed at each flight condition and do not rely on the other maneuvers such as the steps and doublets.

Armed with these results, the ground-based flight test engineer will be able to give the aircrew two vital pieces of information. The first is how close the maneuver was to driving either the load or the helicopter unstable. Along with this information would be a recommendation concerning whether or not to proceed to the next planned maneuver. Second, in the process of analyzing the data, the engineer can determine if the frequency content of the maneuver was satisfactory. If it was not, the engineer can relay what changes are required in order to produce an output with the sufficient frequency content.

## **B. TYPICAL SCENARIO**

It was determined through trial and error and from the needs of the project that having three flight test engineers worked well, each dedicated to particular duties. The lead was responsible for running the flight, talking to the pilots, and relaying any results and concerns. The second was responsible for monitoring and marking the strip charts. This was the individual who would back the pilots up with respect to sweep frequency limitations. The third individual was the data analyst. He was solely responsible for processing the data from the Loral all the way through CIPHER<sup>®</sup>. At this point, it is assumed that the user has a basic understanding of CIPHER<sup>®</sup> and its utilities.

Before aircraft movement but after all systems are on line, the ground engineer must get a compass calibration record of about ten seconds. This is accomplished by simply starting and stopping the recording with the trigger switch connected to "fox-gpx6." The ground engineer running the analysis from "fox-sparrow" will then run the routine 'run\_cal.' This will generate a compass correction to be applied to each of the following records.

Once in flight, for each sweep the pilot will call out when he is about to start, usually by saying “data on.” The flight test engineer simultaneously begins recording data by use of the trigger switch. The pilot will then execute the maneuver and call out when complete, usually by saying “data off.” The engineer running the analysis will then execute the routine ‘run\_real\_time.’ This will convert the data from counts to engineering units, apply necessary scaling and calibrations, decimate the record to 50 Hertz, and transfer the record from “fox-gpx6” to “fox-sparrow.” (At the time of this work “fox-sparrow” was the only machine which was compatible with running CIFER®.) Two UNC3 formatted time history files are generated and placed in the directory ‘/u\_sparrow/cifer/time\_hist.’ One is called ‘EU\_RXXX’ and the other is called ‘cifer\_in.dat.’ A third file, ‘getdataXXX.bin,’ which is a copy of the original file from ‘fox-gpx6,’ is placed in the home directory. XXX refers to the record number. Note, each time ‘run\_real\_time’ is executed it creates the unique files ‘getdataXX.bin’ (the original record, all data in counts) and ‘EU\_RXXX’ (UNC3 format, ready for use), but over-writes the file ‘cifer\_in.dat.’ When all the sweeps in a particular axis at a particular flight condition have been completed, the engineer can run CIFER® and begin the analysis. In the mean time, the flight can continue with the steps and doublets.

As noted in the main text, a typical flight profile consists of a trim point, three frequency sweeps, two steps, and two doublets for each axis of interest at each flight condition. It is recommended that the ground station match the aircraft with respect to the record number of each maneuver. Therefore, although in the analysis only the frequency sweeps are used, it’s a bookkeeping dividend to take a record every time the aircraft takes one.

With the time histories available, CIFER® is then run. It is useful to note that one can enter several inputs and outputs for each run of FRESPID and select the responses to be calculated. This will save time and reduce possible typing errors. Another time saver is to avoid generating plots from within a CIFER® routine such as FRESPID. Use the utility function #19 instead to do the plot generation. Also, note that by only trying to do single input single output (SISO) responses and using only a single window, a significant timesaving can be made. Although this does not produce the best results, they were shown to be adequate. A little prior planning and analysis of the problem to be observed during the flight test, should provide adequate information for window size selection (see also ref. 14).

### **C. STEP-BY-STEP PROCEDURES FOR RUNNING CIFER® NEAR-REAL TIME**

1. Log on to “fox\_sparrow”

```
Username:  cifer
Password:  xxxxxx (See Sunny Ng for password)
```

2. Start the Windows environment. >openwin [cr]
3. Set up the windows, as you like. See figure E.1 for an example. Note that each window is set to a different directory.
4. Set up the “xterm” window for CIFER® (required). >xton [cr]  
>xterm [cr]

If you want to be able to use the window from which “xterm” is started, use the command “*xterm&*” instead of just “*xterm.*”

## 5. Run CIFER®.

A) In the new “xterm” window, initiate CIFER®: `>cifer [cr]`

B) Ensure the file path names are correctly entered (Utility #11).

database	/u_sparrow/cifer/cifroot/data/db
plots	/u_sparrow/cifer/cifroot/jobs/plots
jobs	/u_sparrow/cifer/cifroot/jobs
time history	/u_sparrow/cifer/time_hist

C) Create a new database as necessary.

D) CIFER® should now be ready for the first run.

## 6. Processing the Data.

A) Before a record is ready for CIFER®, it must be processed. This is done by use of the routines ‘run\_cal’ and ‘run\_real\_time.’ To begin, change directory in one of the windows (not the ‘xterm window’) to

```
>cd uh60_slung2_flight.dir [cr]
```

Once a lock is established with the aircraft’s telemetry signal, have the ground station operator run a “rt\_cal” to sample and average 5 seconds of DA02 to be used as the heading bias. When the operator completes this, execute

```
>run_cal [cr]
```

This routine creates a small data file (*uh60\_cal.dat*) to be used by “run\_real\_time.” You will be prompted for the following information, which is available from the pilots:

PS1C - initial magnetic heading of the helicopter  
TOW - take-off gross weight  
XMOMTO - the initial moment as calculated in preflight  
(*ESFW - engine start fuel weight - to be deleted*)

B) After a maneuver is completed and the record of the event generated, execute

```
>run_real_time [cr]
```

When asked, enter the appropriate record number (should match with the flight card). This program processes the raw data file, converting units and decimating the file to 50 hertz. It will take a few moments depending on the size of the file. The output from this is two files:

EU.RXXX     the processed data file, where XXX is the record number entered  
cifer\_in.dat   a temp file, over-written each time "run\_real\_time" is executed.

7. Perform the desired analysis with CIFER<sup>®</sup>.

8. Plotting.

A. Plots are sent from "fox-sparrow" to the printer in the test facility control room.

B. CIFER<sup>®</sup> postscript files can be printed with the command:

```
>lpr <filename>
```

C. When CIFER<sup>®</sup> sends a plot to the screen, that window must be closed in order to return to CIFER<sup>®</sup> proper and the original 'xterm' window.

D. To get a hard copy of the workstation screen, expand the plotting window as large as possible, leaving enough room on an active window to execute the following:

```
>dumpscreen [cr]
```

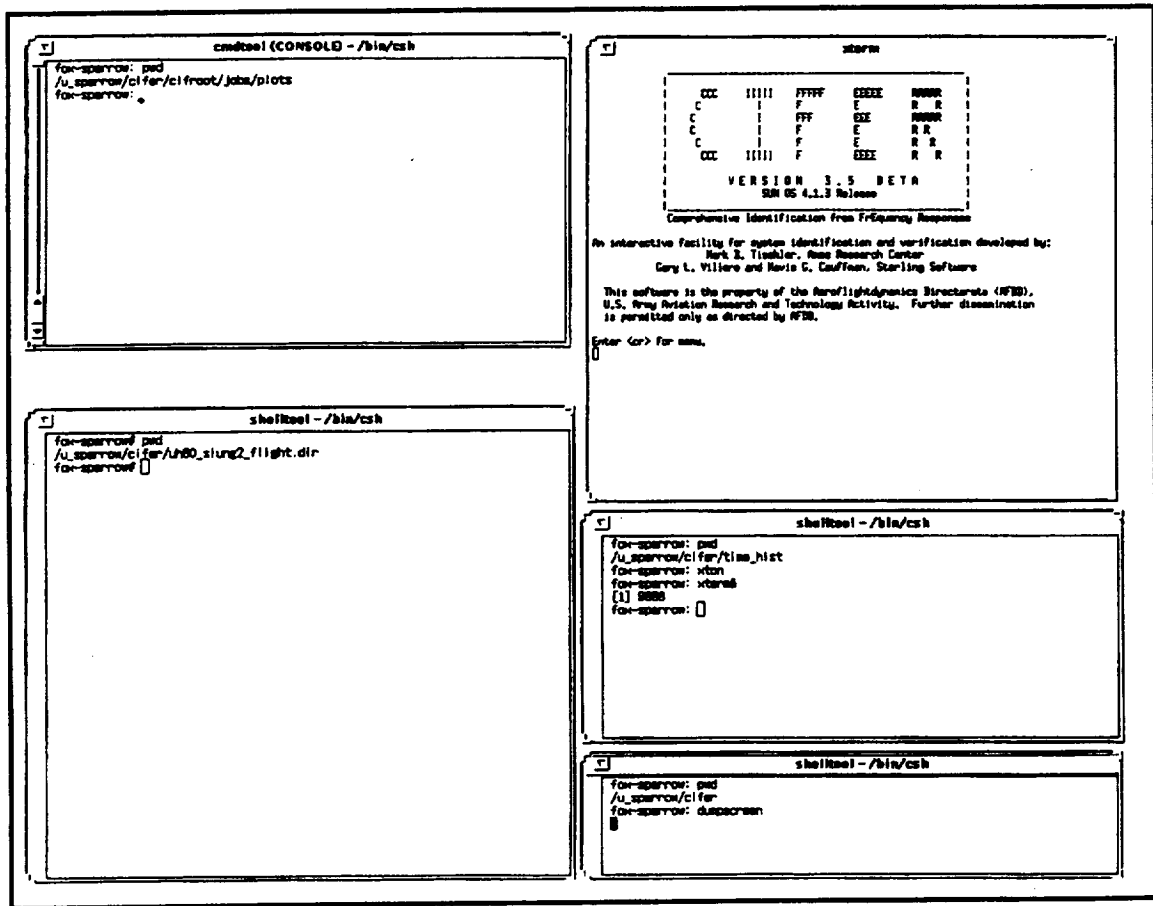


Figure E.1. 'fox-sparrow' screen setup for real time analysis.

## **APPENDIX F. SISO ANALYSIS RESULTS SUMMARY**

Table F.1. Summary of results from SISO analysis of flight data.

Load	Axis	Airspeed (kts)	CLOSED LOOP RESPONSE			BROKEN LOOP RESPONSE				LOAD MOTION		Flight Number	CIFER Database
			-135 deg BW Frequency (rad/sec)	6 dB BW Frequency (rad/sec)	$\tau_{Ld}$ (sec)	Phase Margin (deg)	$\omega_c$ (rad/sec)	Gain Margin (dB)	$\omega_{100}$ (rad/sec)	Damping Ratio	$\omega_n$ (rad/sec)		
NONE	LON	0	2.2437	2.8424	0.1917	106.8910 87.4143	0.2022 1.9994	22.4496	6.5000			170	PF_748
		30	2.3816	3.5620	0.1513	164.0550 110.4960	0.3814 1.7051	20.2886	6.3814			170	PF_748
		50	2.2019	2.6766	0.1590	158.0340 103.3536	0.2843 1.4306	24.3017	7.1839			170	PF_748
		80		2.4236	0.1594			26.3125	5.5340			153	PF_748
	LAT	0	5.1803	3.3319	0.1862	143.0560 141.8840	0.2555 1.0065	18.9243 20.5780	9.6510 10.0909			170	PF_748
		30	4.2098	4.2549	0.1115	179.0500 180.5420 166.8410 155.0780	0.2076 0.4188 0.4553 0.8149	16.0331 16.7882	10.4097 10.7485			170	PF_748
		50	4.1006	4.2704	0.1211	166.6190 135.4870	0.2399 1.0966	15.2483 15.2337 15.6586	9.6938 9.7561 10.0899			170	PF_748
		80	4.1386	4.2584	0.1967	100.3266	1.8725	13.1280	9.7824			153	PF_748
1K INT	LON	80	-	2.4236	0.1594	-	-	26.3125	5.5340			153	PF_748
	LAT	80	4.1386	4.2584	0.1967	100.3266	1.8725	13.1280	9.7824			153	PF_748
1K EXT	LON	0	1.5957	2.1560	0.2111	107.7850 126.4250	0.2676 0.6671	23.2885	5.3622			151	PF_748
		80	2.9552	2.3147	0.1910	92.9259	1.0549	21.3386 21.8763	7.3097 7.3999			160	PF_748
	LAT	0	6.2517	3.3968	0.2079	186.0530 106.4800	0.3578 0.8565	12.7220 12.9402	9.4959 9.5773			151	PF_748
		80	4.4018	4.2968	0.1372	109.5830	1.1749	12.8234	10.2362			160	PF_748
4K EXT	LON	0	2.5745	2.9191	0.2083	125.5130 84.3969	0.2062 2.3646	14.6013 14.6942	6.5947 6.6489			159	PF_748
		80	3.2378	2.3454	0.1693	120.4680 105.4240 106.0460	0.2178 1.3124 1.3254	14.4612	7.1556			161	PF_748
	LAT	0	6.7287	1.7291	0.1988	213.7760 104.2136	0.3909 1.0631	11.8537	9.9193			159	PF_748
		80	6.2953	3.8699	0.1612	97.2334	1.1399	11.1050	10.1749			161	PF_748
2K CONEX	LON	0	2.5285	2.9155	0.1984	82.1574	2.2471	17.3476	6.3342	0.0986	1.4855	167	PF_748
	LAT	0	6.1223	2.8787	0.1815	159.6050 136.6660 136.6350	0.2719 0.7563 0.7608	16.3388 16.5184 16.7572	9.8293 9.9146 10.0008	0.1394	1.6356	167	PF_748
4K CONEX (w/ swivel)	LAT	0	6.3751	2.9981	0.1947	197.9030 110.9170	0.2089 0.8401	14.3627	9.8012	0.2040	1.5173	169	PF_748
	LON	30	2.7219	3.3251	0.1982	150.5870 107.3730 120.7650 108.8280	0.3154 1.1391 1.6220 2.1068	19.3820	7.1820	0.1294	1.4466	169	PF_748
4K CONEX	LON	0	2.6586	3.0290	0.1675	146.6600 86.3652	0.1601 2.4329	20.9999	7.1329	0.1259	1.5162	173/168	PF_748
		30	3.0600	3.3330	0.1981	160.4080 105.8920 119.9020 106.6040	0.3208 1.2226 1.6176 2.1983	20.3759 20.4617	7.0181 7.0888	0.1073	1.4163	172	PF_748
		50	2.8926	3.0071	0.1825	166.1520 99.3068	0.2249 2.5269	23.5966	7.5243	0.1597	1.4433	172	PF_748
		60	3.1115	2.7462	0.1956	143.2270 103.1608 120.9720 102.1835	0.1961 1.1805 1.6557 2.1999	16.2084	7.2246	Poor Coherence		173	PF_748
		70	3.0813	2.7208	0.1718	171.7470 104.5440 111.0600 91.4931	0.2007 1.2277 1.4529 2.7689	17.1142	7.0339	Poor Coherence		173	PF_748
	LAT	0	6.1524	2.8208	0.1902	194.4470 126.1600	0.2399 0.8000	14.6642	9.7277	0.1646	1.5287	172/168	PF_748
		30	5.8716	3.9008	0.1924	181.4740 118.6930	0.2831 0.8176	14.3195	9.9737	0.2016	1.3455	172	PF_748
		50	5.6543	3.7743	0.1500	170.6330 112.1930	0.2128 0.8348	12.9268 13.0158	9.8433 9.9277	0.1994	1.3145	172	PF_748
		60	6.0217	4.2822	0.1511	114.3180 165.0730 164.1400 150.8520	0.8725 1.9836 1.9989 2.1934	13.4955 13.7003	10.0869 10.2519	Poor Coherence		173	PF_748
		70	5.8938	3.8652	0.1477	112.6000	0.7848	12.5880 12.4501	10.6445 10.7260	Poor Coherence		173	PF_748

## REFERENCES

1. Lawrence, T.H., Gerdes, W.H., and Yakzan, S.S.: *Use of Simulation for Qualification of Helicopter External Loads*, American Helicopter Society 50<sup>th</sup> Annual Forum, Washington, D.C., May 1994.
2. *Requirements for the Certification of Externally Transported Military Equipment by Department of Defense Rotary Wing Aircraft*, MIL-STD 913, January 1991.
3. Tischler, M.B. and Kuritsky, A. (editors): *Ten Years of Cooperation: The U.S. / Israel Memorandum of Agreement for Cooperative Research on Rotorcraft Aeromechanics and Man-Machine Integration Technology, 1986-1996*, U.S. Army Aviation and Troop Command, Aeroflightdynamics Directorate, Moffett Field, CA 94035-1000.
4. Presentation of *Task 8 of the U.S. / Israel MOA on Rotorcraft Aeromechanics and Man-Machine Integration Technology* at the 20<sup>th</sup> Semi-Annual Meeting, Ames Research Center, Moffett Field, CA, May 1997.
5. Tucker, G.E.: *Designation of JUH-60A / NASA 748 as a Project Aircraft*, Memorandum, 20 January 1995.
6. *Operator's Manual for Army Models UH-60A, UH-60L, and EH-60A Helicopters*, Technical Manual, TM-1-1520-237-10, 31 August 1994.
7. Prouty, R.W.: Helicopter Performance, Stability, and Control, Robert E. Krieger Publishing Company, 1990.
8. NASA 748, Helicopter Weight and Balance Sheet.
9. *Owner's Manual: E-79 Electronic Load Weigh System for the Sikorsky UH-60A Black Hawk*, May 1996, Onboard Systems, Portland, OR 97231-1038.
10. Multiservice Helicopter External Air Transport: Volume I and II, U.S. Army, FM-55-450-3/4, February 1991.
11. *Helicopter External Load Sling Test*, Ames Research Center Calibration Report, S.R. No. OPF-143, 18 January 1996.
12. Fax from J.C. Smith, Chief, GSE Branch, ATCOM, AVRDEC, to G.E. Tucker, 09 June 1995.
13. Williams, MAJ. J.N., Ham, MAJ. J.A., and Tischler, M.B.: *Flight Test Manual: Rotorcraft Frequency Domain Flight Testing*, AQTD Project No. 93-14, U.S. Army Aviation Technical Test Center, September 1995.

14. Tischler, M.B. and Cauffman, M.G.: *Comprehensive Identification from Frequency Responses: An Interactive Facility for System Identification and Verification*, Volume I – Class Notes, USAATCOM TR-94-A-017, September 1994.
15. Tucker, G.E. and Tischler, M.B.: *OP Division Flight Project Overview: UH-60 Slung Load Flight Dynamics Experiment*, U.S. / Israel MOA, Ames Research Center, April 1995.
16. Tischler, M.B., Villere, G., and Cauffman, M.G.: *CIFER®*, Software Overview Documentation.
17. Maine, R.E.: *Manual for GetData Version 3.1: A Fortran Utility Program for Time History Data*, NASA Dryden Flight Research Facility, October 1987.
18. Vernon, T.: *XPlot – A Utility for Plotting X-Y Data, User Manual / Command Reference*, NASA Dryden Flight Research Facility, September 1991.
19. *Handling Qualities Requirements for Military Rotorcraft*, ADS-33D-PRF, USAATCOM, May 1996.
20. Key, D., Blanken, C., Hoh, R., Mitchell, D., and Heffley, R.: *Cargo / Slung Load Handling Qualities Development: Test Plan*, U.S. Army / NASA Rotorcraft Division, Ames Research Center, March 1997.
21. Ogata, K.: Modern Control Engineering, Prentice Hall, 1990.
22. Tischler, M.B., Fletcher, J.W., Diekmann, V.L., Williams, R.A., and Cason, R.W.: *Demonstration of Frequency-Sweep Testing Technique Using a Bell 214-ST Helicopter*, USAAVSCOM Technical Memorandum 87-A-1, April 1987.
23. Cicolani, L.S.: *Linear Analysis of a UH60 with Slung Load Suspended with Multi-Cable Sling*, Working Paper, November 1996.
24. Balough, D.L.: *Aircraft State Measurements Obtained During UH-60 Airloads Flight Tests*, Memorandum for Record, April 12, 1994.
25. Bondi, M.J. and Bjorkman, W.S.: *TRENDS, A Flight Test Relational Database: User's Guide and Reference Manual*, NASA TM-108806, June 1994.

# REPORT DOCUMENTATION PAGE

Form Approved  
OMB No. 0704-0188

Public reporting burden for this collection of information is estimated to average 1 hour per response, including the time for reviewing instructions, searching existing data sources, gathering and maintaining the data needed, and completing and reviewing the collection of information. Send comments regarding this burden estimate or any other aspect of this collection of information, including suggestions for reducing this burden, to Washington Headquarters Services, Directorate for Information Operations and Reports, 1215 Jefferson Davis Highway, Suite 1204, Arlington, VA 22202-4302, and to the Office of Management and Budget, Paperwork Reduction Project (0704-0188), Washington, DC 20503.

1. AGENCY USE ONLY (Leave blank)		2. REPORT DATE June 1998	3. REPORT TYPE AND DATES COVERED Contractor Report	
4. TITLE AND SUBTITLE Flight Testing and Real-Time System identification Analysis of a UH-60A Black Hawk Helicopter with an Instrumented External Sling Load			5. FUNDING NUMBERS RTOP 581-30-22	
6. AUTHOR(S) Allen H. McCoy			8. PERFORMING ORGANIZATION REPORT NUMBER A-9809853	
7. PERFORMING ORGANIZATION NAME(S) AND ADDRESS(ES) Naval Postgraduate School Monterey, CA 93943-5000			10. SPONSORING/MONITORING AGENCY REPORT NUMBER NASA/CR-1998-196710	
9. SPONSORING/MONITORING AGENCY NAME(S) AND ADDRESS(ES) National Aeronautics and Space Administration Washington, DC 20546-0001			11. SUPPLEMENTARY NOTES Point of Contact: Luigi Cicolani, Ames Research Center, MS 211-1, Moffett Field, CA 94035-1000 (650) 604-5446	
12a. DISTRIBUTION/AVAILABILITY STATEMENT Unclassified-Unlimited Subject Category - 08 Availability: NASA CASI (301) 621-0390			12b. DISTRIBUTION CODE Distribution: Standard	
13. ABSTRACT (Maximum 200 words) Helicopter external air transportation plays an important role in today's world. For both military and civilian helicopters, external sling load operations offer an efficient and expedient method of handling heavy, oversized cargo. With the ability to reach areas otherwise inaccessible by ground transportation, helicopter external load operations are conducted in industries such as logging, construction, and fire fighting, as well as in support of military tactical transport missions. Historically, helicopter and load combinations have been qualified through flight testing, requiring considerable time and cost. With advancements in simulation and flight test techniques there is potential to substantially reduce costs and increase the safety of helicopter sling load certification. Validated simulation tools make possible accurate prediction of operational flight characteristics before initial flight tests. Real time analysis of test data improves the safety and efficiency of the testing programs. To advance these concepts, the U.S. Army and NASA, in cooperation with the Israeli Air Force and Technion, under a Memorandum of Agreement, seek to develop and validate a numerical model of the UH-60 with sling load and demonstrate a method of near real time flight test analysis. This thesis presents results from flight tests of a U.S. Army Black Hawk helicopter with various external loads. Tests were conducted as the U.S. first phase of this MOA task. The primary load was a container express box (CONEX) which contained a compact instrumentation package. The flights covered the airspeed range from hover to 70 knots. Primary maneuvers were pitch and roll frequency sweeps, steps, and doublets. Results of the test determined the effect of the suspended load on both the aircraft's handling qualities and its control system's stability margins. Included were calculations of the stability characteristics of the load's pendular motion. Utilizing CIFER® software, a method for near-real time system identification was also demonstrated during the flight test program.				
14. SUBJECT TERMS Helicopter, External loads, Sling loads			15. NUMBER OF PAGES 97	
			16. PRICE CODE A05	
17. SECURITY CLASSIFICATION OF REPORT Unclassified	18. SECURITY CLASSIFICATION OF THIS PAGE Unclassified	19. SECURITY CLASSIFICATION OF ABSTRACT	20. LIMITATION OF ABSTRACT	

